Chemical Synthesis of Glycosylated Oligoribonucleotides for siRNA Development

Yuyan Zhao, B. Eng.

A thesis submitted to the Department of Chemistry

in partial fulfilment of the requirements for the degree of

Master of Science

July 2009

Brock University

St. Catharines, Ontario

Abstract

In this study, an efficient methodology for the preparation of carbohydrate–RNA conjugates was established, which involved the use of 3,4-diethoxy-3-cyclobutene-1,2-dione (diethyl squarate) as the linking reagent. First, a glycan moiety containing an amino group reacted with diethyl squarate to form an activated glycan, which further reacted with an amino modified oligoribonucleotide to form a glycoconjugate under slightly basic conditions. The effect of glycosylation on the stability of RNA molecules was evaluated on two glycoconjugates, monomannosyl U_{10}-mer and dimannosyl U_{10}-mer.

In the synthesis of aromatic fluorescent ribosides, perbenzylated ribofuranosyl pyrene and phenanthrene were synthesized from perbenzylated ribolactone. Deprotection of benzyl-protected ribofuranosyl phenanthrene and pyrene by boron tribromide gave ribofuranosyl phenanthrene and ribopyranosyl pyrene, respectively. UV/vis and fluorescent properties of the ribosides were characterized.

Acknowledgements

I would like to thank the many individuals whose contributions have made this work possible.

I must first thank my supervisor, Dr. Tony Yan, for giving me the opportunity to work in his research group. Contributing his wisdom and practical experience, he has both guided and assisted me throughout this study.

And I couldn't have finished my study without the unconditional love and support of my parents and my brother who are always there for me.

I am grateful for the efforts of Dr. Art van der Est and Dr. Costa Metallinos while serving my Supervisory Committee; the supports from Kha Tram, Lulu Wang, and Ryan West. Special thanks to Kha Tram for his assistance in the preparation of phosphoramidites and proofreading this thesis.

I would also like to express my gratitude to my friends, Yanming Wang, Huaping Li, and Bin Wang for their belief in me, friendships, and encouragement.

Thank Tim Jones and Razvan Simionescu for assistance in mass and NMR spectroscopy respectively; Anne Noronha for performing the melting studies; and the Natural Sciences and Engineering Research Council of Canada for funding this work.

Table of Contents

List of Tables

List of Figures

List of Schemes

List of Abbreviations

A	adenosine
Ac	acetyl
Ar	aromatic
AcOH	acetic acid
BOP	(benzotriazol-1-yloxy)tris(dimethylamino)phosphonium hexafluorophosphate
Cpep	1-(4-chlorophenyl)-4-ethoxypiperidin-4-yl
CPG	controlled pore glass
d	doublet
dd	double of doublet
DBU	1,8-diazabicyclo[5.4.0]undec-7-ene
DCC	1,3-dicyclohexylcarbodiimide
DMA	*N,N*-dimethylacetamide
DMF	*N,N*-dimethylformamide
DMSO-d_6	deuterated dimethylsulfoxide
DMTr	4,4'-dimethoxytriphenylmethyl
DNA	2'-deoxyribonucleic acid
EI	electron impact
ESI	electrospray ionization
FAB	fast-atom bombardment
h	hour
Hünig's base	*N,N*-diisopropylethylamine
HPLC	high performance liquid chromatography
RP-HPLC	reverse phase HPLC
AE-HPLC	anion-exchange HPLC
m	multiplet
M	molar concentration
Me	methyl
min	minute

m.p.	melting point
NMR	nuclear magnetic resonance
r.t.	room temperature
Ph	phenyl
RNA	ribonucleic acid
R_t	retention time
Squarate	3,4-diethoxy-3-cyclobutene-1,2-dione
s	second
t	triplet
TEAA	triethylammonium acetate
TEAF	triethylammonium formate
THF	tetrahydrofuran
TIPDS	1,1,3,3-tetraisopropyldisiloxyl
TLC	thin layer chromatography
*T*m	melting temperature
U	uridine
UV	ultraviolet

Chapter 1 - Introduction

1.1 Introduction of nucleic acids

In 1869, Miescher isolated a phosphorus containing substance from the pus cell nuclei, which he named "nuclein". In fact, this nuclein was really a nucleoprotein. In 1889, Altman was able to obtain the first protein-free material which he gave the name nucleic acid. In the late 19th century, the pyrimidine and purine bases were isolated and characterized by Kossel and Fischer. The double helix structure of DNA was discovered by Watson, Crick, Franklin, and Wilkins in 1953.[1-3] The discovery of the DNA double helical structure directed enormous development in nucleic acid research.

Nucleic acids may be subdivided into ribonucleic acid (RNA) and deoxyribonucleic acid (DNA). The basic building blocks of nucleic acids are nucleotides **1** (Figure 1.1), which are the phosphate esters of nucleosides **2** (Figure 1.1). Each nucleotide consists of a nitrogen heterocyclic base, a pentose sugar, and a phosphate backbone. Base residues include pyrimidines and purines. The pyrimidine bases are thymine **3**, cytosine **4**, and uracil **5**; the purine bases are adenine **6** and guanine **7**. In nucleosides, the purine or pyrimidine bases are joined from N-1 of pyrimidine or the N-9 of the purines to the anomeric carbon of a pentose sugar. In RNA **2b** (Figure 1.1), the pentose sugar is D-ribose which is a five-membered furanose ring; in DNA **2a** (Figure 1.1), the pentose sugar is 2-deoxy-D-ribose. In the DNA series, the four bases consist of guanine, cytosine, adenine, and thymine; while in RNA uracil replaces thymine.

1.2 Introduction of small interference RNA (siRNA)

In recent years, nucleic acids have found a wide range of therapeutic applications such as gene therapy, antisense oligonucleotides, aptamers, and RNA interference.[4, 5] Of paticular interest, the potential use of siRNAs has attracted great attentions as a novel approach for specific gene silencing.

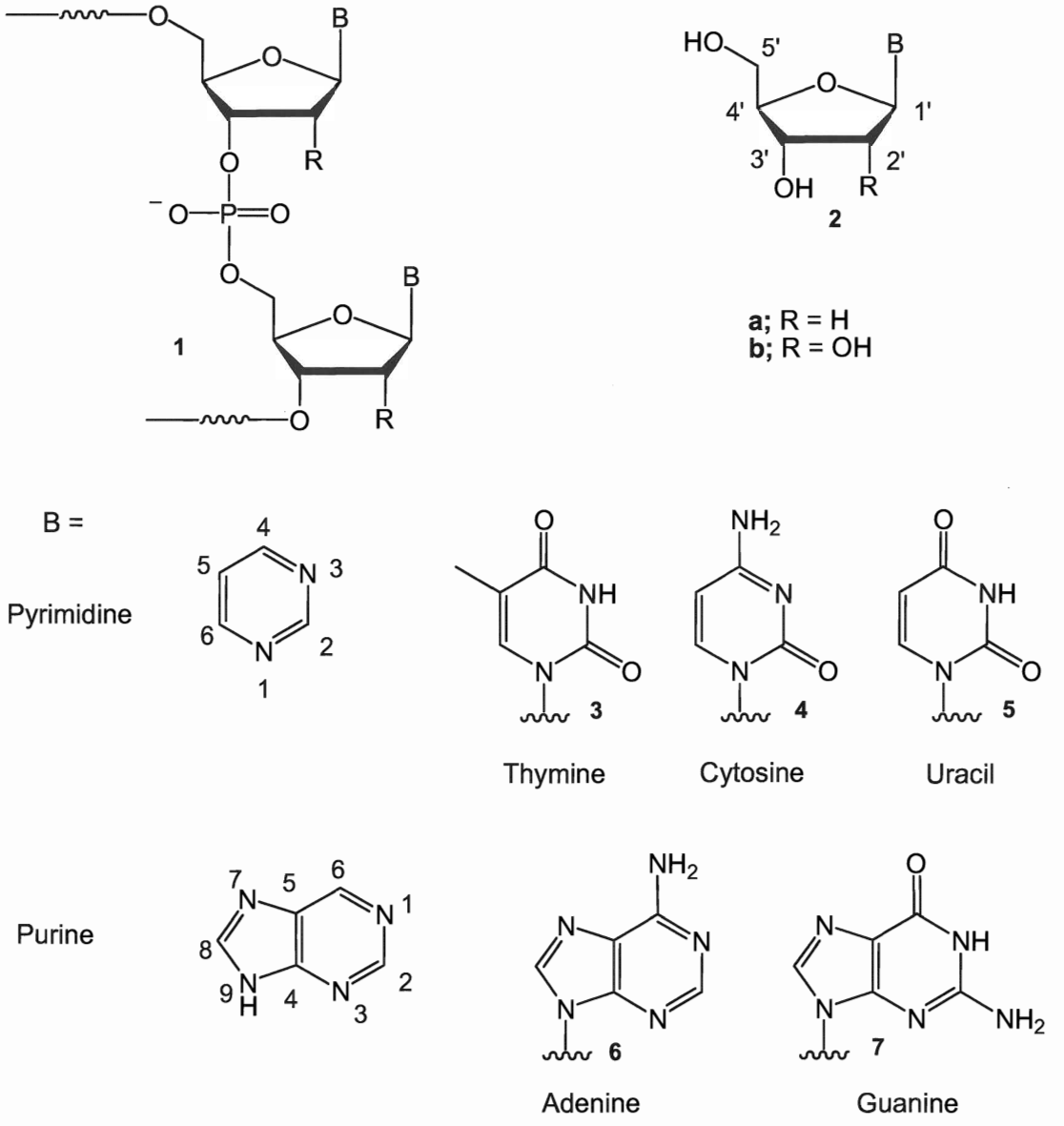

Figure 1.1: Basic structures of nucleic acids

siRNAs are double stranded RNA (dsRNA) molecules which usually contain 21 to 23 nucleotides in length including 2-nucleotide overhangs at the 3'-termini of each strand. When introduced to a cell, siRNAs can silence gene expression through the RNA interference (RNAi) pathway. RNAi is a naturally occurring biological process in which dsRNAs direct the degradation of complementary target RNAs. In 1998 Fire and Mello demonstrated that dsRNA was able to inhibit gene expression in *C. elegans*.[6] Such dsRNA-mediated gene silencing was later identified in Drosophila, zebrafish, and

mammals. RNAi pathways are guided by small RNAs that include siRNAs and microRNAs (miRNAs)[7, 8] as shown in Figure 1.2. First, long dsRNAs or precursor miRNAs (pre-miRNAs) are processed by the RNase III enzyme Dicer into siRNAs or miRNAs repectively. Then, the siRNAs or miRNAs are incorporated into RNA-inducing silencing complexes (RISC). The endonuclease Argonaute 2 (AGO2) in the RISC mediates the cleavage of sense strand of siRNAs or unwinding of the miRNA duplex. The RISC complexes are activated while the single-stranded antisense strand is generated. The antisense strand of the activated RISC complexes acts as a guide sequence to target complementary messenger RNA (mRNA). Finally, the target mRNA is cleaved or degraded by the catalytic domain of AGO2 in RISC, resulting in sequence specific inhibition of gene expression.

Although dsRNAs can cause potent genetic interference, achieving RNAi in mammalian cells was initially unsuccessful because dsRNA induces a powerful interferon response. This response leads to the inhibition of all gene expression and rapid cell death.[9] Fortunately, Tuschl and colleagues discovered that introduction of synthetic siRNAs did not stimulate an interferon response but rather led to sequence-specific mRNA degradation in mammalian cells.[10] These synthetic siRNAs, which are usually 21-23 nucleotides in length, are long enough to induce RNAi, but small enough to avoid inducing interferon response. Further studies demonstrated that duplexes of 21-nucleotide siRNAs with 2-nucleotide 3' overhangs were shown to be the most efficient triggers of RNAi-based mRNA degradation.[11] These studies provided a very powerful tool for researchers working in mammalian systems to selectively and rapidly suppress genes of interest using such synthetic siRNAs.

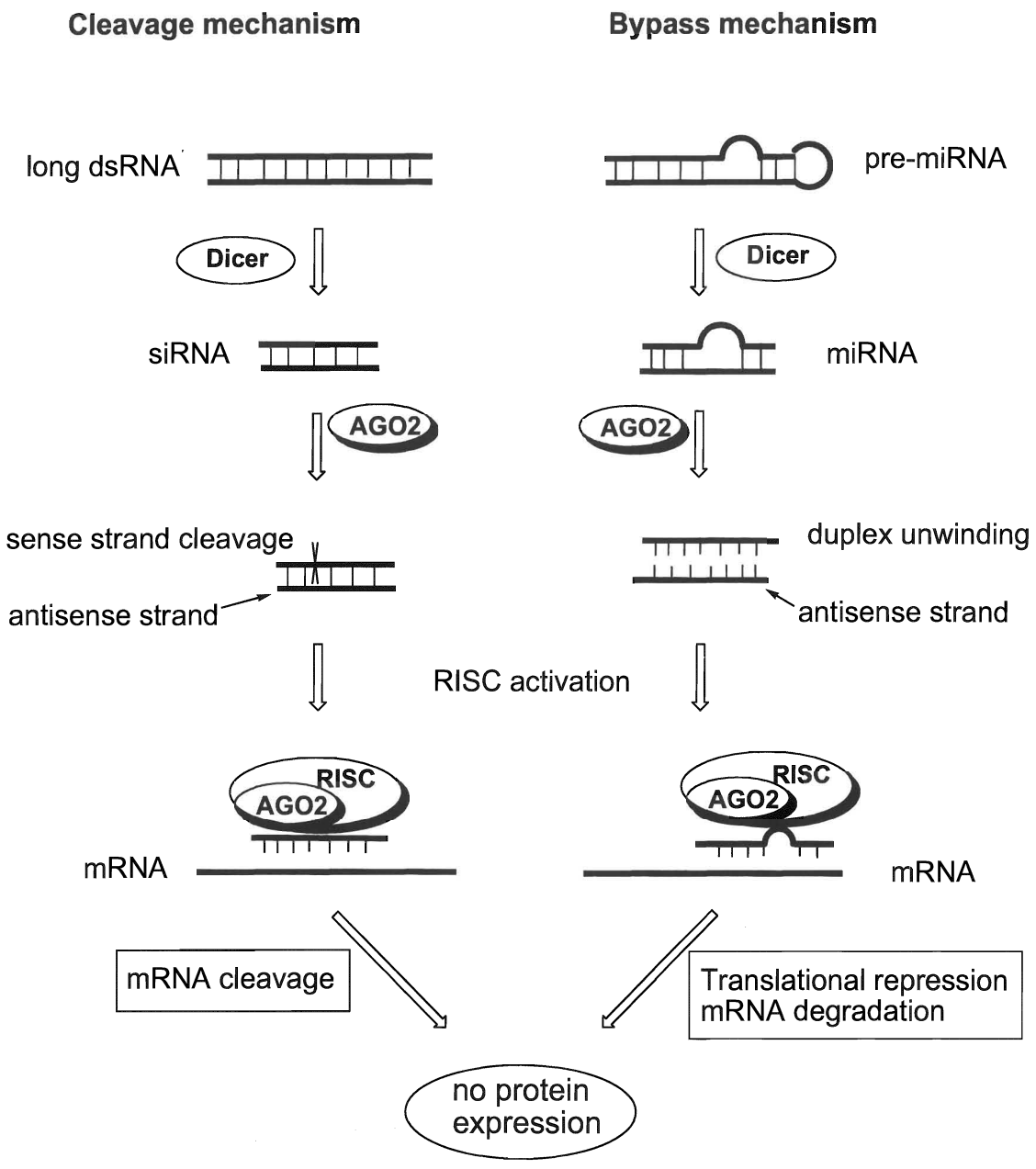

Figure 1.2: Mechanism of RNAi pathway

siRNAs participate in repeated cycles of degradation of specific mRNAs, so protein production can be efficiently inhibited. Theoretically, siRNAs can be used to cure any disease that is caused by the expression of deleterious genes. The major advantage of siRNA therapy is that it interferes with the synthesis of disease-causing proteins at an

early stage of gene expression. Therefore, siRNA is considered as a means of sequence-specific therapeutics against a wide range of diseases. As such, several companies are focusing on the development of RNAi-based therapeutics.[12]

1.3 Challenges in siRNA development

The success of gene silencing by synthetic siRNA in mammalian cells has led to high expectations for siRNA as an important tool in gene regulation for therapeutic development. However, the development of siRNA molecules as therapeutic agents is faced with a number of challenges, particularly their relatively poor *in vivo* stability, poor delivery efficiency, and potential off-target effects.[13]

1.3.1 Improvement of siRNA stability

dsRNAs are quite stable in cell culture media. It was observed that dsRNAs are stable in 5% fetal bovine serum for up to 72 h, while the single stranded (ssRNA) was completedly degraded as short as 30 s under the same condition.[14] However, the situation is more complex *in vivo*. dsRNAs are less stable in higher concentrations of serum.[13] When dsRNAs were incubated in 50% mouse serum, degradation was observed after 24 h.[15] In order to improve the serum stability of siRNAs, a number of chemical modifications have been investigated. Many of these modifications were initially designed for antisense applications. The most important chemical modifications include backbone modifications like phosphorothioate linkages and ribose modifications.

1.3.1.1 Phosphorothioate linkages

In phosphorothioate linkages **9**, one of the non-bridging oxygen atoms in the phosphate backbone **8** is replaced with a sulfur atom (Figure 1.3). It was reported that phosphorathioate modification did not significantly affect RNAi activities.[14] Although introduction of phosphorothioate linkages into duplex RNAs provides significant improvement in serum stability, it decreases hybridization affinity which is indicated by reduction in melting temperature (T_m) values compared with unmodified RNA duplex.[14]

Another study found that the cytotoxicity was observed with phosphorathioate modification of siRNA in human keratinocyte cell line HacaT.[16]

1.3.1.2 Ribose modifications

Many modifications to the ribose residues of RNAs were investigated in order to increase the enzymatic stability of siRNA as well as their hybridization affinity. Among these, 2'-*O*-methyl ribonucleotides **10,** 2'-deoxy-2'-fluoro (2'-F) nucleotides **11**, and locked nucleic acids (LNA) **12** (Figure 1.3) have been well evaluated.

1.3.1.2.1 2'-*O*-Methyl modification

siRNA with 2'-*O*-methyl modification **10** showed resistance to fetal bovine serum and slightly increased hybridization affinity, with an increase of T_m by upto 1°C per modification.[14] Several siRNA sequences with 2'-*O*-methyl residues at different positions have been investigated for their effects on both the stability and silencing efficiency.[17] It was shown that 2'-*O*-methyl modifications at certain positions in the siRNA duplex can increase stability in serum without significant loss of RNAi activity. siRNAs with two to four 2'-*O*-methyl modified nucleotides in either strand efficiently mediated RNAi acitivity. However, siRNA molecules with either one or both strands fully substituted by 2'-*O*-methyl residues were not able to induce RNAi activity in mammalian system.[17]

1.3.1.2.2 2'-F modification

It has been reported that the introduction of 2'-F modification **11** increased the thermal stability of RNA duplexes.[18] In addition, 2'-F modification has been shown to be well tolerated in siRNA applications.[19] When 2'-F modifications were introduced at the 3'-termini or internal positions of RNA strands, the resulting siRNAs led to efficient inhibition of gene expression.[14] These findings suggest that partial substitution with 2'-deoxy-2'-fluoro nucleotides is well accommodated in RNAi pathway. The idea of 2'-F modification provides another option for optimizing RNAi in mammalian cells.

1.3.1.2.3 LNA modification

LNA-RNA duplexes that contain LNA nucleotides **12** at 3'-, 5'-, or both 3'- and 5'-termini (Figure 1.3) were able to block gene expression.[14] In contrast, LNA-RNA duplexes that contained two LNA nucleotides within the central region were ineffective in gene silencing.[14] It was also observed that introduction of LNA nucleotides substantially increased T_m values. Optimization of the numbers and position of LNA substitution may offer a useful strategy for RNAi applications.

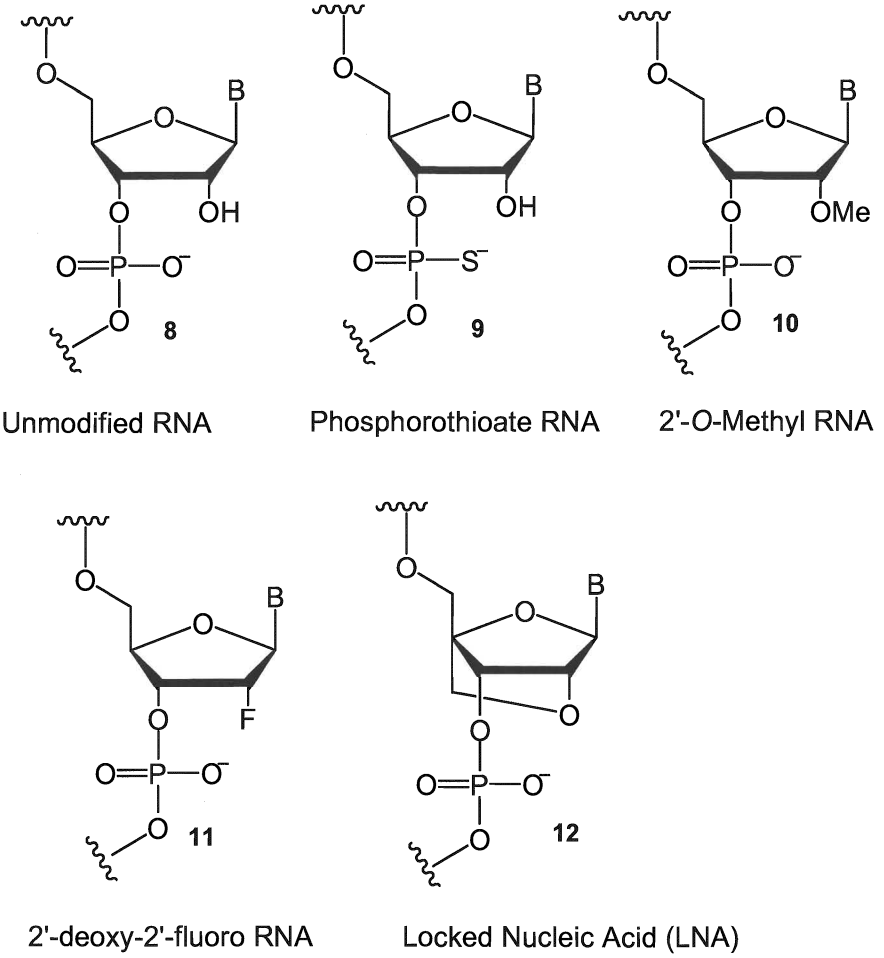

Figure 1.3: Chemical modifications of RNA

1.3.1.2.4 2'-*O*-Methyl **10** in combination with 2'-F **11** or LNA **12** modifications

Recently several groups have demonstrated the advantages of using 2'-*O*-methyl in combination with other modifications in siRNAs. Soutschek *et al.* reported the *in vivo*

silencing of apolipoprotein B (ApoB) using chemically modified siRNAs containing 2'-*O*-methyl modification combined with phosphorothioates. The siRNA that had two modified nucleosides (2'-*O*-methyl combined with phosphorothioate) at the 3'-end of antisense strand and a cholesterol moiety conjugated to 3'-end of sense strand induced potent RNAi activity.[20]

Combination of 2'-*O*-methyl with 2'-F modifications has been examined by Allerson *et al.* [21] In their study, a fully 2'-modified siRNA that consists of alternating 2'-*O*-methyl and 2'-F modifications in both strands displayed an increase of *in vitro* potency as well as enzymatic and thermal stabilities.[21] Therefore, alternating 2'-F/2'-*O*-methyl modifications may prove to be a useful strategy in designing functionally active and stable siRNAs.

1.3.1.3 Chemical modifications of the termini and conjugate groups

A 5'-phosphate on the antisense strand of an siRNA duplex is required for siRNA target cleavage in mammalian cells.[22] siRNAs with a 5'- free hydroxyl on their antisense strands can mediate RNAi function because it can be phosphorylated by cellular kinases. It was found that siRNA in which 5'-hydroxyl termini of the antisense strand was blocked as 5'-methoxy failed to induce RNAi acitivity.[22] In contrast, 5'-modification of the sense strand had no effect on silencing activity.[17] Blocking 3'-hydroxyl of the antisense strand by a C_6-amino modifier group did not affect on efficiency or specificity of RNAi in flies or mammals.[22]

Certain terminal conjugates in the sense strand of siRNAs have been reported to improve RNAi activity. Soutschek *et al.* reported *in vivo* silencing of ApoB mRNA by cholesterol-conjugated siRNAs which contain phosphorothioate backbone modification **9**, 2'-*O*-methyl modification **10**, and a cholesterol moiety.[20] In their study, both sense and antisense strands of siRNAs were modified by phosphorothioate backbone and the antisense strand contains two 2'-*O*-methyl nucleotides at the 3'-end. Cholesterol–siRNAs (Chol-siRNAs) were synthesized by linkage of cholesterol to the 3'-end of the sense strand *via* a pyrrolidine linker. It was found that Chol-siRNAs was significantly more

stable than unconjugated siRNAs in human serum without significant loss of the gene-silencing activity in cell culture. Lorenz *et al.* synthesized the lipid conjugates of siRNAs by covalently linking lipid moieties to the 5'-ends of the siRNA sense strand using phosphoramidite chemistry.[23] General structure of lipid-containing phosphoramidite **13** is illustrated in Figure 1.4. The resulting lipid–siRNAs improved *in vitro* cellular uptake and silencing efficiency in liver cells.

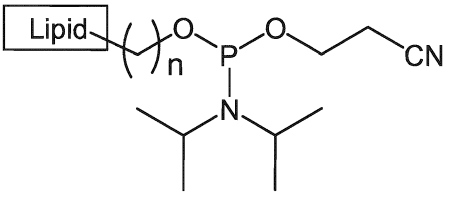

13

Figure 1.4: Lipid-containing phosphoramidite

1.3.1.4 Glycosylation

Naturally glycosylated DNAs in T-even bacteriophages have been discovered to enhance the resistance of these DNA molecules to deoxyribonucleases.[24] It was found that glucose was present as an *O*-glycoside of the 5-hydroxymethyl substituent on the pyrimidine residue of DNA of T2, T4, T6 bacteriophages. Although their biological roles have not yet been fully elucidated, strong evidences show that the glycosylation of DNA protects T-even phages DNA from degradation by deoxyribonucleases. However, the effect of glycosylation on the stability of RNA has not been investigated yet.

1.3.2 Improvement of siRNA delivery efficiency

siRNAs are relatively large molecules with multiple negative charges. Because of the electrostatic repulsion between these negative charges and the negative charges on cell membranes, their cellular uptake is inefficient. Several approaches have been investigated in order to develop an appropriate delivery tool for siRNA therapies.

1.3.2.1 Lipids

Development of potential siRNA therapeutics against liver cell-specific diseases such as hepatitis C is hampered because human liver cells show poor uptake of these nucleic

acids. Since the liver is involved in lipid and steroid metabolism, several studies employed lipids to assist siRNA delivery *via* a receptor mediated mechanism or by an increased membrane permeability of the negatively charged RNA. A series of lipid-modified siRNAs were synthesized by Hadwiger and co-workers in order to investigate the silencing potency of reporter gene expression.[23] In their studies, the lipid moieties were covalently linked to the 5'-ends of the RNAs using phosphoramidite chemistry. It was found that siRNAs with a modified sense strand inhibit gene expression to a higher extent than siRNAs with a modified antisense strand or both strands modified. Unmodified siRNAs did not affect gene expression under the same conditions.

1.3.2.2 Cholesterol

In order to improve the delivery of siRNA into liver cells without transfection agents, a series of lipophilic siRNAs conjugated with derivatives of cholesterol were synthesized. Results by Soutschek and co-workers demonstrated that cholesterol conjugation may be able to address the siRNA delivery problem.[20] The cholesterol–siRNA conjugates (Chol-siRNA) were synthesized by incorporation of cholesterol to the 3'-end of the sense strand of an siRNA molecule *via* a pyrrolidine linker. The silencing effect on an ApoB gene by cholesterol- modified siRNAs was investigated. Chol-ApoB-siRNA, but not unconjugated ApoB-siRNA, resulted *in vivo* silencing of ApoB mRNA in liver and jejunum.

1.3.2.3 Liposomes

Although neutral liposomes have been successfully used to deliver siRNA *in vivo*,[25] cationic liposomes are more commonly used for siRNA delivery. Cationic liposomes are termed as "stable nucleic acid lipid particles" (SNALPs).[26] In this approach, the negatively charged siRNA molecules interact electrostatically with cationic liposomes to form complexes that are able to be transferred into the cells (Figure 1.5).

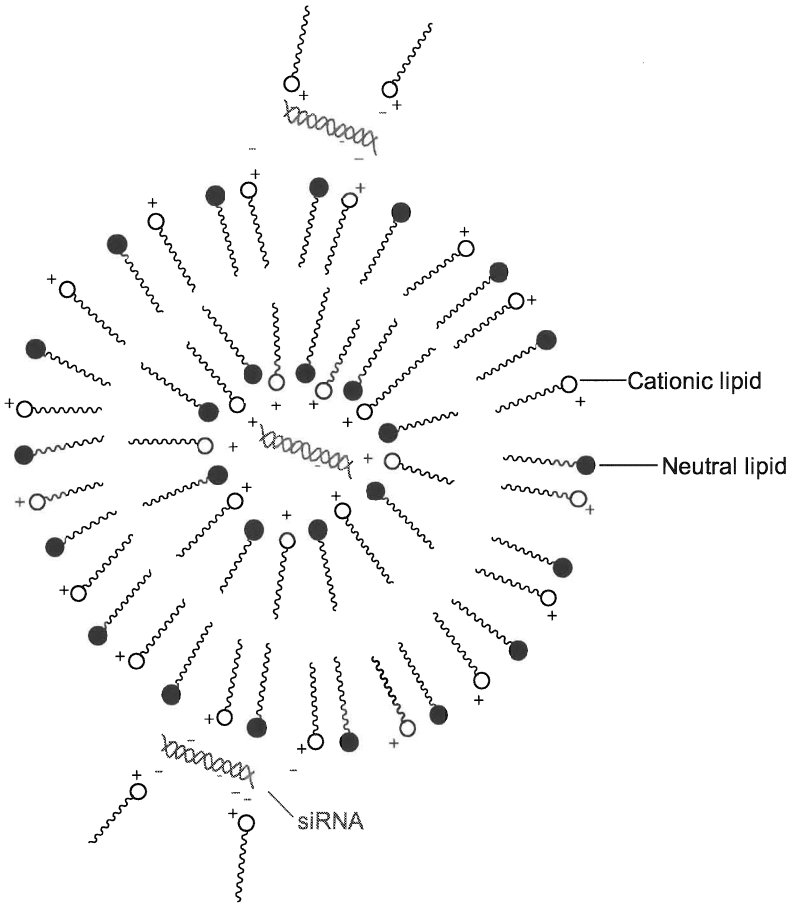

Figure 1.5: siRNA delivery by cationic liposomes

Torchilin and colleagues[27] successfully delivered siRNA into lung tumor cells using siRNA encapsulated in liposomes bearing arginine octamer (R8) molecules attached to their surface. R8 belongs to a group of cell-penetrating peptides (CPP), which are positively charged and can enter cells more readily. In their studies, siRNA-loaded R8 liposomes showed very high transfection efficiency in lung tumor cells and high stability in serum.

In another study by Zimmermann *et al.*, the disease target ApoB in non-human primates was successfully silenced by systemic delivery of siRNAs in a liposomal formulation.[28] In their studies, the ApoB-specific siRNAs were encapsulated in stable SNALP and administered by intravenous injection to cynomolgus monkeys. The results suggest that delivery of siRNAs for targeting specific genes in higher species is possible, therefore

RNAi may represent a new strategy for reducing LDL–cholesterol levels in clinical settings.

1.3.2.4 Peptides

Peptide-based gene delivery system has been under investigation for nucleic acid delivery for over ten years.[29-32] Divita *et al.* investigated MPG-mediated siRNA delivery.[33] MPG, a short peptide vector (27 amino acid residues), contains a hydrophobic domain derived from the fusion sequence of HIV gp41 and a hydrophilic domain derived from the nuclear localisation sequence of SV40 large T-antigen.[32] MPG forms stable non-covalent complexes with nucleic acids by electrostatic interactions. Results[32] showed that MPG promotes the delivery of siRNA into mammalian cells in less than 1 h with efficiency of over 90%. In the absence of MPG, siRNA was taken up by at a very low level.

1.3.2.5 Antibodies

Lieberman and colleagues recently reported the development of antibody–protamine fusion proteins as vehicles for receptor-directed delivery of siRNA.[34] They combined the nucleic acid-binding properties of the small basic protein protamine with the specific ligand-recognition properties of antibodies to achieve cell-type-specific siRNA delivery both *in vitro* and *in vivo*. The fusion protein (F105-P) was designed with the protamine coding sequence linked to the C terminus of the Fab fragment of an HIV-1 envelope antibody. siRNA binds to fusion protein non-covalently. With the assistance of protamine-antibody fusion proteins, the siRNA was successfully delivered to HIV-infected cells and induced efficient gene silencing. Additionally, F105-P-complexed siRNA only targeted the cells expressing HIV-1 envelope, but not normal tissues. These results demonstrate that silencing using antibody-mediated delivery is both efficient and specific.

1.3.2.6 Viral vectors

Viral vectors are highly efficient delivery systems for nucleic acids. Different viral vectors encoding short hairpin RNA (shRNA) including lentiviruses,[35] adenoviruses,[36]

and adeno-associated viral vector[37] are being developed for delivery of siRNA. However, their clinical application is hindered by induction of adverse immune responses and inadvertent changes in gene expression following random integration into the host genome.

1.3.2.7 Glycotargeting to improve cellular delivery efficiency of siRNAs

Apart from the above approaches, utilizing interactions on cell surfaces is another strategy in the design of efficient delivery platform in siRNA therapies. Using carbohydrate ligands to target protein receptors by the mechanism of receptor-mediated endocytosis is called glycotargeting.[38] The idea of using carbohydrates to create a targeted drug delivery system was first demonstrated in 1971.[39] Lectins, which are proteins existing on cell surfaces, recognize and bind to carbohydrates with high specificity. Utilizing lectin-glycan interactions to mediate cell targeting and cellular uptake of molecules has been under intense investigation during the past two decades.[40]

A nucleic acid delivery system that exploits the interactions between glycans and lectins is a relatively recent technique first implemented by Wu and Wu.[41] Carbohydrate moieties have been proved to improve cellular delivery efficiency of deoxyribonucleic acid. Following this pioneer study, many different variations using lectin-ligand interactions in nucleic acid delivery have been developed. The developments in nucleic acid glycosylation are summarized in comprehensive review articles by Yan[42] and Oretskaya[43] respectively.

Nucleic acid glycosylation can be prepared as non-covalently associated carbohydrate-nucleic acid complexes and covalently-linked carbohydrate-nucleic acid conjugates. In the first approach, the non-covalent nucleic acid complexes (glycoplexes) can be formed through ionic interactions, protein-ligand interactions,[44] nucleic acid-intercalator interactions,[45] and nucleic acid-polysaccharide interactions.[46] In the second approach, carbohydrates and nucleic acids are linked by covalent bonds. So far, a number of systems have been investigated in the preparation of carbohydrate-nucleic acid conjugates including:

- Coupling of sugar phosphoramidites with oligonucleotides;[47]
- Enzymatic elaboration of carbohydrate moiety of a glycosylated oligonucleotide;[48]
- Derivatization from the nucleoside base residues;[49]
- Diazocoupling;[50]
- Oximation;[51]
- Reductive amination;[52]

Compared to glycoplexes, the conjugates from the second approach tend to be more homogeneous and easily characterized. However, the difficulties in the preparation of covalent conjugates and steric effects caused by some covalent linkages on binding properties make the second approach quite challenging.

1.4 Chemical synthesis of oligoribonucleotide sequences

1.4.1 Overview of chemical synthesis of oligonucleotides

Since the discovery of the double helical structure of DNA in 1953,[1-3] tremendous efforts have been made in the chemical synthesis of oligonucleotides. The essence of oligonucleotide synthesis is the formation of internucleotide 3'→5' phosphodiester linkages. However, this reaction is complicated by the presence of two or three hydroxyl functions in nucleosides and reactive functional groups in the base residues. It is very important to protect these groups appropriately to ensure formation of correct internucleotide linkages during the coupling reaction and subsequent purification.

The first chemical synthesis of an oligonucleotide with a natural 3'→5' internucleotide linkage was reported by Michelson and Todd.[53] Over the past fifty years, several methods for the syntheis of oligonucleotides have been established. Based on the ways of making the internucleotide linkage, these methods are grouped into the phosphodiester,[54] phosphotriester,[53] phosphite triester,[55] phosphoramidite[56] and H-phosphonate approaches.[57]

1.4.2 Phosphoramidite approach

Among the methods described above, phosphoramidite chemistry is the most widely used approach in oligonucleotide synthesis on solid phase since its invention. In this approach, first introduced by Beaucage and Caruthers,[56] monofunctional nucleoside phosphoramidites are used as a new class phosphorylating reagent. In their original studies (Scheme 1.1), 5'-*O*-dimethoxytrityl (DMTr) **20** protected deoxyribonucleoside was first allowed to react with chloro-*N*,*N*-(dimethylamino)-methoxyphosphine (R^1=R^2=Me in **15**) in the presence of *N*,*N*-diisopropylethylamnine to give the corresponding nucleoside phosphoramidite **16**. Upon activation, the phosphoramidite **16** coupled rapidly with a second nucleoside **17** bearing a free 5'-hydroxyl function to afford a phosphite triester **18**. After oxidiation by iodine, the stable phosphate triester **19** was produced.

1*H*-Tertrazole was chosen as a suitable activating agent in the phosphoramidite approach. Since 3'-*O*-(methoxy-*N*,*N*-dimethyl)phosphoramidites (R^1=R^2=Me in **16**, Scheme 1.1) were found to be unstable in solution, several stable phosphoramidite derivatives have been developed. Among them, 3'-*O*-(2-cyanoethyl-*N*,*N*-diisopropyl)phosphoramidites (R^1=CH_2CH_2CN, R^2=Me_2CH in **16,** Scheme 1.1) were proved to be stable in solution. The cyanoethyl groups for protecting internucleotide linkages are readily removable under the conditions required for the removal of the nucleobase protecting groups, i.e. incubation in concentrated aqueous ammonium hydroxide.[58] Since then, 2-cyanoethyl-*N*,*N*-diisopropylphosphoramidites (R^1=CH_2CH_2CN, R^2=Me_2CH in **16,** Scheme 1.1) have been used widely in phosphoramidite-based solid phase oligonucleotide synthesis.

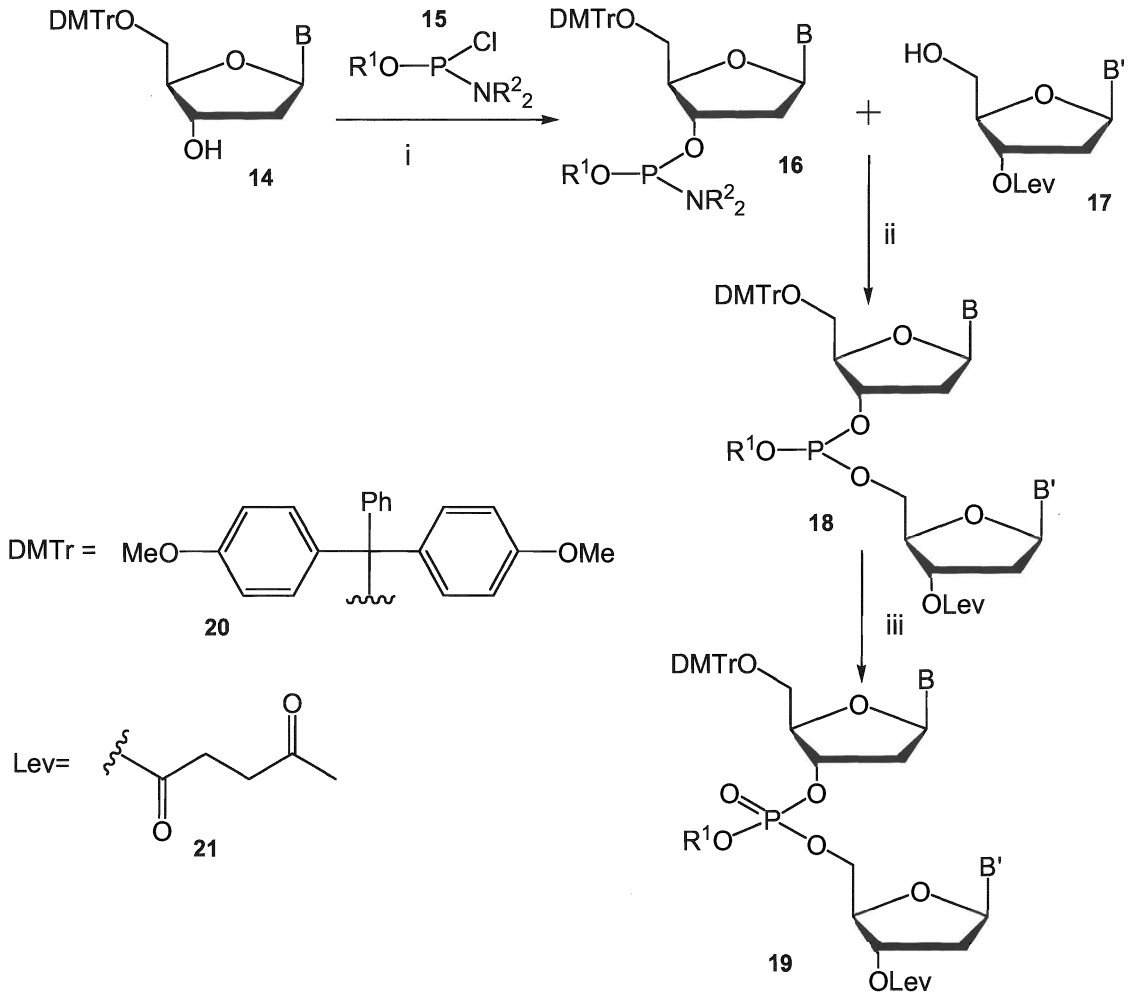

Scheme 1.1: The original phosphoramidite chemistry. *Reagent and conditions*: i, (*i*-Pr)$_2$NEt, $CHCl_3$, r.t.; ii, 1*H*-tetrazole, CH_3CN; iii, iodine.

1.4.3 Solid phase oligonucleotide synthesis

Solid phase oligonucleotide synthesis involves the addition of one nucleotide residue or a blockmer at a time to a protected nucleoside or oligonucleotide on a solid support. Controlled-pore glass (CPG)[59] and higly crosslinked polystyrene[60] are both robust materials and are used as choices of solid support. CPG has proved to be generally useful solid supports and have been used successfully in the automated solid phase oligonucleotide synthesis since 1981.[59] The terminal nucleoside is commonly attached to solid supports via a succinoyl group **22** as in Figure 1.6.

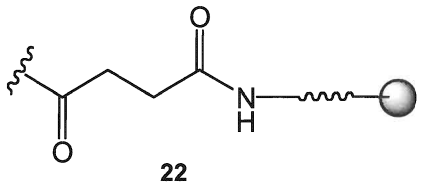

22

Figure 1.6: Succinoyl group attached to CPG

Solid phase oligonucleotide synthesis *via* the phosphoramidite approach has been widely used for synthesis of DNA and RNA sequences since 1980s because of (i) commercial availability of automatic synthesizers, phosphoramidite building blocks and reagents; and (ii) efficiency in the synthesis of oligonucleotides. In this approach, the various steps involved in each cycle of synthesis are illustrated in Scheme 1.2. Each cycle starts with the detritylation step which is the removal of the DMTr group to free the 5'-hydroxyl for the coupling reaction. Coupling is achieved by the addition of an activator such as 1*H*-tetrazole, 5-(ethylthio)-1*H*-tetrazole (ETT), and 5-(benzylthio)-1*H*-tetrazole (BTT). Then the capping step follows, which terminates any unreacted chains with a free 5'-OH by acetylation using acetic anhydride and *N*-methylimidazole. Subsequent oxidation step converts the unstable phosphite triester linkages to the stable phosphate triester linkages. Once the chain is assembled, the oligonucleotide is then cleaved from the solid support by treatment with aqueous ammonia. Meanwhile, all the protecting groups are also cleaved, including the cyanoethyl protecting groups for the internucleotide linkages and the acyl protecting groups for the bases.

1.5 2'-Hydroxyl protecting groups in the synthesis of oligoribonucleotide sequences

There has been increased interest in the chemical synthesis of oligoribonucleotides since the discovery of the siRNA technology. However, the chemical synthesis of oligoribonucleotides lagged a long way behind the well-established oligodeoxyribonucleotide synthesis. Compared to the synthesis of DNA, preparation of RNA sequence is more complex due to the presence of 2'-hydroxyl function in RNA which causes undesirable side reactions. Protection of 2'-hydroxyl function lowers coupling yields in chain assembly because of steric hindrance of protecting groups.

Besides the inefficiency in coupling reaction, the instability of RNA in both acidic and basic media is another hurdle in RNA chemistry.[61]

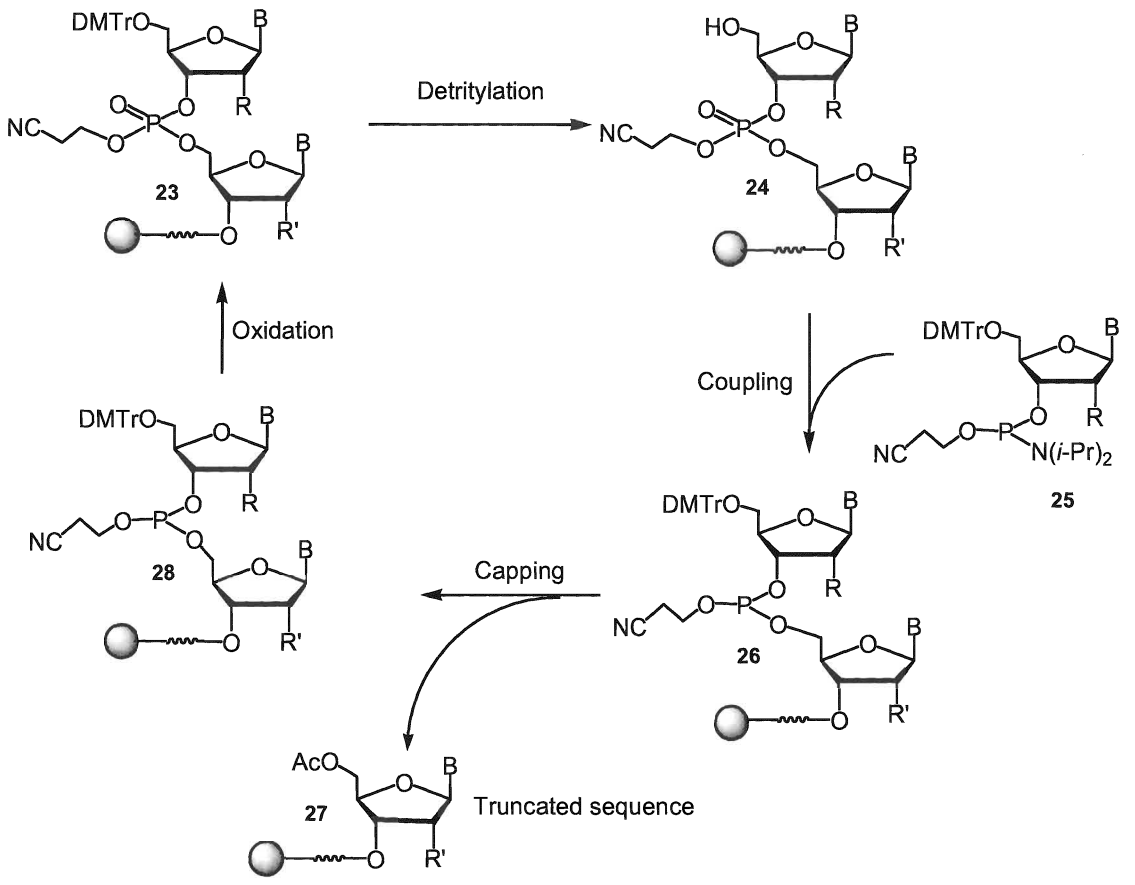

Scheme 1.2: Solid phase synthesis of oligonucleotide using the phosphoramidite chemistry

It is therefore obvious that the most crucial decision to be taken in the chemical synthesis of RNA sequences is the choice of 2'-OH protecting groups. This protecting group must remain completely intact throughout the synthesis and must then be removed in the final deblocking step without causing any cleavage or migration of internucleotide chain. These are very demanding requirements, since the internucleotide linkage of RNA easily undergoes both base-catalyzed hydrolysis and acid-catalyzed hydrolysis and migration.[62] It is possible to separate synthetic oligonucleotide from the cleavage products by either HPLC or polyacrylamide gel electrophoresis (PAGE). However, it is virtually impossible

to separate the oligonucleotide from the impurities containg 2'-5' internucleotide linkage resulted from migration. If an acid labile group is used to protect the 2'-hydroxyl function in oligonucleotide synthesis, it must be removable under very mild conditions to avoid degradation and migration of the internucleotide linkages.

Based on the deblocking conditions, the 2'-OH protecting groups can be grouped into four major categories: protecting groups removable under nearly neutral conditions, base labile protecting groups, acid labile protecting groups, and protected protecting groups (which are usually removed in two steps).

1.5.1 Protecting groups removable under nearly neutral conditions

1.5.1.1 Benzyl

The benzyl protecting group is removable by catalytic hydrogenolysis.[63] The major drawbacks of this protecting group are incomplete 2'-deblocking and hydrogenation of the 5,6-double bonds of cytosine and uracil residues. This protecting group has very rarely been used in oligoribonucleotide synthesis.

1.5.1.2 2-Nitrobenzyl

The 2-nitrobenzyl group **29** (Figure 1.7) is removable photolytically above 280 nm under acidic conditions.[64] However, phosphoramidite monomers derived from 2'-*O*-nitrobenzyl group ribonucleosides need extended coupling time due to steric hindrance by the bulky 2'-protecting group. A more serious problem is the formation of photoadducts under the conditions for the removal of nitrobenzyl.

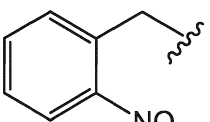

29

2-Nitrobenzyl

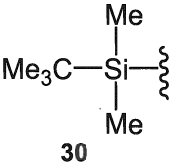

30

TBDMS

Figure 1.7: Protecting groups removable under nearly neutral conditions

1.5.1.3 *tert*-Butyldimethylsilyl (TBDMS)

TBDMS group[65] **30** (Figure 1.7) is the most widely used 2'-OH protecting group. TBDMS is moderately stable to the acidic conditions used for deblocking of the 5'-*O*-DMTr group and is removable by treatment with tetrabutylammonium fluoride (TBAF).[66] The problems associated with TBDMS group are rather long coupling times (*ca.* 10 min), lack of regio-selectivity in its introduction, and base-catalyzed migration[67] in Scheme 1.3(a). Despite the ease of migration, relatively pure monomeric phosphoramidites (R=TBDMS in **33**, Figure 1.8) with a very small quantity of isomeric 3'-*O*-TBDMS-2'-phosphoramidites are commercially available and have served well in the solid phase RNA synthesis.

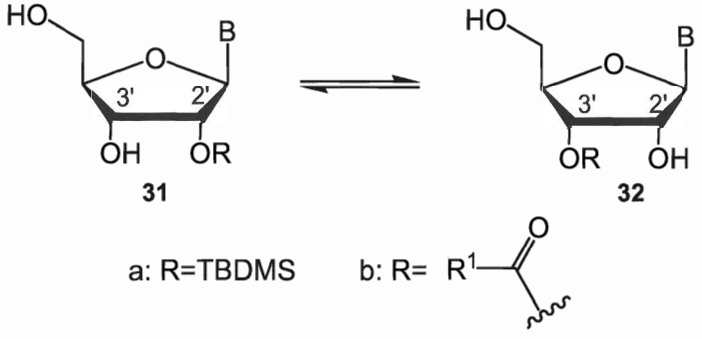

Scheme 1.3: Base-catalyzed migration of TBDMS protected ribonucleotides

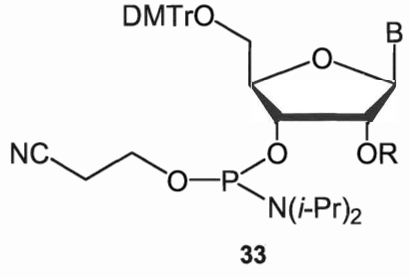

Figure 1.8: RNA phosphoramidite building blocks

1.5.2 Base labile protecting groups

Acyl groups are the most common base-labile protecting groups for 2'-hydroxy functions. The use of base-labile protecting group is very limited because acyl groups very readily undergo base-catalyzed migration[68] as shown in Scheme 1.3(b).

1.5.3 Acid labile protecting groups

The use of acid-labile 2'-protecting groups has the considerable advantage of being stable under the basic conditions which are used to remove the protecting groups from the nucleoside residues and the internucleotide linkages, as well as to cleave the fully-assembled RNA sequences from solid support.

DMTr **20** (Scheme 1.1) group has been used for the temporary protection of 5'-hydroxy functions in most solid phase synthesis of oligoribonucleotides. Obviously, if the acid-labile groups are to be used to protect 2'-hydroxy functions, they must be compatible with the 5'-hydroxy DMTr protecting groups and be readily removable under the mildest possible conditions of acidic hydrolysis in the final deblocking step. Acetal protecting groups are most commonly used acid-labile 2'-protecting group with the advantages in that they can be introduced regiospecifically to the 2'-hydroxy function of a ribonucleoside derivative and, once in place, they do not migrate.

1.5.3.1 Thp and Mthp

Tetrahydropyran-2-yl (Thp) group **34** (Figure 1.9) was the first acid-labile 2'-protecting group investigated.[69] The cleavage and migration of the 2'-*O*-Thp uridine dinucleotide were found to occur in a negligible extent under the deprotection conditions (pH 2.0). Later, the Thp group was abandoned due to its chirality. Soon after, the achiral 4-methoxytetrahydropyran-4-yl (Mthp) protecting group **35** (Figure 1.9) was developed.[70] The Mthp group is more than twice as labile as the Thp group at pH 2.0. However, both Thp and Mthp groups can not withstand repeated exposure to the relatively drastic acidid conditions used for detritylation in oligonuceotide synthesis on a solid support. A series of studies were followed in order to pursue suitable 2'-hydroxyl protecting groups which are compatible to the use of 5'-DMTr group and removable under conditions similar to those required for the cleavage of the Mthp group.

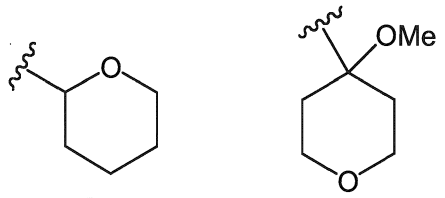

34 **35**

Thp Mthp

Figure 1.9: Acid labile protecting groups: Thp and Mthp

1.5.3.2 Acetals with a piperidine moiety

In the pioneer studies on the design of protection groups for 2'-hydroxyl function in chemical synthesis of oligonucleotides, Reese and co-workers[71] found that the rate of acid-catalyzed hydrolysis of acetal systems (Scheme 1.4) is very sensitive to the inductive effect of the atom or group X. The sulfone acetal ($X=SO_2$ in **36**) is less acid labile than the Mthp (X=O in **36**) group; in contrast, the sulfur-containing protecting group (X=S in **36**) is more acid labile than Mthp group.

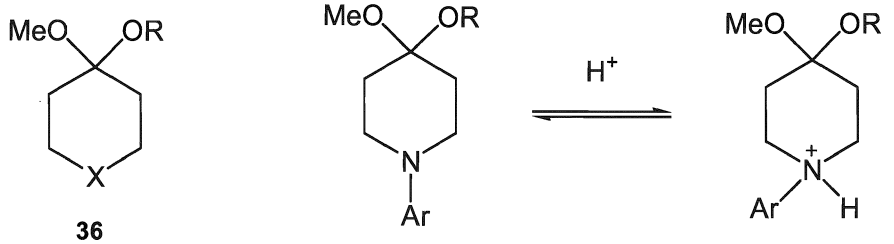

36 **37** **38**

Scheme 1.4: Acid-catalyzed hydrolysis of acetal systems

In a typical acetal system, the rate of hydrolysis is pH dependant and increases logarithmically with decreasing pH which were observed in the unblocking of Thp and Mthp groups.[72] Designing an acetal system which has virtually pH independent hydrolysis properties in the pH range of 0–2.5 led to the discovery of the acetal systems with piperidine moiety.

In a 1-arylpiperidin-4-one acetal system, the weakly basic tertiary amine function (pKa *ca.* 2) has this desired property. It would be largely protonated **38** in the presence of excess of trichloroacetic acid (pKa 0.66) during the 'detritylation' step and largely

unprotonated **37** (Ar = aryl, Scheme 1.4) during the final deblocking step (above pH 3). The difference in the inductive effect of the protonated *N*-aryl group **38** and the unprotonated *N*-aryl group **37** would result in the rate hydrolysis of the acetal being several orders of magnitude faster than that of the acetal in its conjugate acid. It can be concluded that the rate of hydrolysis of acetal system should be pH independent within a specific pH range from somewhere below to somewhere above the pKa of the tertiary amino function. Carefully choosing aryl constituent would ensure that rate of acetal hydrolysis is pH independent in the desired range of pH.

1.5.3.2.1 Ctmp

l-(2-Chloro-4-tolyl)-4-methoxypiperidin-4-yl (Ctmp) **39** (Figure 1.10) is the first piperidine acetal system used for the protection of 2'-hydroxyls in oligoribonucleotide synthesis.[72] The rate of acetal hydrolysis hardly changes between pH 0.5–2.0. In addition, this 1-arylpiperidin-4-one acetal system has an acid lability similar to that of Mthp group **35** under mild acidic conditions (pH 2.0–2.5, room temperature). These findings proved that Ctmp group **39** meets the requirements of 2'-hydroxy protecting groups, *i.e.* stable under the acidic conditions required for the detritylation step and removable under mild acid conditions.

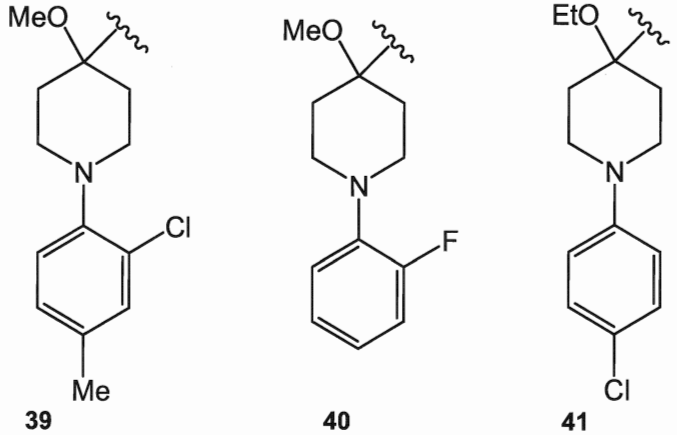

Figure 1.10: Acetals with a piperidine moiety

1.5.3.2.2 Fpmp

Although Ctmp **39** is an effective group for protecting 2'-hydroxyl function in RNA synthesis, the original development of the Ctmp **39** was limited by the difficulty in the preparation of the enol ether reagent **45a** (Scheme 1.5) required for the introduction of the Ctmp protecting group. Subsequent studies on the synthesis of the enol ether reagents **45** led to the development of 1-(2-fluoropheny1)-4-methoxypiperidin-4-yl (Fpmp) **40** (Figure 1.10).[73] The enol ether reagents required for the introductions of Ctmp **39** and Fpmp **40** protecting groups can be prepared using the general method[74] illustrated in Scheme 1.5a and Scheme 1.5b, respectively. As a halogenated piperidinyl protecting group, the Fpmp has almost the same hydrolysis properties as Ctmp protecting group. Studies suggest that Fpmp is able to withstand the acidic conditions required for detritylation and it is readily removable at pH 3.0 without detectable migration or cleavage of the internucleotide linkages.[75] Fpmp has been used successfully in the preparation of the protected ribonucleoside building blocks in the solid phase synthesis.

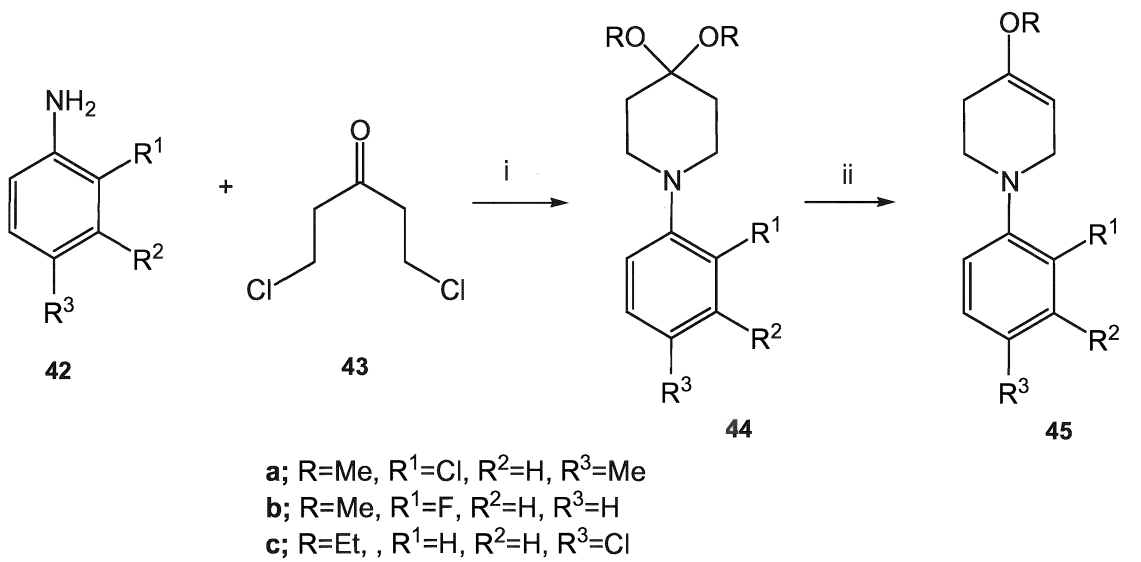

Scheme 1.5: Preparation of enol ether reagents. *Reagents and conditions*: i, (a) $TsOH{\cdot}H_2O$, ROH, reflux, 1.5 h; (b) $(RO)_3CH$, reflux, 30 min; ii, $(i\text{-}Pr)_2NEt$, $Et_2O{\cdot}BF_3$, CH_2Cl_2, 0°C.

1.5.3.2.3 Cpep

Althgouh there is no doubt that Fpmp **40** is suitable for the protection of 2'-hydroxy functions in the chemical synthesis of RNA sequences, it is evident that the internucleotide linkages of certain RNA sequences readily undergo cleavage and migration under even very mild acidic conditions for unblocking Fpmp protecting group (pH 2.0–2.5). Therefore, it would be beneficial if 2'-protecting group is removed at or above pH 3.25.[75] Ideally, a 1-aryl-4-alkoxypiperidin-4-yl protecting group should be as stable as Fpmp group at pH 0.5 but more labile at pH 3.5 or higher. Among the fourteen piperidinyl protecting groups examined, the 1-(4-chlorophenyl)-1-ethoxypiperidin-4-yl (Cpep) group **41** (Figure 1.10) had advantages over the others including Fpmp.[75]

The Cpep protecting group has a better acid hydrolysis profile (Figure 1.11) than the Fpmp group.[75] Compared with Fpmp, Cpep is more stable to acidic hydrolysis in the pH range of 0.5 to 2.0 but more than twice as labile at pH 3.75. Thus, rate of hydrolysis of Cpep at pH 3.75 is only 3.73 times slower than at pH 0.5. The half-life of hydrolysis of 2'-*O*-Cpep-uridine is only 170 min versus 266 min for Fpmp at pH 3.75 and 30°C, so that it can be removed in approximately one-half of the time required for deblocking Fpmp under the same conditions. The half-life of hydrolysis of 2'-*O*-Cpep-uridine is almost pH independent in the range of pH 0.5–2.5.

In addition, preparation of Cpep group precursor is straightforward.[74] The enol ether precursor, 1-(4-chlorophenyl)-4-ethoxy-1,2,5,6-tetrahydropyridine (**45a**) can be prepared from 4-chloroaniline in two-steps in 90% overall yield (Scheme 1.5a).

The 2'-*O*-Cpep protected phosphoramidites (R=Cpep in **33**) can be prepared in the traditional approach. Complete removal of the 2'-protecting groups at pH 4.4 and 35°C required *ca.* 7 and 4 h for r[$(Up)_{19}$U] protected at 2'-positions with Fpmp and Cpep, respectively. No migration or cleavage of internucleotide linkages was observed in either case. From this study, the Cpep group showed very promising properties in protecting 2'-hydroxy function in oligoribonucleotide synthesis.

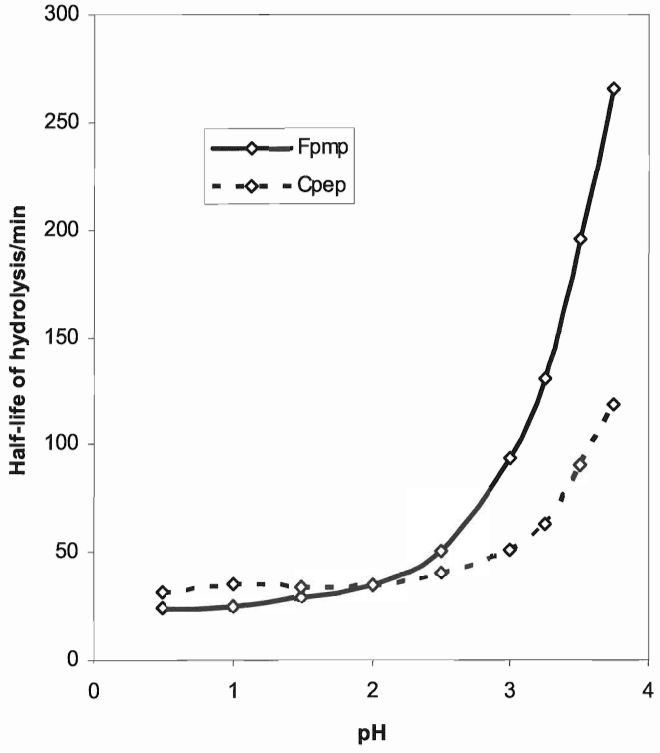

Figure 1.11: Dependence of the half-lives of hydrolysis at 30°C of the 2'-*O*-Fpmp- and 2'-*O*-Cpep-uridines on pH

1.5.4 Protected protecting groups

1.5.4.1 Nitrobenzyloxymethyl (NBOM)

Nitrobenzyloxymethyl (NBOM) groups **46** were developed to relieve the steric crowding in the vicinity of the phosphoramidite function by incorporating a flexible arm into the structure at the 2-OH.[76-78] In the 2-nitrobenzyloxymethyl (2-NBOM) **46a** and 4-nitrobenzyloxymethyl (4-NBOM) **46b** groups, formaldehyde acetal linkers were used to connect the bulky 2-nitrobenzyl to 2'-*O* position of ribonucleosides. Introduction of 2'-*O*-NBOM group led to coupling yields of over 98% under DNA coupling conditions. The 2'-*O*-(2-NBOM) group could be removed by UV photolysis at pH 3.7;[76] and the 2'-*O*-(4-NBOM) group could be removed by treatment with TBAF.[77] Recently, Beaucage *et al.* reported that the convertion of 4-nitro group to 4-amino group in 2'-*O*-(4-NBOM) facilitated the cleavage of 2'-*O*-acetal in 0.1 *M* AcOH.[78]

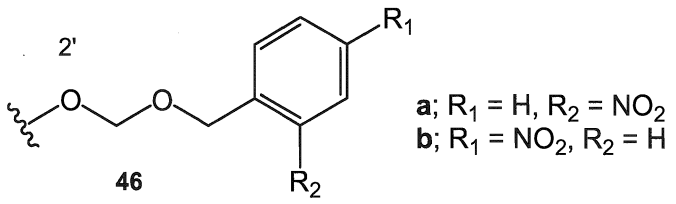

2'-*O*-NBOM

1.5.4.2 Bis(2-acetoxyethoxy)methyl (ACE)

In the late 1990s, Scaringe *et al.* developed the 2'-*O*-ACE protecting group **48** (Scheme 1.7) for the RNA synthesis *via* the phosphoramidite chemistry.[79] In this approach, the 5'-hydroxy is protected with a silyl ether group (SIL) **47** (Figure 1.12) instead of a DMTr group. These silyl ether protecting groups could be removed with fluoride ions under neutral conditions which are compatible with an acid labile 2'-hydroxyl protecting group. In the ACE chemistry, the 3'-hydroxyl is phosphitylated as the methoxy *N,N*-diisopropylphosphoramidite **47** (Figure 1.12) because the cyanoethyl phosphoramidites are not compatible with fluoride reagents used for removal of 5'-*O*-SIL protecting group.

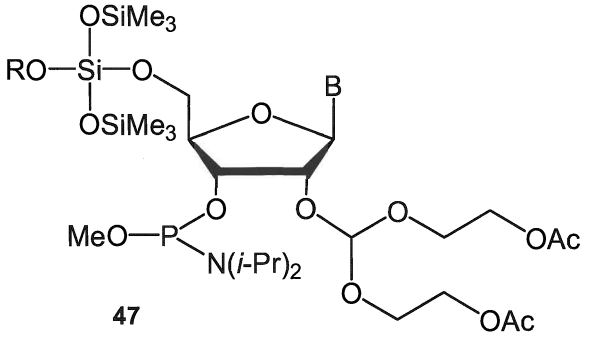

R=cyclooctyl or cyclododecyl

Figure 1.12: 5'-*O*-SIL-2'-*O*-ACE RNA phosphoramidite building blocks

As a protected protecting group, removal of ACE is achieved in two steps (Scheme 1.6). First, ACE **48** undergoes ester hydrolysis under basic conditions used for nucleoside base deprotection to result in 2'-*O*-bis(2-hydroxyethoxy)methyl orthoester **49** which is 10 times more acid labile than ACE itself. Then the 2'-*O*-bis(2-hydroxyethoxy)methyl orthoester **49** is completely removed under mild acidic conditions (pH 3, 10 min, 55°C).

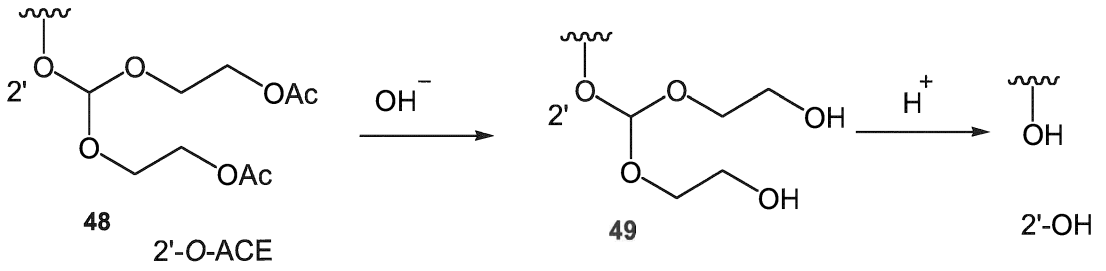

Scheme 1.6: Deprotection of 2'-*O*-ACE group

An advantage of this chemistry is that the ACE group proved to be stable in oligonucleotide synthesis, purification, and storage. However, the ACE strategy is not compatible with the conventional automated synthesizer. Substantial changes in synthetic cycle and reagents were required in order to incorporate the 5'-*O*-SIL-2'-*O*-ACE phosphoramidite building blocks **47** (Figure 1.12) in solid phase synthesis. Nevertheless, these phosphoramidite building blocks have been commercially available and widely used in custom synthesis of RNA sequences.

1.5.4.3 [(Triisopropylsilyl)oxy]methyl (TOM)

[(Triisopropylsilyl)oxy]methyl (TOM) group **50** (Scheme 1.7), a silyl-protected acetal, was first used to protect the 2'-hydroxy functions in Pitsch's Lab.[80] As a variant of TBDMS **30**, the TOM group **50** is deprotected in a two step process: (i) attack of Si-atom by fluoride ions results in cleavage of Si-O bond **51**; and (ii) addition of aqueous buffer solution results in fragmentation to free 2'-OH (Scheme 1.8).

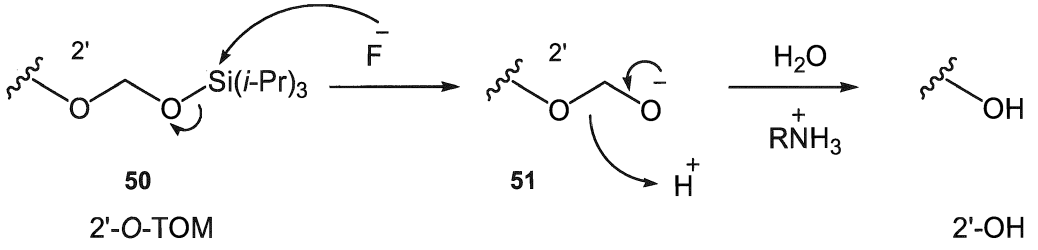

Scheme 1.7: Deprotection of 2'-*O*-TOM group

The TOM group has several advantages over TBDMS group. First, in contrast to TBDMS protecting group, TOM group does not migrate from the 2'-*O* to the 3'-*O* position. Therefore very pure phosphoramidites (R=TOM in **33**, Fugure 1.8) could be

prepared *via* this approach. Second, because of the minimal steric demand of the TOM group, excellent coupling yields of 99.5% with coupling time of 60-150s are obtained with 2'-*O*-TOM phosphoramidites. Furthermore, good stability of the 2'-*O*-TOM group allows for a variety of nucleobase, sugar, and backbone modifications in the preparation of the RNA sequences. However, TOM-protected oligoribonucleotides can not be purified by HPLC because of the hydrophobic nature of the silyl group.

1.5.4.4 2-(Trimethylsilyl)ethoxymethyl (SEM)

In order to improve the regioselectivity of 2'-*O*-protection and the slow coupling reaction, Sekine *et al.* developed the 2-(trimethylsilyl)ethoxymethyl (SEM) protecting group **52** (Figure 1.13) which could be removed by treatment with fluoride ion.[81] The regioselective introduction of the SEM group into the 2'-position was achieved in 78-84% yields. The corresponding 2'-*O*-SEM phosphoramidite building blocks were found to be more reactive than 2'-*O*-TBDMS protected amidites in the solid phase synthesis.

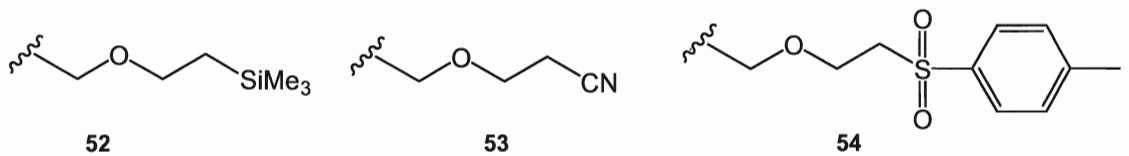

52 SEM **53** CEM **54** TEM

Figure 1.13: Protected protecting groups: SEM, CEM, and TEM

1.5.4.5 2-Cyanoethoxymethyl (CEM)

2-Cyanoethoxymethyl (CEM) **53** (Figure 1.13) is readily removable by treatment with 1 *M* TBAF/THF for several hours.[82] This formaldehyde acetal type protecting group posesses relatively less steric hindrance toward the vicinal 3'-phosphoramidite, therefore high coupling efficiency could be achieved. CEM method allows RNA synthesis with high coupling yields and gives products of high purity. Homo- and mixed-base RNA oligomers up to 55 bases in length have been synthesized *via* CEM chemistry with coupling yields greater than 99% in 60-150 s. Regio-selective introduction of 2'-*O*-CEM is still under investigation and the yields of the corresponding amidites need to be

optimized. Nevertheless, after suitable optimization, CEM method may have the potential for the synthesis of long RNA sequences.

1.5.4.6 2-(4-Tolylsulfonyl)ethoxymethyl (TEM)

Very recently Chattopadhyaya *et al.* introduced the 2-(4-tolylsulfonyl)ethoxymethyl (TEM) **54** (Figure 1.13) as a new 2'-OH protecting group for solid phase RNA synthesis using phosphoramidite chemistry.[83] As a 2'-OH protecting group with a formaldehyde acetal linker, TEM was developed based on the modulation of the CEM group. It was found that the TEM group can be removed with TBAF in 5 min at room temperature. The TEM chemistry allows for relatively fast coupling reactions (120 s) to give relatively high average coupling yield (97-99%).

1.5.4.7 4-(*N*-Dichloroacetyl-*N*-methylamino)benzyloxymethyl

Recently Beaucage reported the use of 4-(*N*-dichloroacetyl-*N*-methylamino) benzyloxymethyl group **55** (Scheme 1.9) for 2'-hydroxyl protection in solid phase synthesis of RNA sequences *via* phosphoramidite chemistry.[84] 4-(*N*-Dichloroacetyl-*N*-methylamino)benzyloxymethyl **55** is also a protected protecting group. 4-(*N*-Dichloroacetyl-*N*-methylamino)benzyl alcohol was used for the preparation of the corresponding phosphoramidite building blocks. RNA phosphoramidites protected with a 4-(*N*-dichloroacetyl-*N*-methylamino)benzyloxymethyl group for 2'-*O*-protection allow rapid and efficient solid-phase RNA synthesis. It was reported that average coupling yields of 99% with 5-ethylthio-1*H*-tetrazole as an activator and 3 min coupling resulted in high quality products without purification, which is comparable to standard solid-phase DNA synthesis.

N-Dichloroacetyl groups were cleaved under aqueous ammonium treatment which was used for the cleavage of nucleobase and phosphate protecting groups (Scheme 1.8). Consequently, the resulting 2'-*O*-(4-MABOM)-protected RNA oligonucleotide **56** was released from the solid support. The 2'-*O*-(4-MABOM) group was completely removed by treatment with 0.1 *M* AcOH (pH 3.8) in the presence of *N,N,N',N'*-

tetramethylethylenediamine at 90°C for 30 min without significant internucleotidic chain cleavage and migration (Scheme 1.9).

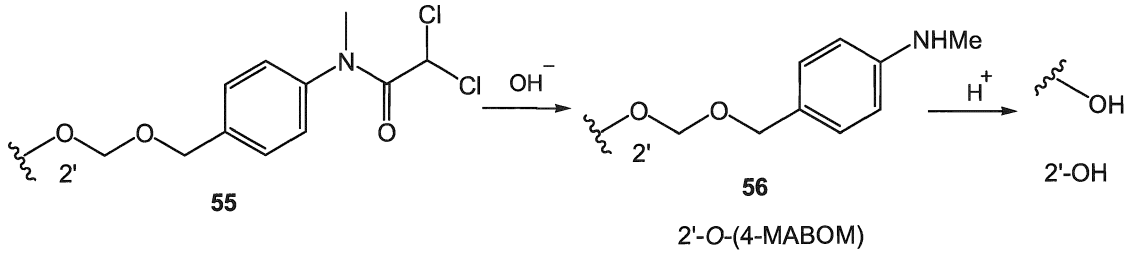

Scheme 1.8: Deprotection of 4-(*N*-dichloroacetyl-*N*-methylamino)benzyloxymethyl group

Although the 4-(*N*-dichloroacetyl-*N*-methylamino)benzyloxymethyl group **55** allows for highly efficient coupling and facile deprotection, methods for convenient preparation of the four RNA building blocks still need to be optimized.

1.6 Objectives of this thesis

The principal aim of this thesis is to use specific glycosylation of synthetic RNA sequences to improve their stability, allow for specific cell targeting, and enhance their cellular uptake by addressing the following objectives:

1) To synthesize RNA sequences by solid phase phosphoramidite chemistry using Cpep to protect 2'-hydroxyls;
2) To establish a conjugation chemistry for the preparation of carbohydrate–RNA conjugates;
3) To evaluate the effects of glycosylation on the stability of RNA molecules;
4) To synthesize and evaluate pyrene- and phenanthrene-based fluorescent ribosides.

Chapter 2 - Results and Discussions

2.1 General strategy

In this study, we aimed to use specific glycosylation of synthetic siRNA sequences to improve stability, specificity, and cellular uptake. The general strategy to achieve carbohydrate–RNA conjugates involved using 3,4-diethoxy-3-cyclobutene-1,2-dione (diethyl squarate)[85] **57** as the linking reagent. We previously reported a method that allows for easy incorporation of carbohydrate moieties into oligodeoxynucleotides under mild conditions.[86] In this approach, a glycan moiety **58** containing an amino group reacts with diethyl squarate to form an activated glycan **59**, which further reacts with an oligonucleotide **60** to form a glycoconjugate **61** under slightly basic conditions (Scheme 2.1).

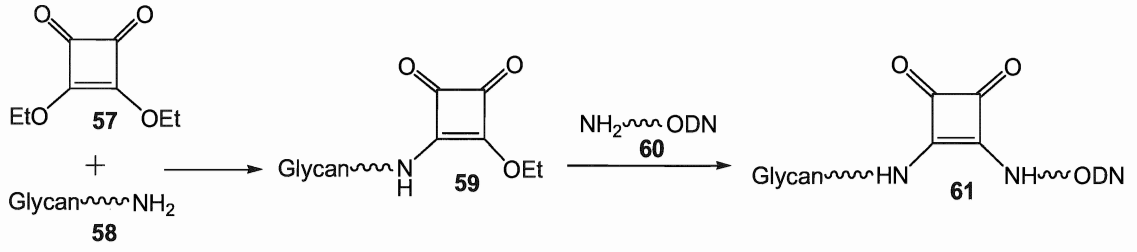

Scheme 2.1: Squarate linker in the synthesis of glycosylated oligodeoxyribonucleotides

In the current project, the dendritic cell was chosen as the target cell type to evaluate the impact of carbohydrate-derivatization on the bioavailability and silencing efficiency of siRNA. Dendritic cells (DCs) are potent antigen presenting cells and play important roles in the immune system. Lectins on dendritic cells are relatively well characterized.[87, 88] Since the target lectins express macrophage mannose receptors, mannosides were chosen as glycan moieties and designed to be covalently attached to synthetic RNA sequences *via* diethyl squarate linker **62**.

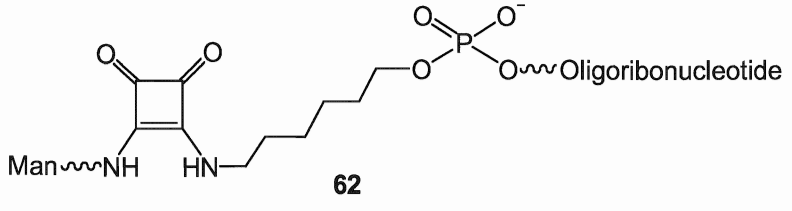

62

2.2 Synthesis of squarate-activated monovalent mannosides

Fully-protected 2'-chloroethyl mannoside **67** was prepared from mannose **63** *via* the trichloroacetimidate chemistry.[89] The subsequent substitution by sodium azide gave fully-protected 2'-azidoethyl mannoside **68** (Scheme 2.2). Deacetylation of **68** followed by catalytic hydrogenation afforded the fully deprotected 2'-aminoethyl mannoside **69** (Scheme 2.2). Catalytic hydrogenation of fully-protected 2'-azidoethyl mannoside **68** in the presence of trifluoroacetic acid (TFA) gave the trifluoroacetate salt of fully-protected mannoside **70**. In the reaction, TFA was added to avoid the acetyl migration.

The trichloroacetimidate method[89] is a widely applicable procedure for formation of glycosidic bonds. In this approach, the anomeric hydroxyl of a suitably protected saccharide is treated with trichloroacetonitrile under basic conditions to give a glycosyl trichloroacetimidate. The glycosylation step is then effected by a Lewis acid. The stereochemical outcome of trichloroacetimidate formation is subjected to both kinetic and thermodynamic control. The thermodynamically more stable α-trichloroacetimidate can be obtained using a strong base such as DBU. If glycosylation is carried out in nonpolar solvents at low temperatures, SN^2-type reactions can be frequently carried out; thus α-trichloroacetimidate yield β-glycosides. This approach was successfully used to generate β-2-aminoethyl glucosides and β-2-aminoethyl lactosides in our lab.[86] However, in the present study, α-2-aminoethyl mannoside **69** was obtained when glycosylation was effected by boron trifluoride. The difference in anomeric stereochemistry of mannosides, glucosides and lactosides is due to the neighbouring 2-*O*-acetate participation. 2-*O*-Acetate protecting group interacts with the glycosyl cation and thus effectively blocks the β-face, leading to the formation of α-mannosides (Scheme 2.3).

The anomeric stereochemistry of α-2-aminoethyl mannoside **69** is evident based on the following NOE observations: lack of NOEs between H-1' and H-3', and H-1' and H-5', which were observed in the β-anomers.

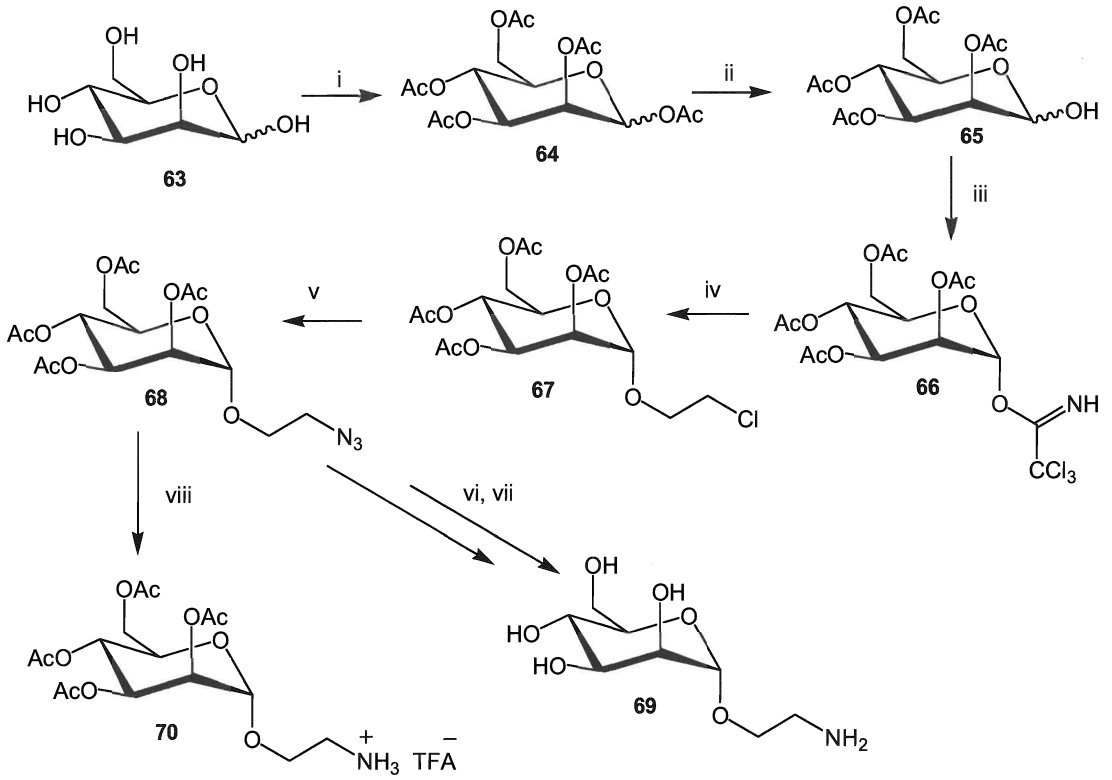

Scheme 2.2: Preparation of 2'-aminoethyl mannosides. *Reagents and conditions*: i, $(Ac)_2O$, C_5H_5N, r.t., 24 h; ii, $NH_2NH_2{\cdot}H_2O$, AcOH, DMF, r.t., 45 min, 64.1% over 2 steps; iii, Cl_3CCN, CH_2Cl_2, DBU, 0°C, 35 min, 79.8%; iv, $BF_3{\cdot}Et_2O$, $HOCH_2CH_2Cl$, 71.5%; v, NaN_3, DMF, 55°C, 3 d, 95.3%; vi, NaOMe, MeOH, 30 min; vii, Pd/C, H_2, H_2O, r.t., 6 h, 66.9% over 2 steps; viii, Pd/C, H_2, MeOH, r.t., 6 h, quatitative.

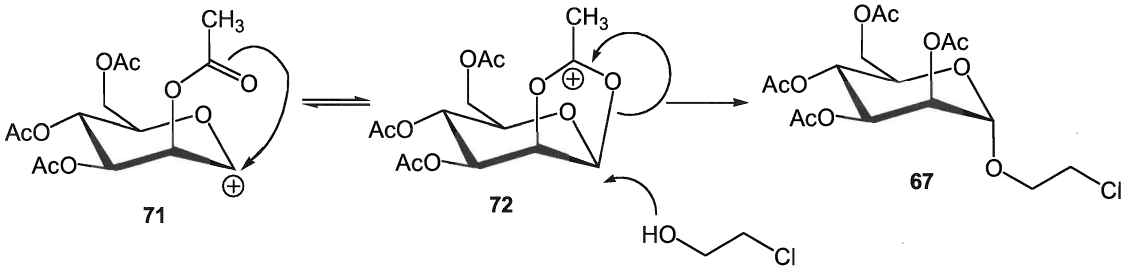

Scheme 2.3: 2-*O*-Acetate participation in glycosylation

The reaction between the α-2-aminoethyl mannoside **69** and diethyl squarate **57** was carried out in aqueous methanol solution in the presence of trace amount of triethylamine

[86] (Scheme 2.4). The product **73** was purified by size exclusion chromatography on Bio-Gel P_2 gel eluted with milliQ water.

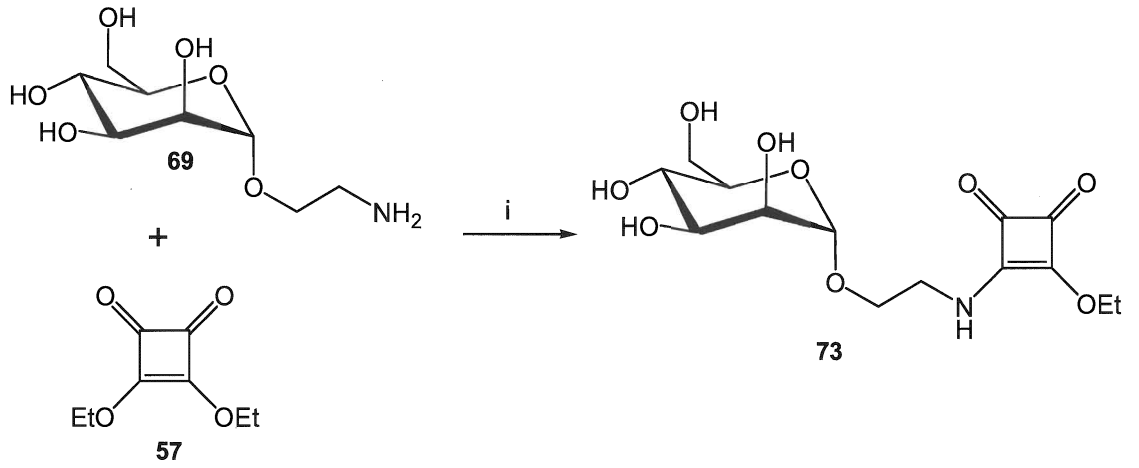

Scheme 2.4: Synthesis of squarate-activated monovalent mannosides. *Reagents and conditions*: i, H_2O, MeOH, NEt_3, r.t., 5 min, 41.4%.

2.3 Synthesis of squarate-activated bivalent mannosides

Because the interaction between glycans and their receptor lectins is relatively weak, it is desirable to introduce multivalent mannosides in order to enhance the cluster glycoside effect.[90] Therefore, bivalent mannosides were synthesized in order to increase the binding affinity between mannosylated siRNAs and lectins. The synthesis of bivalent mannosides was achieved by peptide coupling of a bivalent linker **76** with acetate protected aminoethyl mannoside **70** (Scheme 2.6).

Bis-carboxylic acid linker **76** was prepared in two steps in a total yield of 63% (Scheme 2.5). Tris(2-aminoethyl)amine **74** was used as the core structure. First, one amino group of tris(2-aminoethyl)amine was protected by benzyloxycarbonyl (Cbz) group **75**. Upon addition of succinic anhydride, the bis-carboxylic acid linker **76** was obtained *via* amide bond formation.

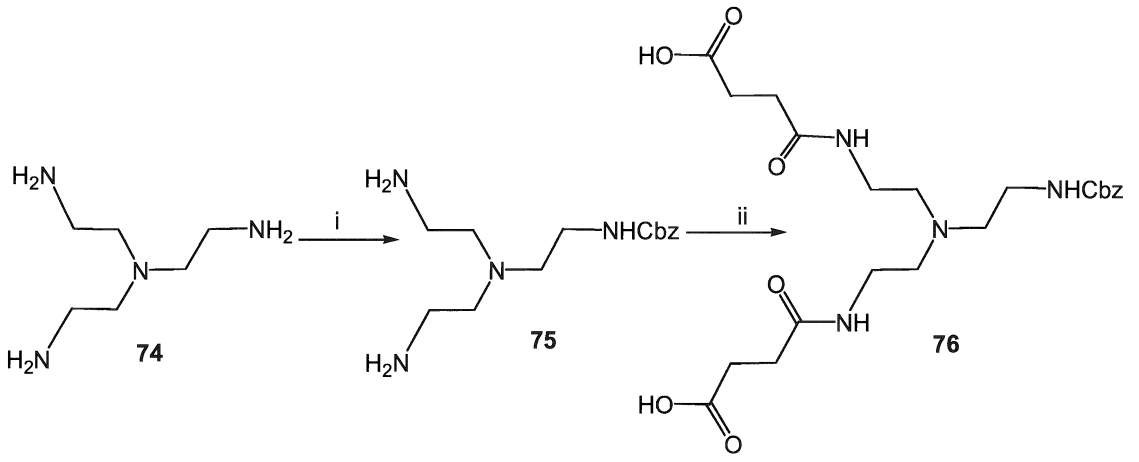

Scheme 2.5: Preparation of bivalent linker. *Reagents and conditions*: i, $PhCH_2OCOCl$, CH_2Cl_2, 74.4%; ii, succinic anhydride, C_5H_5N, 84.3%.

Peptide coupling of the bivalent linker **76** with acetate-protected aminoethyl mannoside **70** was first attempted using dicyclohexylcarbodiimide (DCC) as the activator and *N*-hydroxy succinimide or 1-hyroxyl benzotriazole (HOBT) to trap DCC-activated carboxylic acid. However, formation of the desired amide bond was not observed. (Benzotriazol-1-yloxy)tris(dimethylamino)phosphonium hexafluorophosphate (BOP) **78** (Scheme 2.6),[91] a derivative of HOBT, in the presence of the Hünig's base, led to amide bond formation in a moderate yield (52.5%).[92]

Removal of the acetates and Cbz groups from fully-protected bivalent mannoside **77** gave the fully-deprotected bimannoside **79** bearing a primary amino function, which was subsequently treated with diethyl squarate. The product, squarate-activated bivalent-mannoside **80,** was readily purified by size exclusion chromatography on a Bio-Gel P2 column. The purified product was now ready for conjugation with oligoribonucleotides.

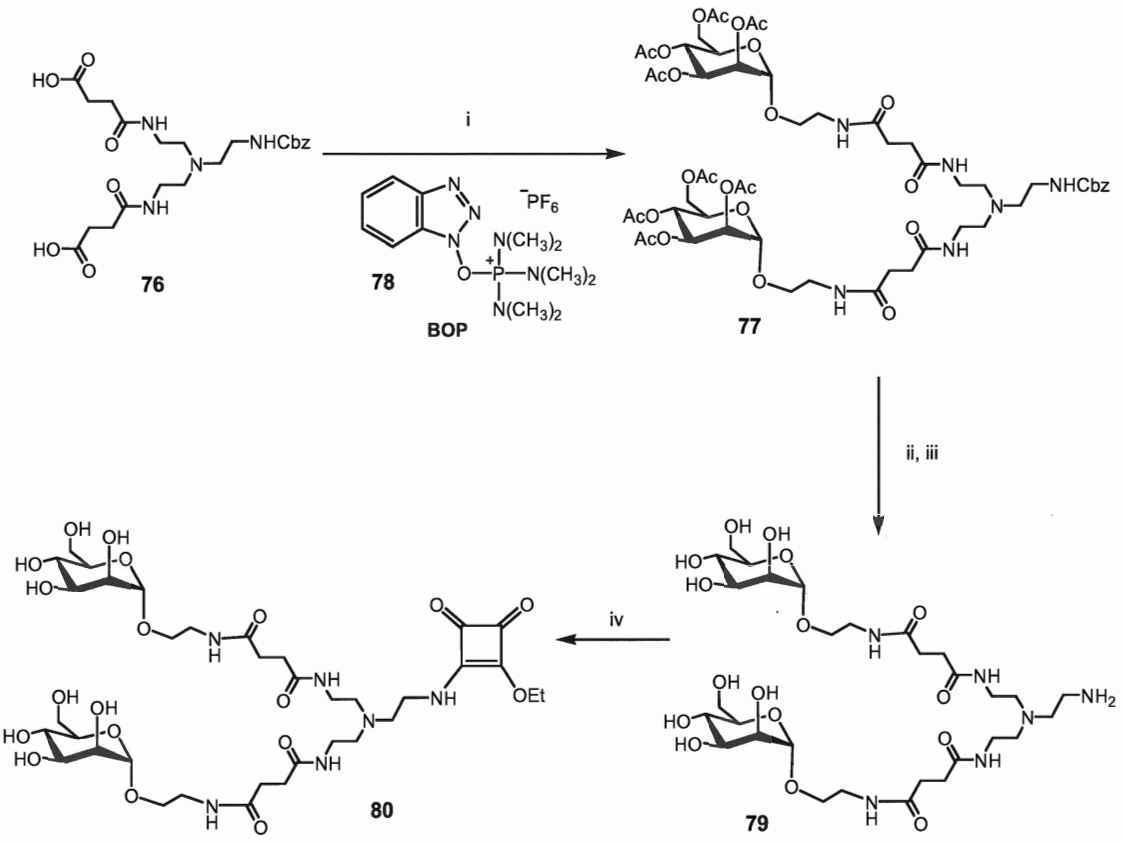

Scheme 2.6: Preparation of squarate-activated bivalent mannosides. *Reagents and conditions* i, **70**, BOP, (*i*-Pr)$_2$NEt, CH_2Cl_2, 52.5%; ii, NaOMe, MeOH; iii, Pd/C, H_2, MeOH, 96.2%; iv, H_2O, MeOH, NEt_3, r.t., 7 min, 55.6%.

2.4 Synthesis of oligoribonucleotides

Oligoribonucleotides were prepared by solid phase phosphoramidite chemistry using the 1-(4-chlorophenyl)-4-ethoxypiperidin-4-yl **41** (Cpep) to protect the 2'-hydroxyls. The Cpep chemistry was chosen because it allows for stable oligoribonucleotide "precursor", i.e. oligoribonucleotides protected at 2'-*O* with Cpep, to be prepared for conjugation with carbohydrates.

2-Cyanoethyl-*N*,*N*-diisopropylphophoramidites **33** are commonly used phosphoramidite RNA monomers. However, the coupling reactions proceed relatively slowly when the Cpep is used to protect the 2'-hydroxyl function due to steric hindrance (Yan, H.; Tram,

K. *unpublished results*). Previous studies in our lab have examined a series of phosphoramidite derivatives from secondary amines. It was found that 2-cyanolethyl-*N,N*-diethylphophoramidites as RNA monomers **88** are more reactive than the corresponding *N,N*-diisopropylphophoramidites **33** and possess reasonable shelf-lives (Yan, H.; Tram, K. *unpublished results*). In this regard, when 2-cyanolethyl-*N,N*-diethylphophoramidites were used, the coupling time was effectively reduced from 10 to 2 min. Therefore, *N,N*-diethylphosphoramidites **88** instead of the more traditional *N,N*-diisopropylphosphoramidites **33** were used in this study. The 2'- and 5'-hydroxyls of the RNA monomers were protected by the Cpep **41** and DMTr **20**, respectively (Scheme 2.8). Adenine, cytosine, and guanine residues were protected as 6-*N*-pivaloyladenine (**b**, Scheme 2.8), 4-*N*-benzoylcytosine(**c**, Scheme 2.8), and 2-*N*-phenylacetylguanine (**d**, Scheme 2.8), respectively, and uracil (**a**, Scheme 2.8) was left unprotected. Uridine **84a**, 4-*N*-benzoylcytidine **84c**, and 6-*N*-pivaloyladenosine **84b** were commercial products from Rasayan Inc. 2-*N*-Phenylacetylguanosine **83** was obtained by treatment of 2',3',5'-*O*-triacetyl guanosine[93] **82** with phenylacetyl chloride followed by deacetylation (Scheme 2.7).

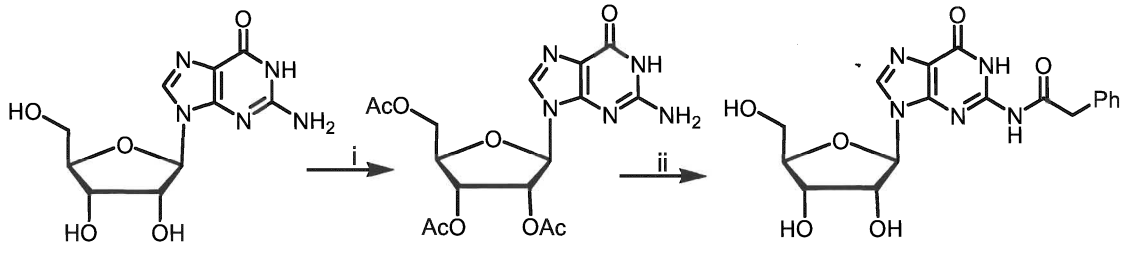

Scheme 2.7: Preparation of 2-*N*-phenylacetylguanosine. *Reagents and conditions*: i, DMF–C_5H_5N (2:1, v/v), $(Ac)_2O$, r.t. 1 h, then 75°C, 2 h, 85.4%; ii, phenyl acetylchloride, CH_3CN–C_5H_5N (3:1, v/v), 60°C, overnight, 23.3%.

The preparation of RNA phosphoramidite building blocks **88** is illustrated in Scheme 2.8. First, 5'- and 3'-hydroxyls of ribonucleosides **84** were temporarily protected with 1,1,3,3-tetraisopropyldisiloxyl group (TIPDS) **85**, followed by introduction of Cpep at 2'-hydroxyl. After removal of TIPDS from **86**, the DMTr group was introduced at the 5'-

position.* The 2'-*O*-Cpep-5'-*O*-DMTr ribonucleosides **87** were then converted to corresponding phosphoramidites **88** by treatment with 2-*O*-cyanoethyl-*N*,*N*-diethyl phosphorochloridite.

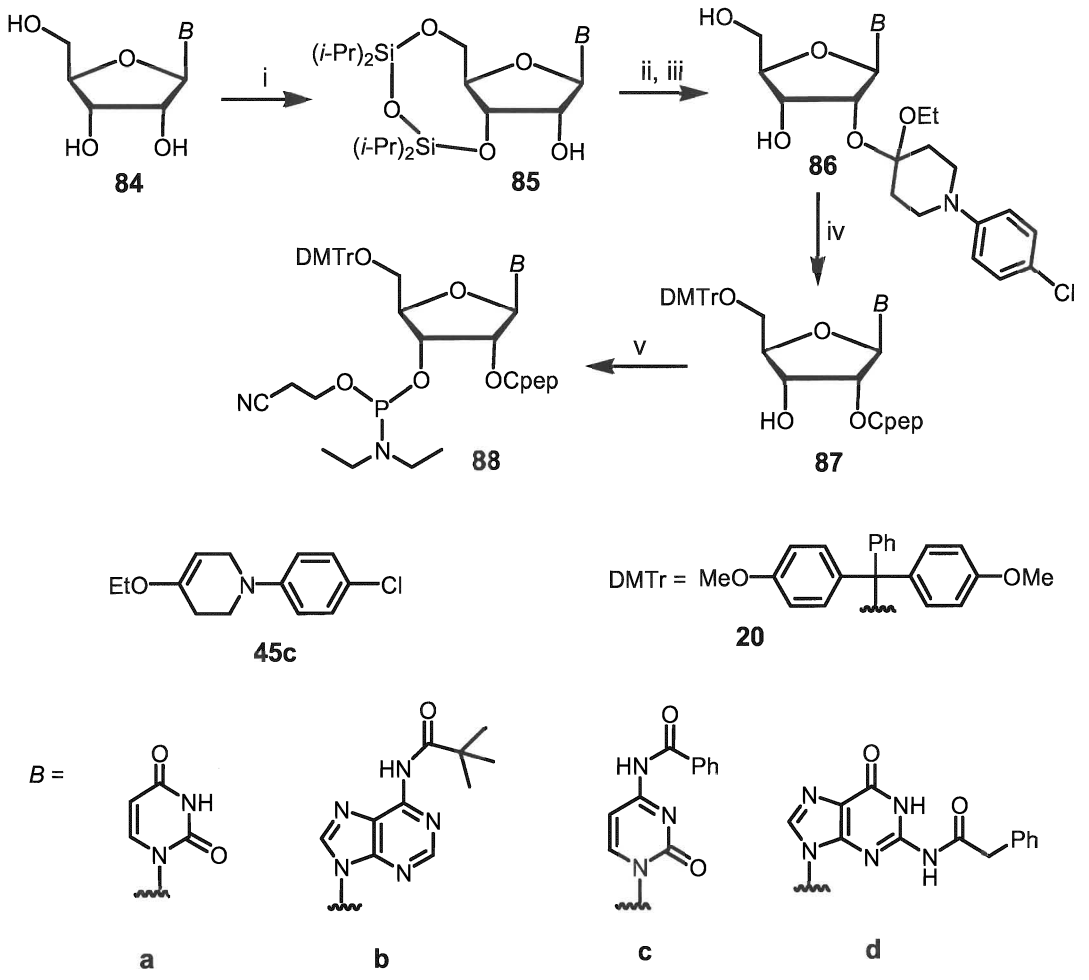

Scheme 2.8: Preparation of the RNA phosphoramidite building blocks. *Reagents and conditions*: i, (*i*-Pr)Si(Cl)OSi(Cl)(*i*-Pr), C_5H_5N, 80-90%; ii, **45c**, CF_3COOH, CH_2Cl_2,; iii, $Et_4N^+F^-$, CH_3CN, 80-90% over two steps; iv, DMTr-Cl, C_5H_5N, >90%; v, $CNCH_2CH_2OP(Cl)NEt_2$, $(i\text{-}Pr)_2NEt$, CH_3CN, 70-90%.

* 2'-*O*-Cpep-5'-*O*-DMTr 6-*N*-pivaloyladenosine and 2'-*O*-Cpep-5'-*O*-DMTr uridine were prepared by Kha Tram.

The purified 2-*O*-cyanoethyl-*N*,*N*-diethylphosphoramidites **88a**, **88b**, **88c**, and **88d** were characterized by ^{1}H and ^{31}P NMR. The ^{31}P NMR spectra (Figure 2.1) indicated that the purities of all RNA phosphoramidite building blocks are over 95% in all four cases.

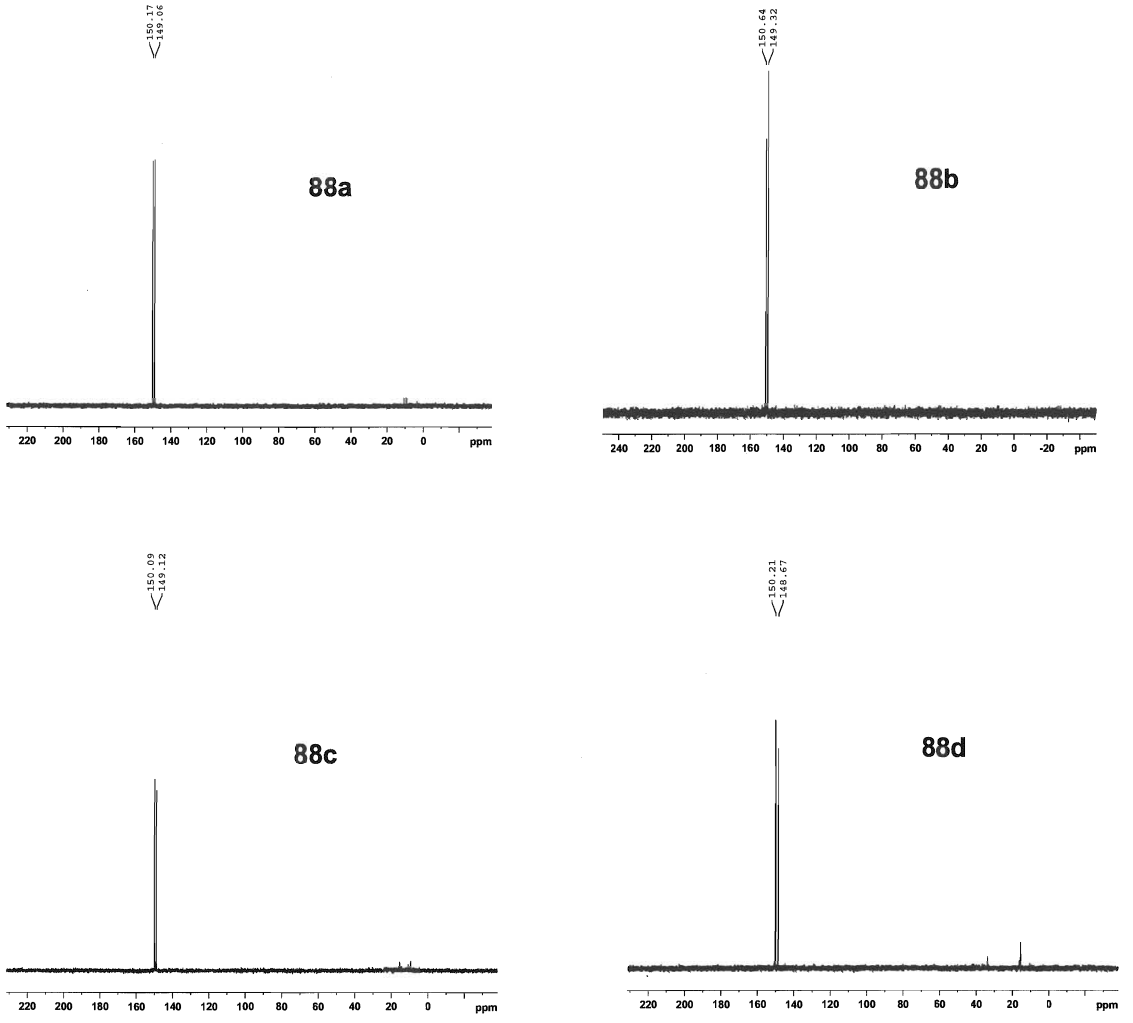

Figure 2.1: The ^{31}P NMR spectra of the RNA phosphoramidte building blocks

In our study, the amino modifier linkers were chosen because they can be coupled to the 5'-end of RNA sequences as a final step in solid-phase synthesis *via* phosphoramidite chemistry. C_6-amino modifier phosphoramidite building block **92** was synthesized in two steps (Scheme 2.9).* In the first, the amino group of 6-amino-1-hexanol **90** was

* Although this phosphoramidite is commercially available, we chose to prepare our own due to its relatively poor stability.

protected as trifluoroacetamide using a method reported in the literature.[94] The reaction of 6-trifluoracetamidohexanol **91** with 2-*O*-cyanoethyl-*N,N*-diisopropylphosphorochloridite gave the C_6-amino modifier phosphoramidite **92** as a colorless oil after purification by column chromatography. The amino modifier amidite **92** was analyzed by ^{31}P NMR which indicated purity of over 98% (Scheme 2.9).

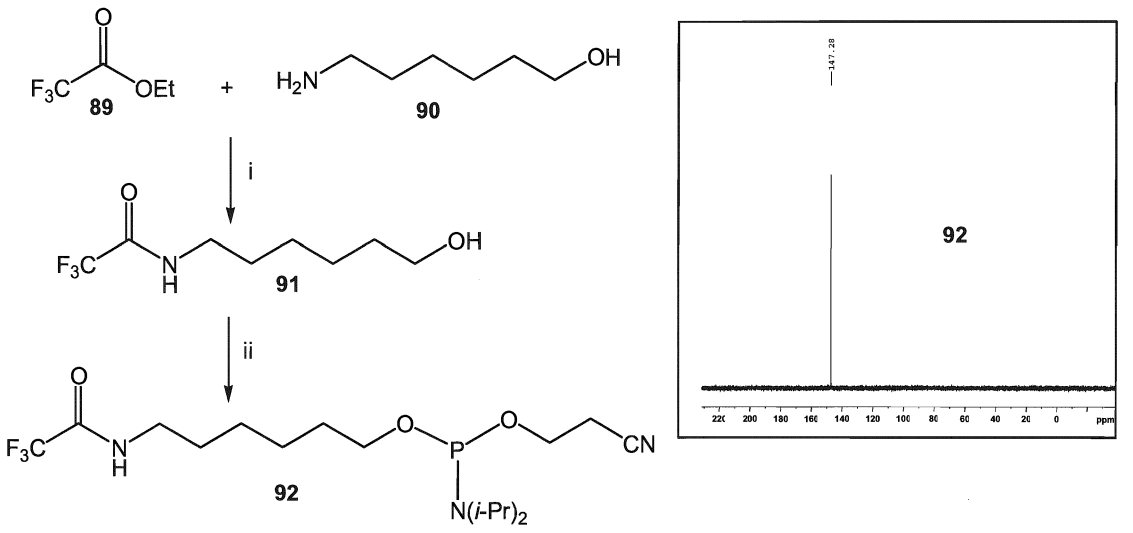

Scheme 2.9: Preparation of C_6-amino modifier phosphoramidite building block and ^{31}P NMR spectrum of **92**. *Reagents and conditions*: i, CH_2Cl_2, r.t., 3 h, 87.1%; ii, $CNCH_2CH_2OP(Cl)N(i\text{-}Pr)_2$, $(i\text{-}Pr)_2NEt$, CH_2Cl_2,15 min, r.t., 57.8%.

Oligoribonucleotide sequences were assembled by solid phase synthesis on an ABI 3400 DNA synthesizer. After the synthesis was complete, oligoribonucleotides were cleaved from CPG solid supports by incubation in concentrate ammonium hydroxide at 55°C for 12 h. This treatment also removed the cyanoethyl protecting groups for the internucleotide linkages, the acyl protecting groups for the base, and the trifluoroacetyl protecting group for the C_6-amino modifier. The crude 2'-protected RNA sequences were analysed by ESI-Mass.

Several conditions were investigated for the removal of Cpep groups. Cpep groups were found to be completely removed under the following two conditions: (1) *N,N*-dimethylacetamide (DMA)–triethylammonium formate (TEAF) buffer (pH 3.75) (2:3

v/v), 12 h, 40°C; (2) DMA–TEAF buffer (pH 2.52) (3:2 v/v), 6 h, 40°C. The latter condition was used in the following studies to remove the Cpep groups.

Some physical data of synthesized oligoribonucleotides are summarized in the Table 2.1. U_{10} homo decamers were used as model RNA sequences to establish the conjugation chemistry. The decamers were modified at the 5'-terminus using the standard phosphoramidite chemistry by a C_6-amino modifier **92**. Amino modified U_{10} homo decamers were used to conjugate with squarate-acitived mannosides **73** and **80**, respectively. Unmodified U_{10} homo decamers (U_{10}) **98** were used as a non-glycosylated control for the stability studies. A_{10} homo decamers (A_{10}) **99** were used as the complementary sequence to U_{10}-mers in the thermal stability studies.

Table 2.1: Physical data of the oligoribonucleotides and glycoconjugates

entry	oligoribonucleotides/ glycoconjugates	Formula	R_t (min)	required Mass	observed Mass
93	U_9U	$C_{207}H_{254}Cl_9N_{29}O_{87}P_9^-$	8.53[a]	5138.2	5138.5
94	A_9A	$C_{217}H_{264}Cl_9N_{59}O_{67}P_9^-$	8.90[a]	5168.6	5368.7
95	C_6-amino modifier-U_9U	$C_{213}H_{268}Cl_9N_{30}O_{90}P_{10}^-$	8.52[a]	5317.4	5316.4
96	Man-U_9U	$C_{225}H_{283}Cl_9N_{31}O_{98}P_{10}^-$	7.63[a]	5618.6	5319.4
97	Bi-Man-U_9U	$C_{247}H_{322}Cl_9N_{36}O_{108}P_{10}^-$	7.34[a]	6152.2	6152.6
98	U_{10}	$C_{90}H_{110}N_{20}O_{78}P_9^-$	2.79[b]	2998.7	2998.4
99	A_{10}	$C_{100}H_{120}N_{50}O_{58}P_9^-$	2.95[b]	3229.1	3229.2
100	C_6-amino modifier-U_{10}	$C_{96}H_{124}N_{21}O_{81}P_{10}^-$	3.40[b]	3177.8	3177.7
101	Man-U_{10}	$C_{108}H_{139}N_{22}O_{89}P_{10}^-$	3.66[b]	3479.1	3479.1
102	Bi-Man-U_{10}	$C_{130}H_{178}N_{27}O_{99}P_{10}^-$	2.70[b]	4012.7	4012.6

Notes: (i) [a]RP-HPLC (C_{18}); [b]AE-HPLC (DNAPac PA100); for detailed chromatographic conditions, see Experimental Section. (ii) Uridine and adenosine protected by Cpep at the 2'-OH are indicated by the italic *U* and *A*, respectively; unprotected uridine and adenosine are indicated by U and A, respectively.

2.5 Studies of the conjugation reaction

We then carried out conjugation reactions between squarate-activated mono- and bivalent mannosides and with U_{10}-mer bearing a C_6-amino modifier. Two routes were attempted. First, conjugations were carried out by using amino modified U_{10} homo decamers **100** (C_6-amino modifier-U_{10}, in which all the Cpep protecting groups were removed), and the conjugations took place in a triethylammonium acetate buffer (TEAA, pH 8, 0.1 *M*). Second, conjugations were performed in a DMA–TEAA buffer, and amino modified U_{10} homo decamers **95** (C_6-amino modifier-U_9U, in which all the uridine except the 3'-terminal one were protected by Cpep at the 2'-OH) was used as a precursor. Neither approach was efficient enough to give the conjugates in reasonable yields. In the first approach, less than 50% conversion was observed after the incubation proceeded for five days, as indicated by anion exchange chromatography on a DNAPac PA100 column. The second route did not give any significant amount of product after 10 days.

Addition of trace amount of triethylamine, however, accelerated the conjugation reaction dramatically. Thus, when Cpep-protected C_6-amino modifier-U_9U **95** (in Scheme 2.10) was treated with squarate-activated monovalent mannoside **73** in methanol–water containing trace triethylamine, the reaction was complete after 5 h at room temperature as indicated by both electrospray (ESI) mass spectrometry and reverse phase HPLC (Figure 2.2).

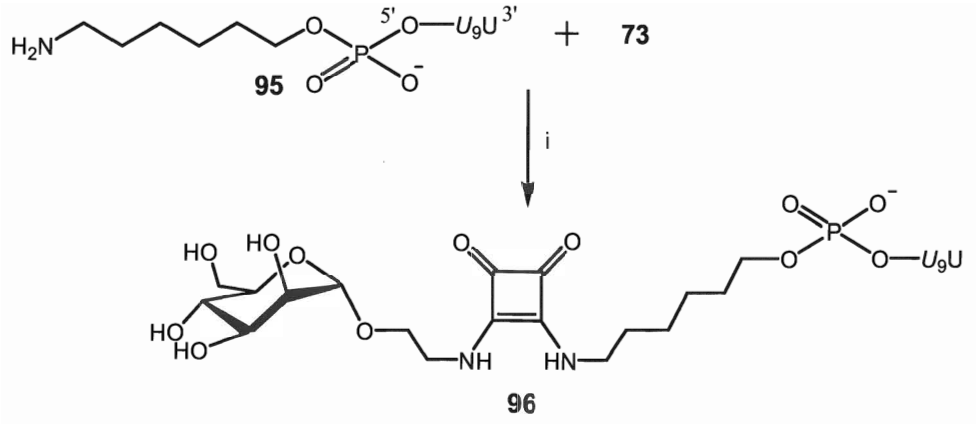

Scheme 2.10: Conjugation reaction of Man-U_9U*. *Reagents and conditions*: i, MeOH, H_2O, NEt_3 (*U*: uridine protected at 2'-position by Cpep; U: fully-unprotected uridine).

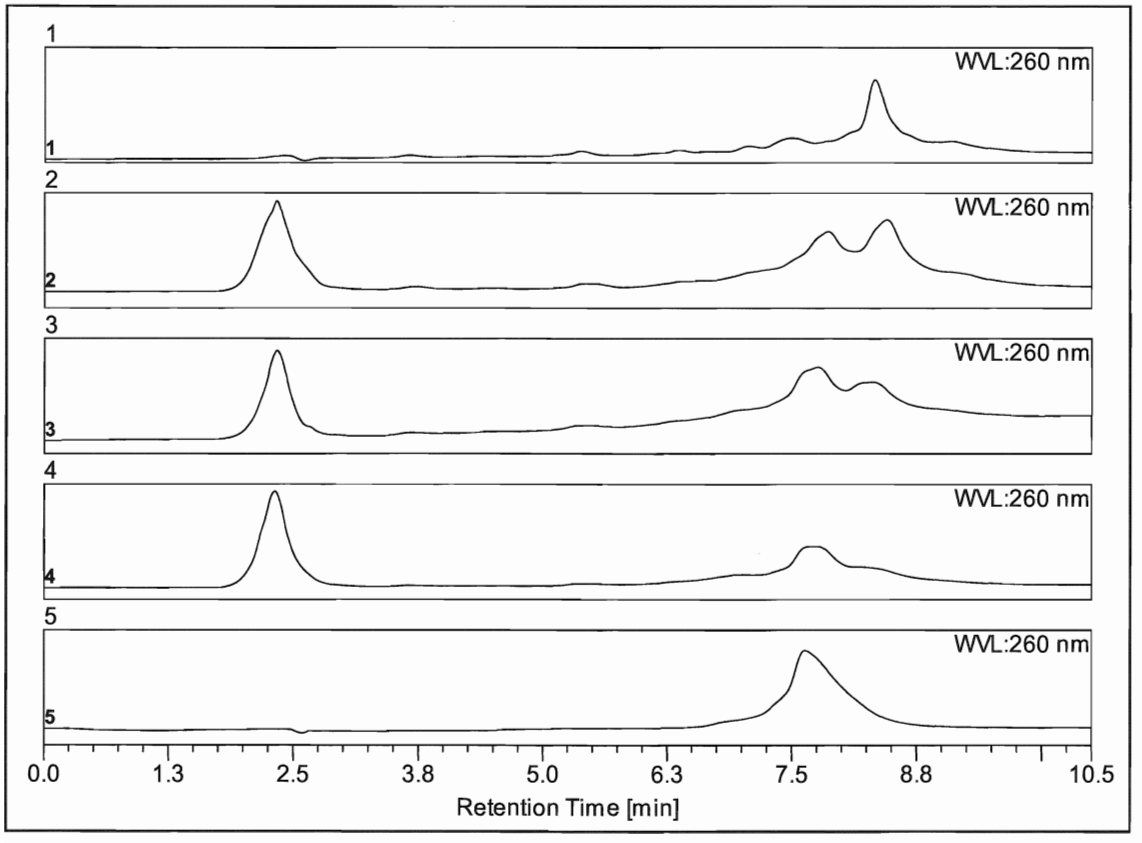

Figure 2.2: Stack plots of reverse phase HPLC profiles of conjugation reaction of Man-U_9U. 1). C_6-amino modifier-U_9U **95**; 2). conjugation reaction mixture after 1 h; 3). conjugation reaction mixture after 3 h; 4). conjugation reaction mixture after 5 h; 5).

* For simplicity, Cpep-protected monomannosyl U_{10}-mer conjugate **96** is abbreviated as Man-U_9U.

purified conjugate Man-U_9U **96**. Samples were run on C_{18} RP column. Linear gradient of 0.1 *M* of TEAA buffer–acetonitrile (70 : 30 v/v to 20 : 80 v/v) over 15 min and then isocratic elution. Flow rate 1.0 ml/min.

The chemistry was similarly efficient when the bimannoside **80** was allowed to conjugate with U_{10}-mer **95**. Reverse phase HPLC profiles of the reaction mixture indicated that the conjugation was complete in 9 h (Figure 2.3).

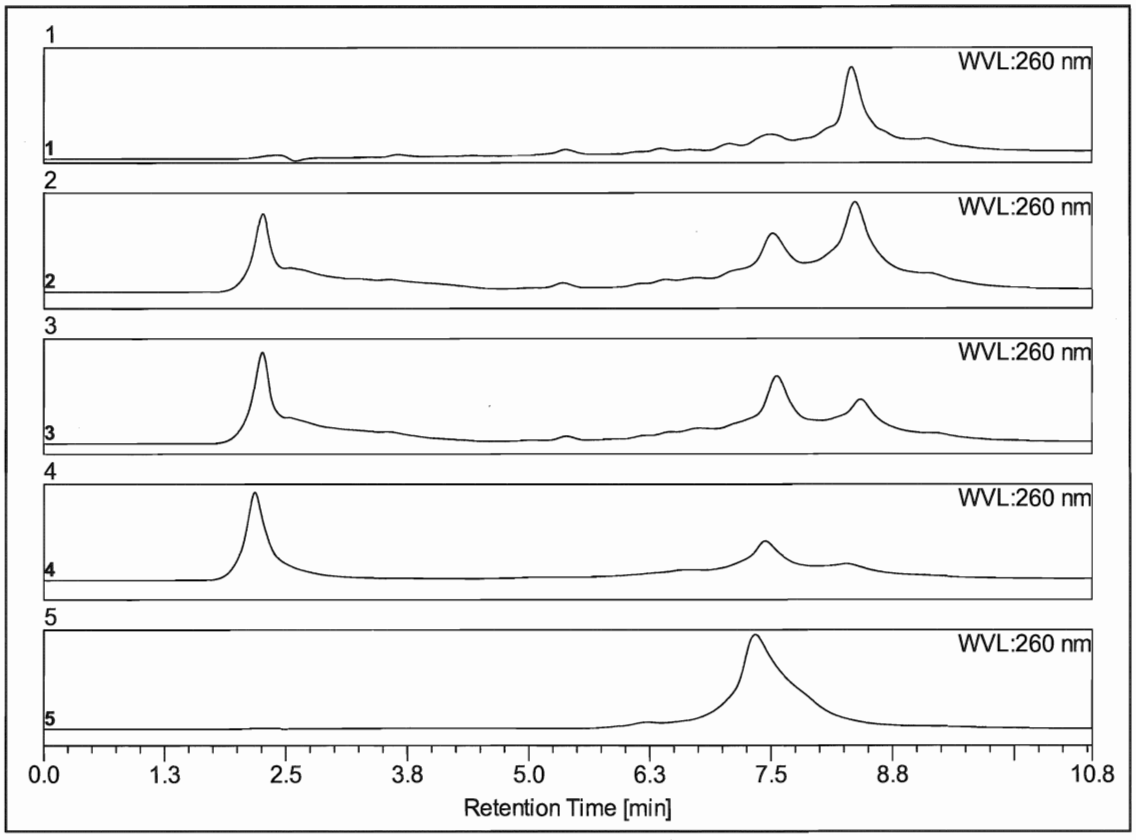

Figure 2.3: Stack plots of reverse phase HPLC profiles of conjugation reaction of Bi-Man-U_9U*. 1). C_6-amino modifier-U_9U **95**; 2). Conjugation reaction mixture after 3 h; 3). Conjugation reaction mixture after 6 h; 4). Conjugation reaction mixture after 9 h; 5). Purified conjugate Bi-Man-U_9U **97**. Samples were run on C_{18} RP column. Linear gradient of 0.1 *M* of TEAA buffer–acetonitrile (70 : 30 v/v to 20 : 80 v/v) over 15 min and then isocratic elution. Flow rate 1.0 ml/min.

* For simplicity, Cpep-protected dimannosyl U_{10}-mer conjugate **97** is abbreviated as Bi-Man-U_9U.

After the conjugations were complete, the crude conjugates were purified by semi-preparative reverse phase HPLC and the products were identified by electrospray mass spectrometry. Some analytical results of the conjugates **96** and **97** are listed in Table 2.1. The Cpep-protected conjugates **96** and **97** were then deprotected (removal of Cpep) by incubation in a mixture of DMA–TEAF (pH 2.52) (3:2 v/v) to give the unprotected conjugates Man-U_{10} **101** and Bi-Man-U_{10} **102** (Scheme 2.11).

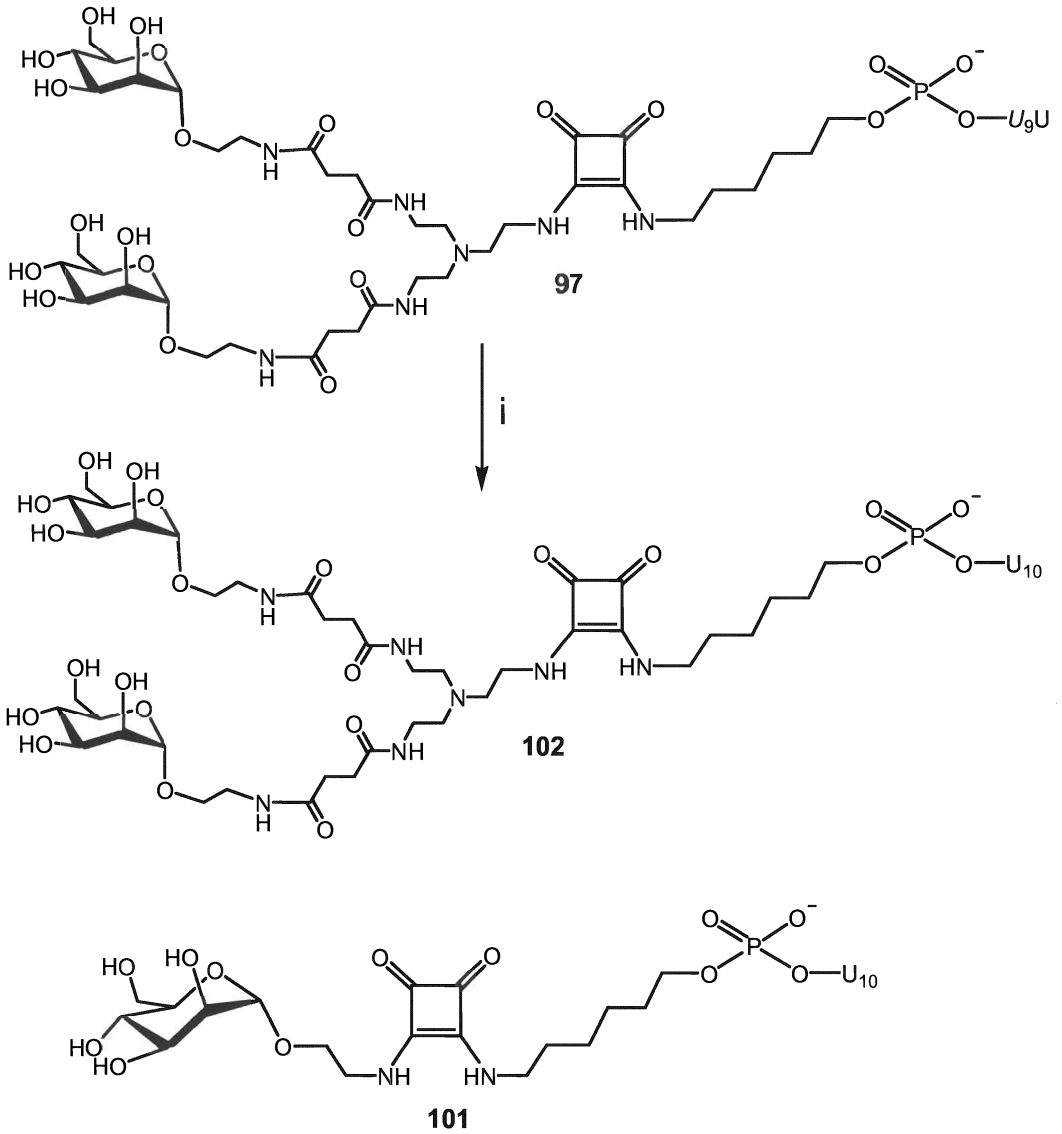

Scheme 2.11: Removal of Cpep groups. *Reagents and conditions*: i, $(CH_3)_2NCONH_2$, $Et_3N^+H{\cdot}HCOO^-$ buffer (pH 2.52), 40°C, 6 h.

The final mono- and bivalent conjugates **101** and **102** were identified by ESI mass spectrometry and analyzed by anion exchange chromatography on a DNAPac PA100 column (Figure 2.4). Some physical properties of mono- and bivalent conjugates **101** and **102** are listed in Table 2.1. These conjugates can be easily further purified by anion exchange chromatography if necessary.

a)

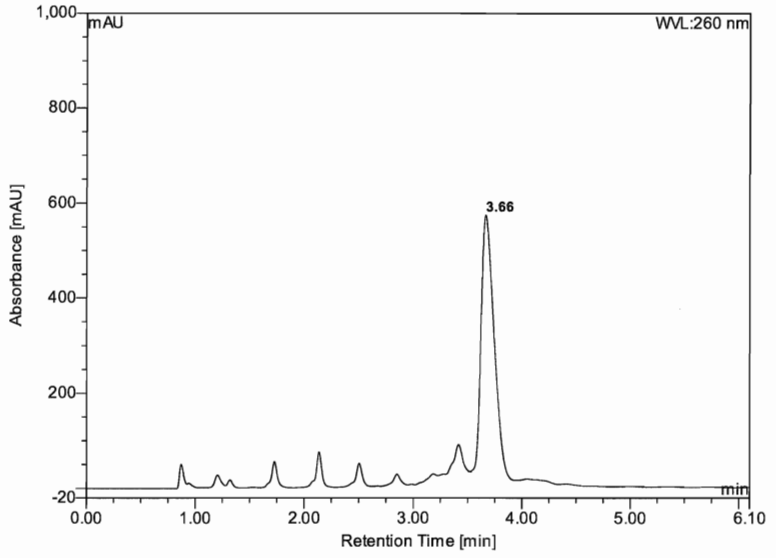

b)

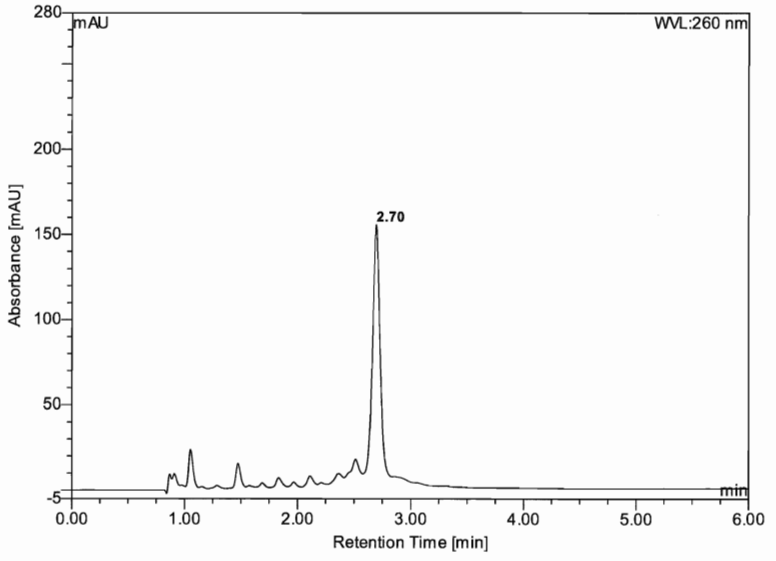

Figure 2.4: Anion exchange chromatography (DNAPac PA100, Dionex) profiles of fully-deprotected conjugates. a) monomannosyl U_{10}-mer conjugate (Man-U_{10}) **101** and b) dimannosyl U_{10}-mer conjugate (Bi-Man-U_{10}) **102**. Eluent 1: TrisCl (0.1 *M*, pH 8.0, 10%),

eluent 2: water, eluent 3: NaCl (1.0 *M*); flow rate: 1.5 ml/min. Concave gradient of NaCl from 0.1 *M* to 0.55 *M* over 20 min.

2.6 Stability tests

Enzymatic stability and thermal stability tests were conducted to evaluate the impact of glycosylation on the stability of RNA molecules.

2.6.1 Enzymatic stability

The enzymatic stability tests were conducted in tris hydrochloride (Tris-Cl) buffer (pH 8.0) with the presence of ribonuclease A (Rnase A) and bacterial alkaline phosphatase. Initially, the enzymatic stability tests were conducted by incubation of samples with the presence of stock solutions of Rnase A and bacterial alkaline phosphatase* for 24 h. It was found that both modified and unmodified U_{10}-mers were completely digested to uridine monomer under the above condition. In order to investigate whether the glycosylation has any effect on the stability of RNA molecules, a number of tests were conducted to establish a milder condition in which U_{10}-mers can be digested by enzymes and the progress of degradation can be monitored. When the 100-fold dilution of stock solution of enzymes was used, the degradation progress was able to be monitored. Figure 2.5 illustrated the progress of enzyme degradation monitored by anion exchange HPLC. No significant difference was observed when the enzymatic stability of mono- and dimannosyl U_{10}-mers **101** and **102** were compared with unmodified U_{10}-mer **98**. Both the modified and unmodified U_{10}-mers were digested by the enzymes at a similar rate under the same conditions. The effects of glycosylation on the stability of siRNA molecules will be investigated in the future.

* See experimental section for the preparation of stock solution.

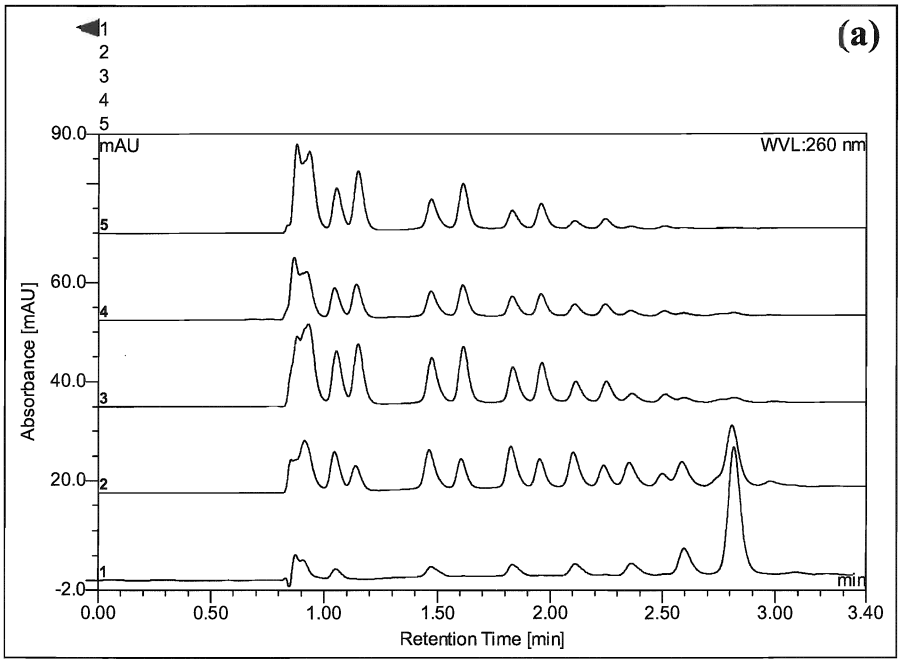
(a)
mAU
WVL:260 nm
Absorbance [mAU]
90.0
60.0
40.0
20.0
-2.0
min
0.00
0.50
1.00
1.50
2.00
2.50
3.00
3.40
Retention Time [min]

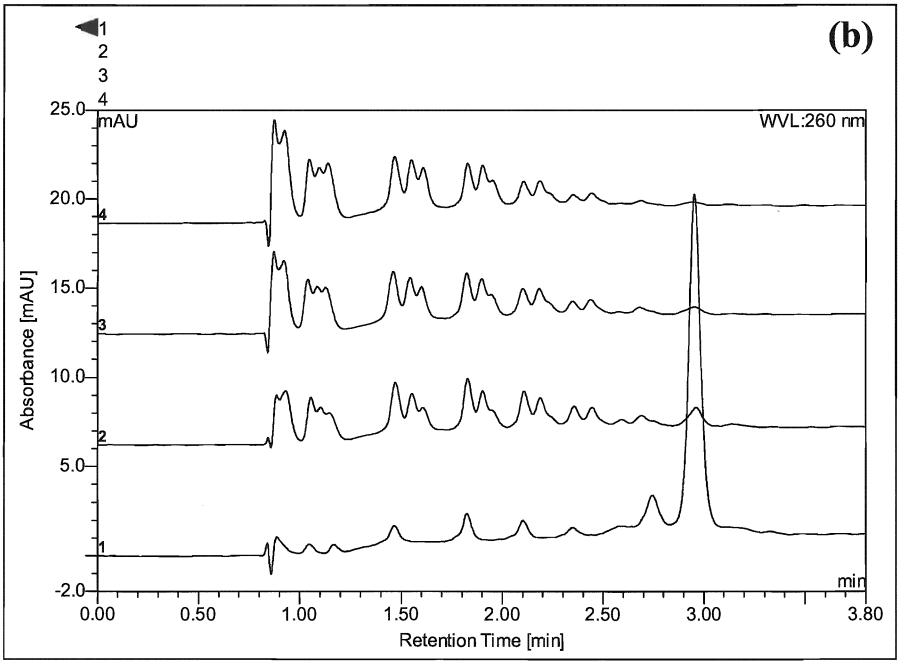
(b)
mAU
WVL:260 nm
Absorbance [mAU]
25.0
20.0
15.0
10.0
5.0
-2.0
min
0.00
0.50
1.00
1.50
2.00
2.50
3.00
3.80
Retention Time [min]

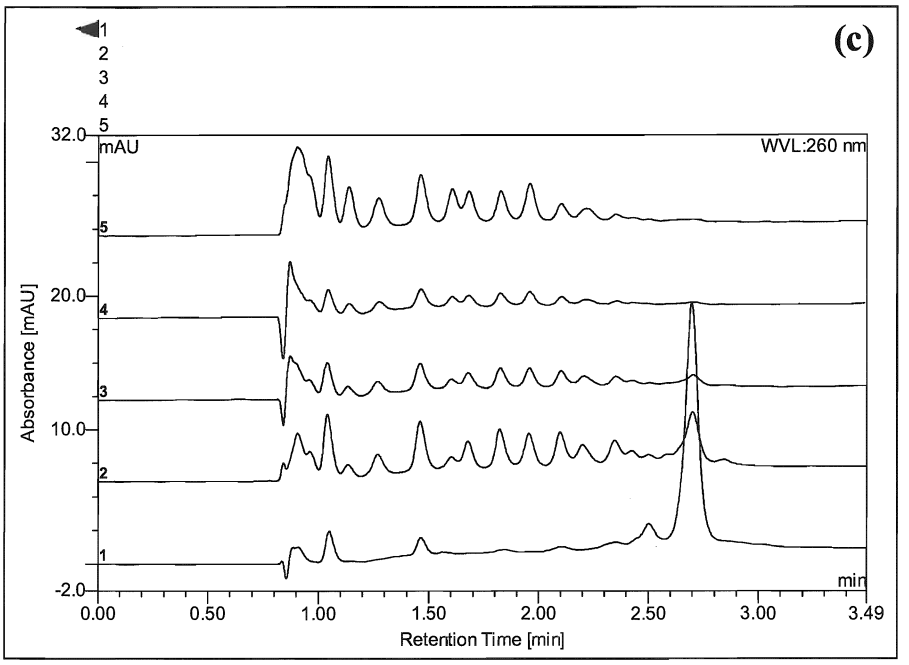

Figure 2.5: Anion exchange HPLC profiles of the enzymatic digests of U_{10}, Man-U_{10}, and Bi-Man-U_{10}. 1). (a): U_{10}; (b): Man-U_{10}; (c) Bi-Man-U_{10}; 2). reaction mixture after 2 min digestion; 3). reaction mixture after 5 min digestion; 4). reaction mixture after 10 min digestion; 5) reaction mixture after 15 min digestion.

2.6.2 Thermal stability

The effect of glycosylation on the duplex stability was determined by measuring the melting temperature. In this test, unmodified A_{10}-mer (A_{10}) was used as the complementary sequence; U_{10}:A_{10} is a non-glycosylated control duplex; Man-U_{10}:A_{10} and Bi-Man-U_{10}:A_{10} are two glycosylated conjugates. UV thermal denaturation studies of the umodified U_{10}-mers **98** and modified U_{10}-mer conjugates **101** and **102**, revealed similar thermal behaviors (Figure 2.6).

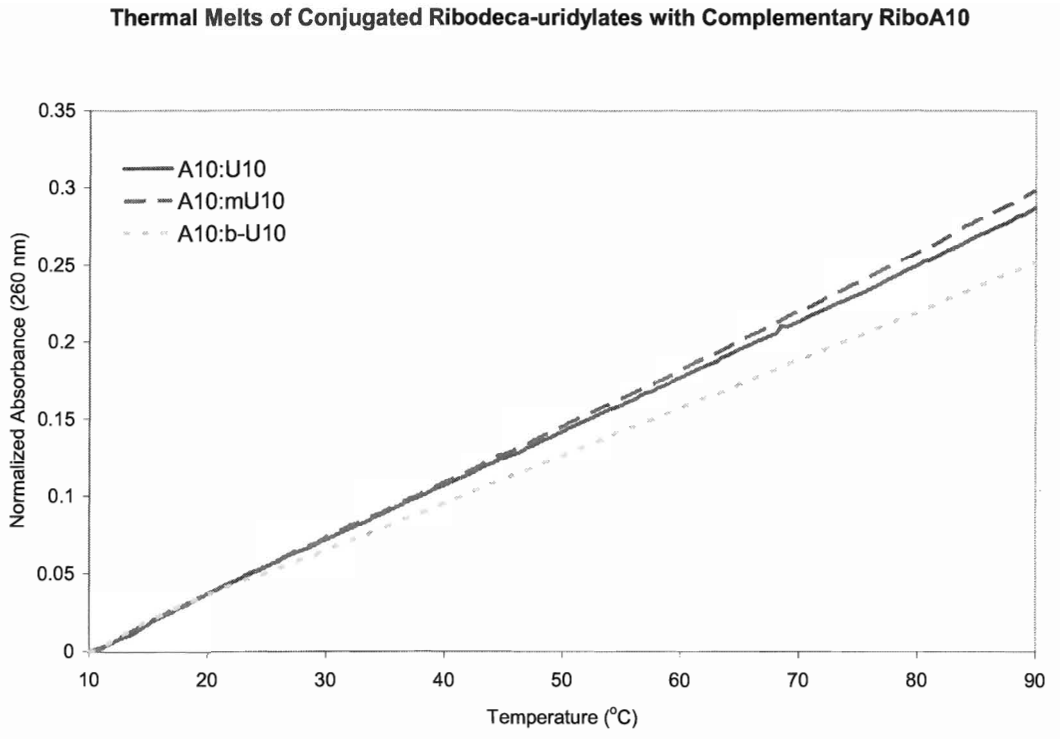

Figure 2.6: Thermal melts on conjugates and unmodified U_{10}-mer. Unmodified A_{10}-mer was used as the complementary sequence. Man-U_{10}:A_{10} is indicated as A10:mU10, and Bi-Man-U_{10}:A_{10} is indicated as A10:b-U10 in this graph.

2.7 Synthesis of fluorescent ribosides

Fluorescent nucleosides have been widely used as probes for hybridization, mis-matches, single nucleotide polymorphism etc.[95, 96] Non-polar aromatic fluorescent *C*-nucleosides such as 1-pyrenyl **103a** and 9-phenanthrenyl deoxynucleosides **103b**[97] represent steric mimics of the natural analogs with little or no hydrogen bonding potentials. They have been shown to be useful tools as biophysical probes for the study of noncovalent interactions such as aromatic π-stacking in DNA.[97-99]

The ribonucleoside series of these non-polar aromatic fluorescent analogues **104a** and **104b**, however, have not been synthesized. With the increasing importance of oligoribonucleotides in applications such as RNA silencing,[6] access to these compounds will allow for investigation of RNA–RNA and RNA–DNA interactions.

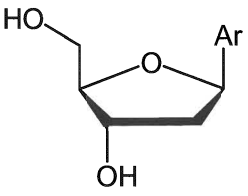

103 **a**; Ar = 1-pyrenyl
b; Ar = 9-phenanthrenyl

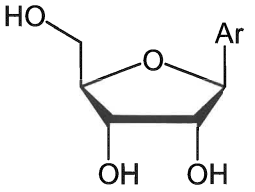

104 **a**; Ar = 1-pyrenyl
b; Ar = 9-phenanthrenyl

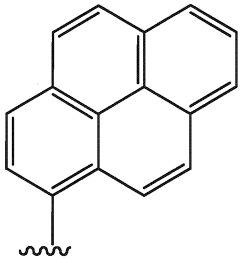

1-pyrenyl

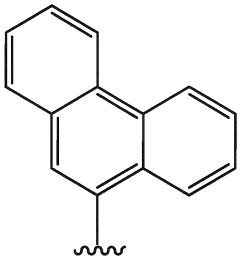

9-phenanthrenyl

In the present project, the sense strand of siRNA is designed to be covalently tagged with a fluorescent dye at the 5'-terminal for evaluation of targeting and cellular uptake of the mannosylated siRNAs by DCs. A convenient way to introduce a fluorescent dye is to use a base modified phosphoramidite, in which the base residue is replaced by a fluorophore. The phenanthrene and pyrene modified *C*-ribonucleosides (**104a** and **104b**) were initially chosen as reporter groups and will be incorporated into RNA sequence through phosphoramidite chemistry.

A number of approaches for the synthesis of *C*-nucleosides have been reported and recently reviewed.[100] Among these methods, the lactone approach[101, 102] is efficient and gives good selectivity for the β-anomer. In this approach, lactone is an electrophilic sugar and C1-glycosidic coupling was achieved by nucleophilic attack on electrophilic anomeric carbon in the sugar moiety. Perbenzylated lactone **110** (Scheme 2.12) has been employed in the preparation of *C*-nucleosides and *C*-ribonucleosides analogue by Leumann[103] and Brown[104]. Lactone derivative **105** was used by Reese *et al.* in the

synthesis of a series of *C*-(2'-deoxyribonucleosides).[105] This chemistry was therefore chosen to prepare the fully protected *C*-nucleosides in this study.

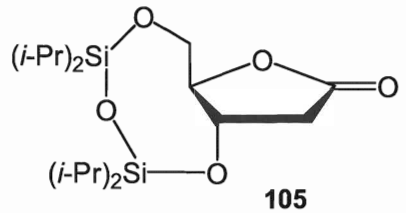

105

In the current study, D-ribose was used as a starting material to prepare the perbenzylated lactone **110** (Scheme 2.12). First, D-ribose **106** was converted to methyl D-riboside **107**, followed by global benzylation with NaH/BnBr in dry THF to give 2,3,5-tri-*O*-benzyl-methyl-D-riboside **108**.[106] 2,3,5-Tri-*O*-benzyl-D-ribose **109** was obtained by acidic hydrolysis of corresponding methyl riboside **108**.[107] Modified Swern oxidation of lactol **109** gave 2,3,5-tri-*O*-benzyl lactone **110** in a yield of 40% over four steps.[108]

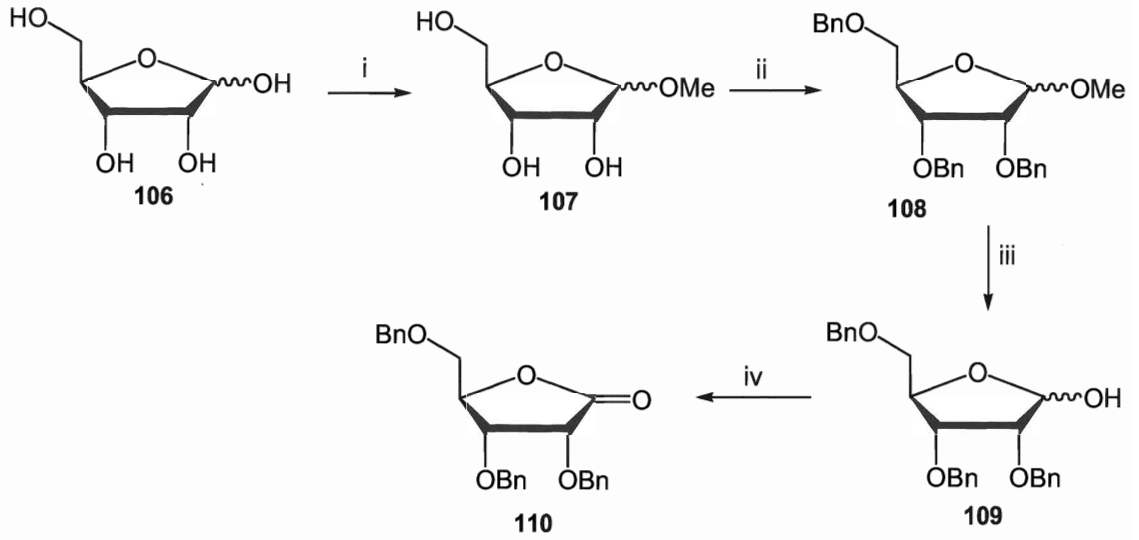

Scheme 2.12: Preparation of perbenzylated lactone. *Reagents and conditions*: i, HCl-MeOH, r.t., 24 h, quantitatively; ii, NaH, BnBr, DMF, 0°C-r.t., 24 h, 61.4%; iii, dioxane–0.12 *N* HCl (4:1 v/v), reflux 9 h, 83.5%; iv, DMSO, Ac_2O, r.t., 20 h, 79.9%.

Bromine-lithium exchange in aromatic bromides **113** with *n*-butyllithium furnished aryl lithium which reacted *in situ* with perbenzylated lactone **110** at -78°C to give the hemiacetal intermediate **111**. The hemiacetals **111** were subsequently reduced to the *C*-

riboside **112** using triethylsilane and boron trifluoride etherate.[103] The β-anomeric isomers were isolated in moderate yields (52% and 34% for the phenanthrenyl **112a** and pyrenyl *C*-riboside **112b**, respectively) (Scheme 2.13).

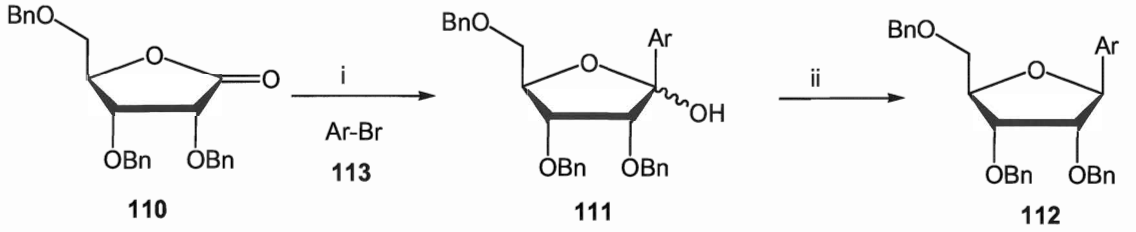

a; Ar = 1-phenanthrene, 52% over 2 steps
b; Ar = 9-pyrene, 34% over 2 steps

Scheme 2.13: C1-glycosidic coupling *via* lactone approach. *Reagents and conditions*: i, *n*-BuLi, THF, -78°C, 5 h; ii, Et_3SiH, $Et_2O{\cdot}BF_3$, -78°C, 3.5 h.

The stereochemistry (β-anomers) of the fully-protected *C*-ribosides was evident base on the following NOEs observation: 1). NOEs between H-3' of the ribose and the aromatic proton of the phenanthrene and pyrene, respectively; 2). NOEs between H-1' and H-4'; and 3) absence of NOEs between H-1' and H-3'. The NOEs of perbenzylated phenanthrene **112a** is illustrated in Figure 2.7. Perbenzylated pyrene **112b** showed similar NOE observations.

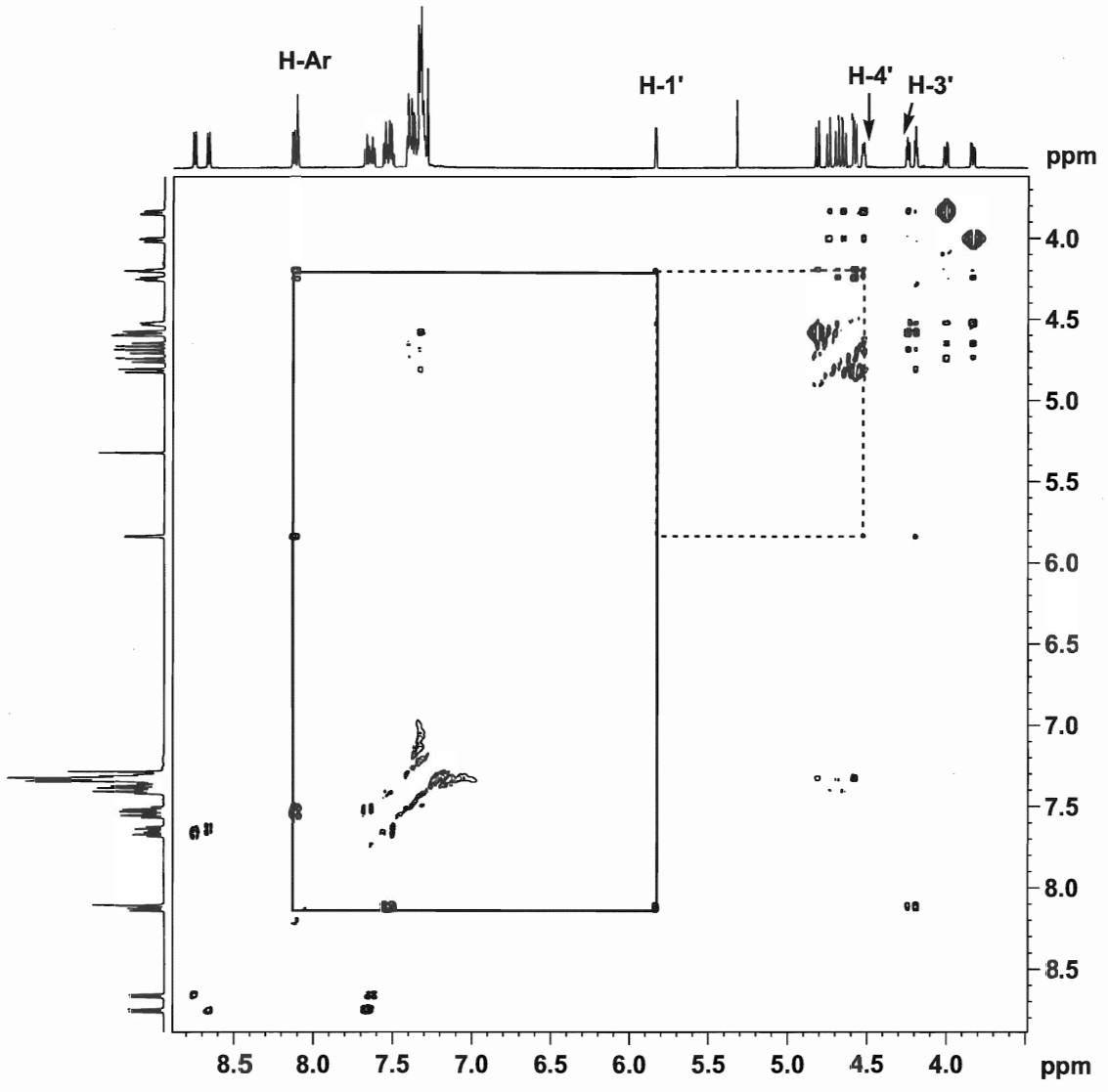

Figure 2.7: NOESY spectrum of perbenzylated β-ribofuranosyl phenanthrene **112a**

Removal of the benzyl protecting groups from the perbenzylated ribofuranosyl phenanthrene **112a** and pyrene **112b** proved to be very challenging. Attempts to remove the benzyl groups by a number of approaches failed to give the desired products. Thus, catalytic hydrogenation, transfer hydrogenation, acid hydrolysis, and oxidative removal by DDQ were either extremely slow or did not give desired products.

Boron tribromide-promoted debenzylation effected quick removal of the benzyl protecting groups from both perbenzylated ribofuranosyl phenanthrene **112a** and pyrene **112b** (Scheme 2.14). Ribofuranosyl phenantharene **114** was obtained as an anomeric

mixture in 63% yield. However, ring expansion was observed in the case of the pyrene analogue to give an anomeric mixture of ribopyranosyl pyrene **115** in only 26% yield. In the latter case, no ribofuranosyl pyrenes were isolated (Table 2.2). Formation of 6-membered ribopyranosyl pyrenes **115** was supported by the disappearance and appearance of 5'-OH and 4'-OH, respectively, which is clearly shown in the COSY spectra of both α- and β-anomers (Figure 2.8 and 2.9).

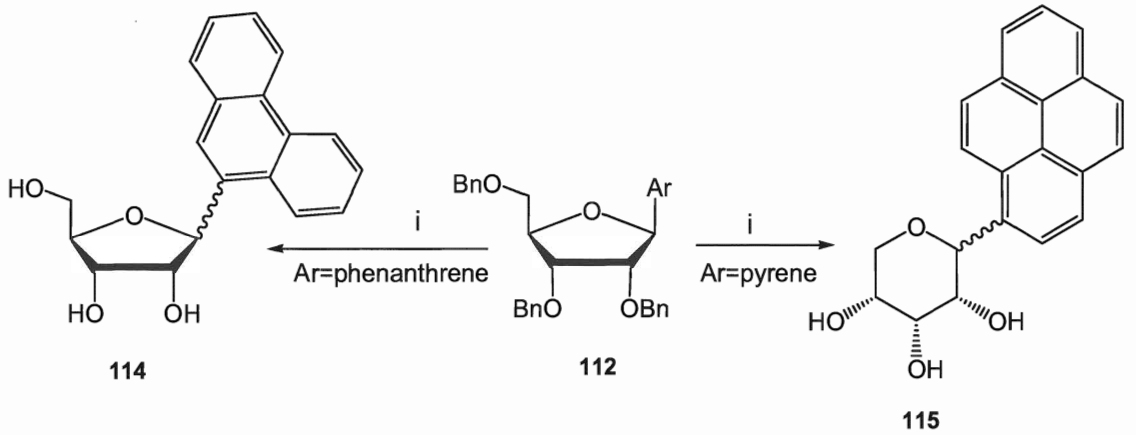

114 **112** **115**

Scheme 2.14: Debenzylation of perbenzylated ribofuranosyl phenanthrene and pyrene. *Reagents and conditions*: i, BBr_3, CH_2Cl_2, -78°C.

Table 2.2: ^1H Resonance of anomeric protons in ribofuranosyl phenantharene and ribopyranosyl pyrene, and ratios of the anomeric isomers

	δ(H-1')(ppm)	Ratio of α- and β-anomers*
Ribofuranosyl phenantharene	5.41 (d, J=3.7, α-)	1:1.84
	5.75 (d, J=2.6, β-)	
Ribopyranosyl pyrene	5.39 (d, J=9.6, β-)	1:1.08
	5.41 (s, α-)	

* As determined by ^1H NMR of crude reaction mixture.

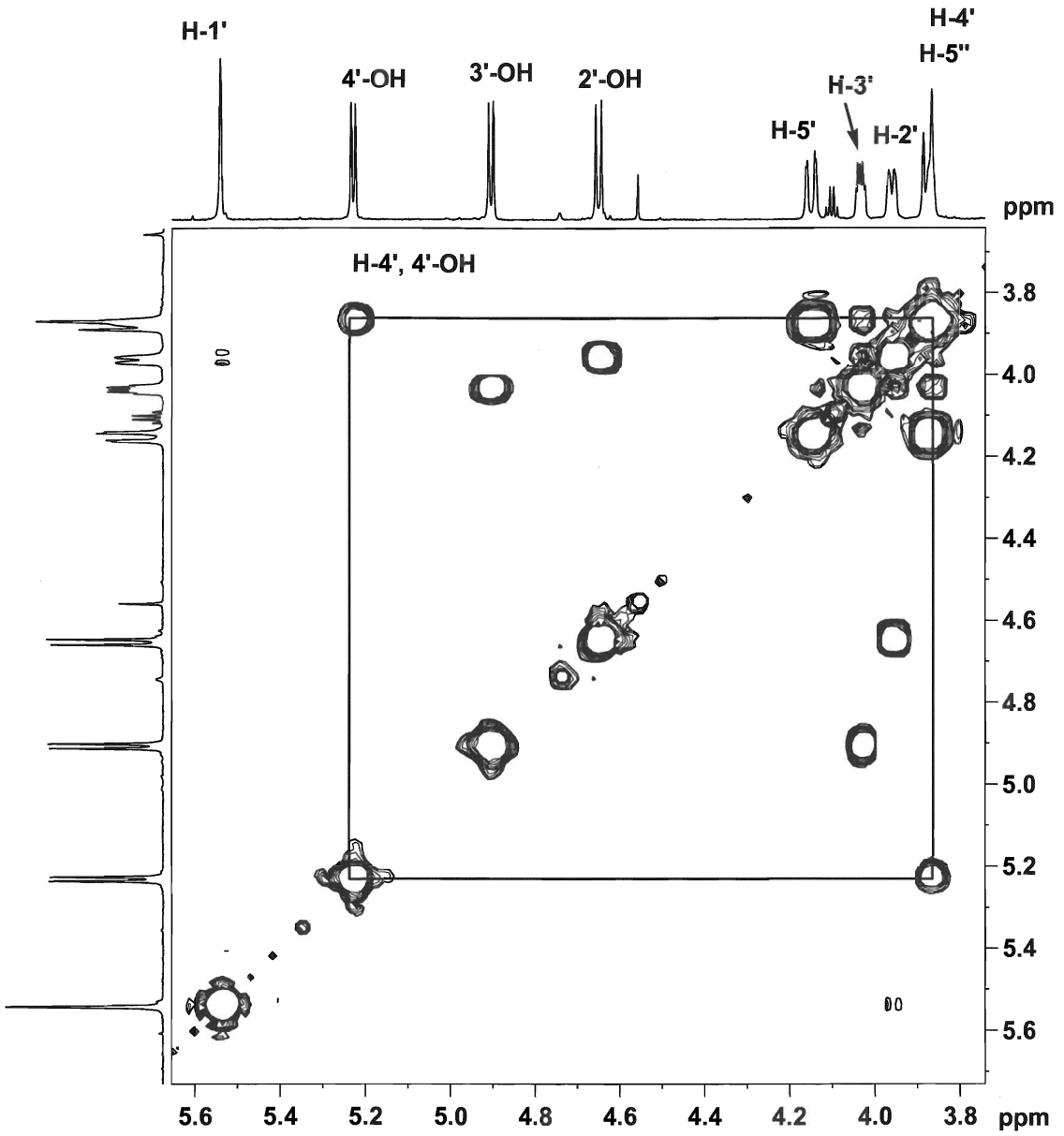

Figure 2.8: COSY spectrum of *9*-*α*-D- ribopyranosyl pyrene **115b**

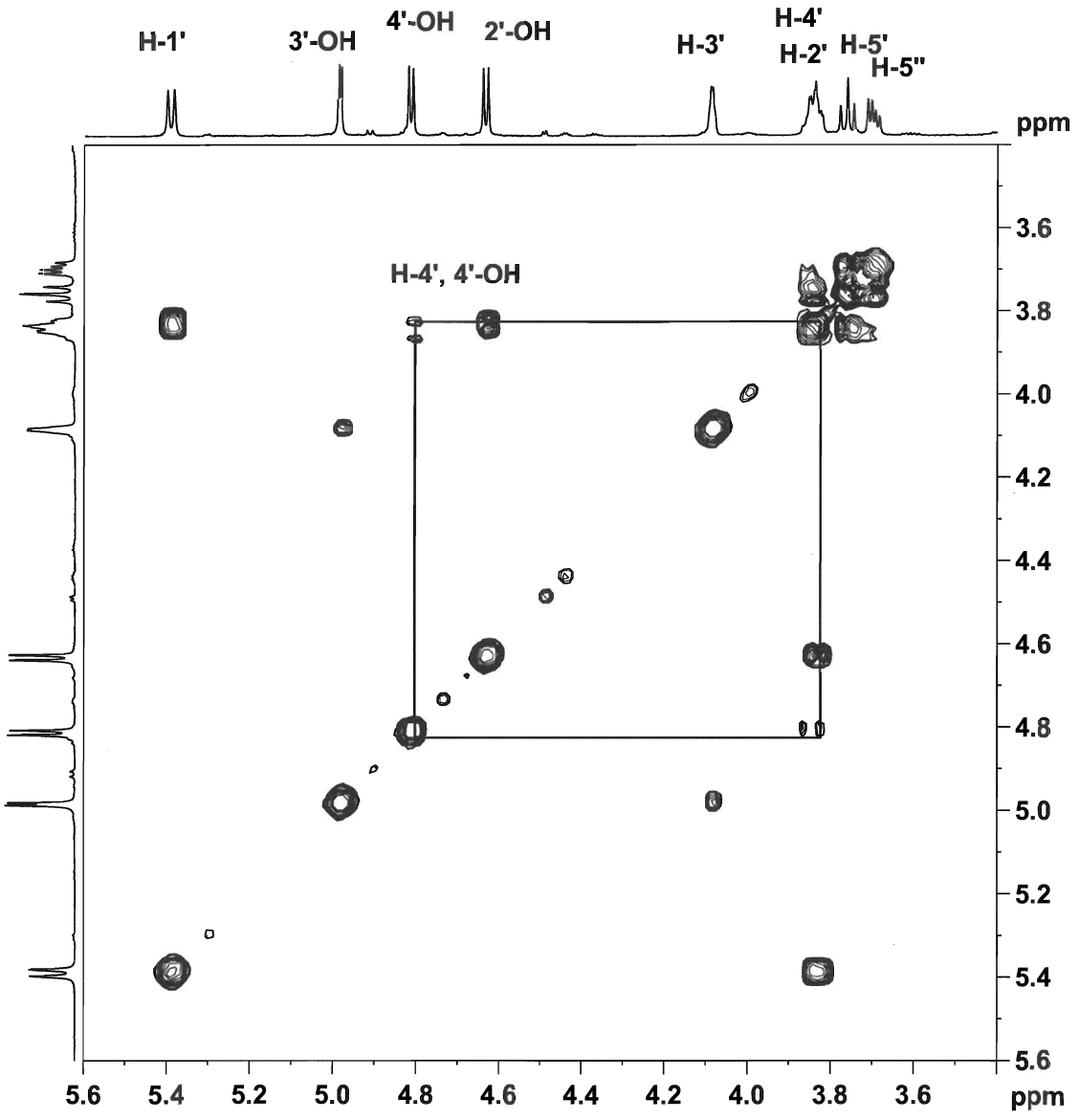

Figure 2.9: COSY spectrum of *9-β*-D- ribopyranosyl pyrene **115a**

The anomeric isomers **114** and **115** were isolated by column chromatography and fully-characterized. The *α*- and *β*-ribofuranosyl phenanthrenes were assigned based on the following NOE observations: 1). NOE between H-1' and 2'-OH in the *β*-anomer **114a**, and 2). NOE between H-1' and H-3' in *α*-anomer **114b** (Figure 2.10). Similar results were obtained in the debenzylated pyrene ribosides **115a** (*β*-anomer) and **115b** (*α*-anomer), respectively.

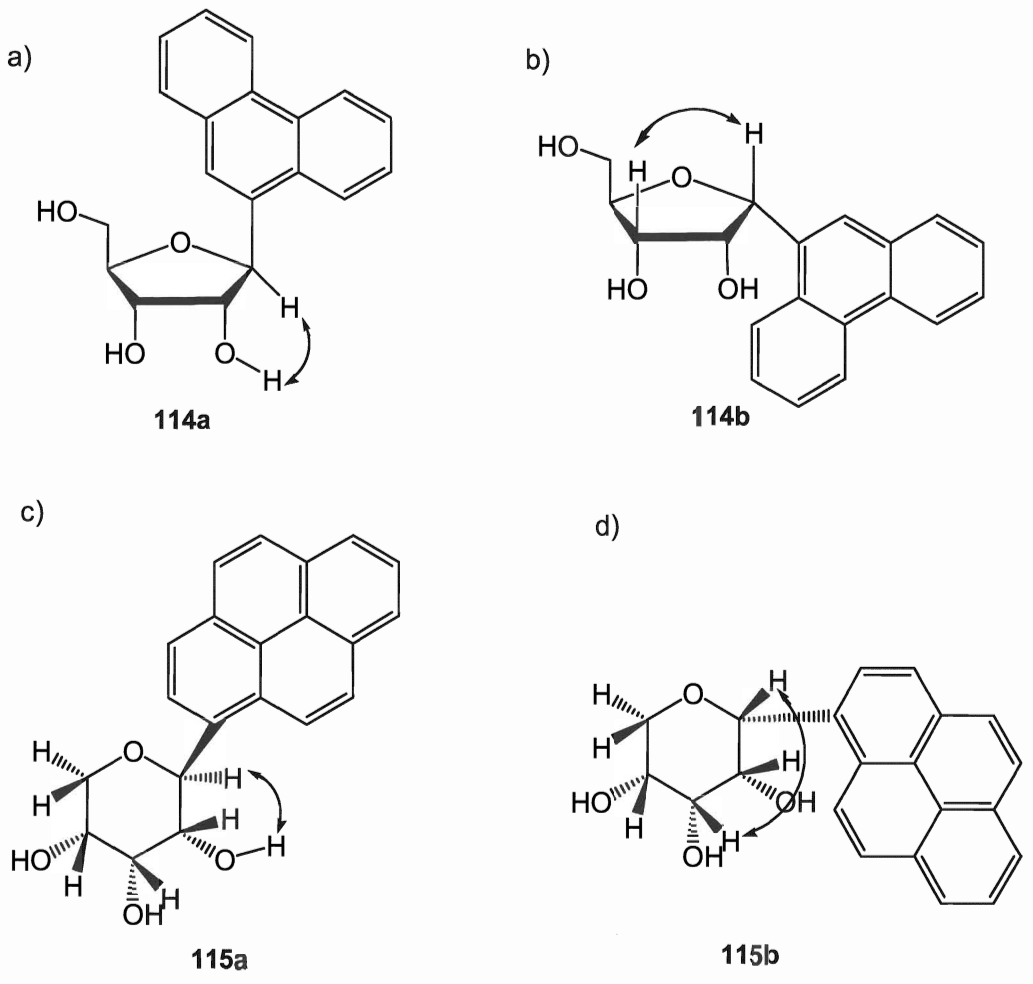

Figure 2.10: NOEs observed in the fully-deprotected ribofuranosyl phenanthrene and ribopyranosyl pyrene. (a) β-ribofuranosyl phenanthrene **114b**, (b) α-ribofuranosyl phenanthrene **114a**, (c) β-ribopyranosyl pyrene **115a**, and (d) α-ribopyranosyl pyrene **115b**.

The UV/vis and fluorescent emission spectroscopy of ribopyranosyl pyrene **115** and ribofuranosyl phenanthrene **114** (both anomers) were measured in methanol. The absorption and emission spectra are shown in Figure 2.11. The molar extinction coefficients (ε), maximal absorption wavelengths (λ^{ex}), and maximal emission wavelengths (λ^{em}) are summarized in Table 2.3. All these compounds show weak fluorescent intensity. Relative fluorescent quantum yields (Φ_f) of these *C*-ribosides were determined against L-tryptophan using the method described in the literature.[109]

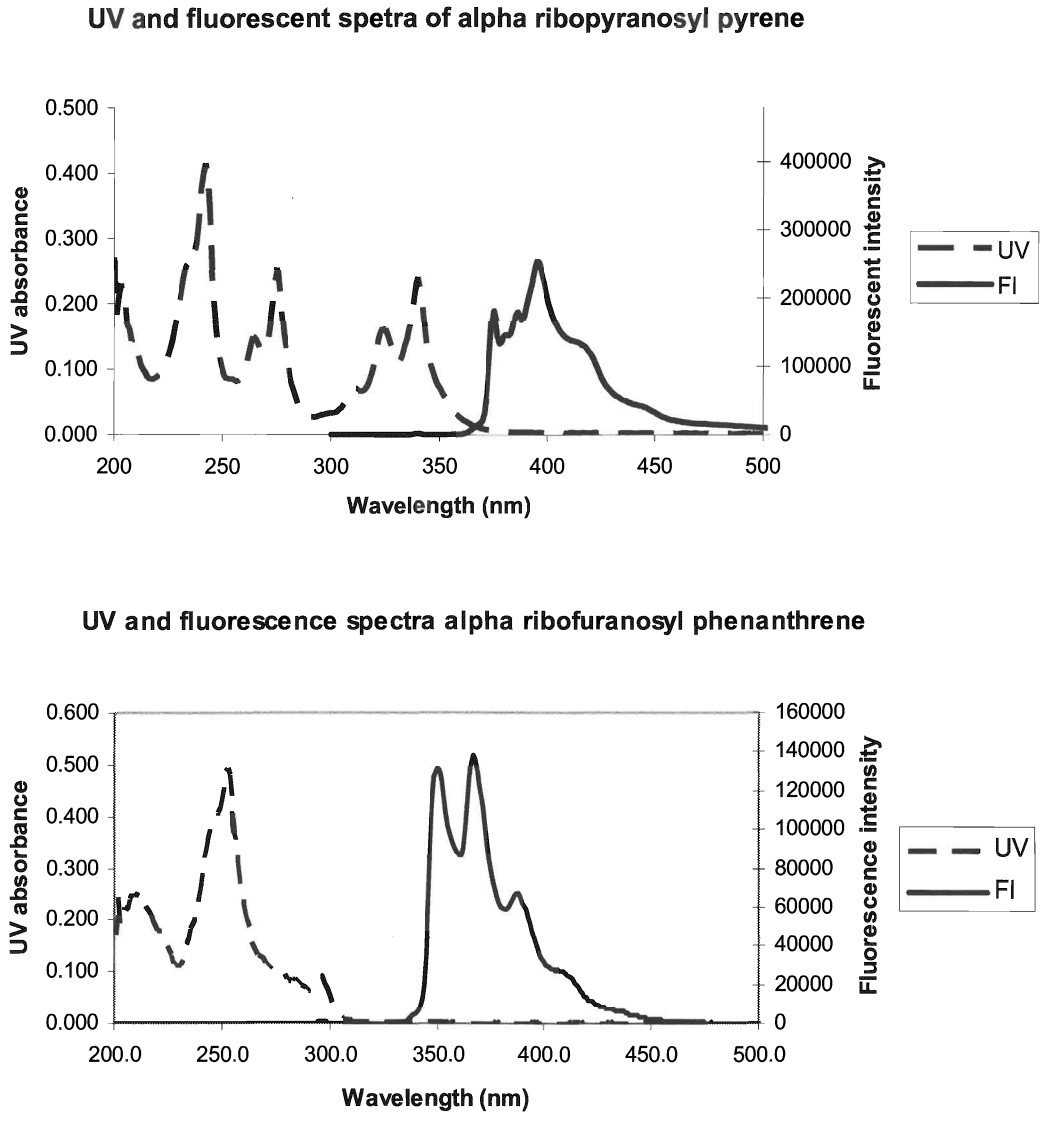

Figure 2.11: Absorption and emission spectra of the α-ribopyranosyl pyrene **115b** and α-ribofuranosyl phenanthrene **114b**

Table 2.3: Molar extinction coefficients, maximal absorption wavelengths, maximal emission wavelengths, and fluorescent quantum yields of ribofuranosyl phenanthrene and ribopyranosyl pyrene

	ε ($M^{-1}cm^{-1}$)	λ^{ex} (nm)	λ^{em} (nm)	Φ_f
α- ribofuranosyl phenanthrene **114b**	9200	251	350	0.055
β- ribofuranosyl phenanthrene **114a**	8350	251	350	0.062
α- ribopyranosyl pyrene **115b**	24600	335	395	0.11
β- ribopyranosyl pyrene **115a**	25600	335	395	0.092
L-tryptophan	5600	280	350	0.13

Chapter 3 - Conclusions and future work

In conclusion, homo RNA sequences have been synthesized using Cpep as 2'-hydroxyl protecting group by solid phase phosphoramidite chemistry. An efficient conjugation chemistry has been established for the preparation of carbohydrate–RNA conjugates using the squarate linker. Two glycoconjugates, monomannosyl U_{10}-mer and dimannosyl U_{10}-mer, were synthesized using the established protocol. The effects of glycosylation on the stability of RNA molecules were evaluated, however no significant improvement was observed.

This chemistry is currently being used to prepare carbohydrate–siRNA conjugates. In this conjugate, 5'- termini of sense strand of siRNA will be attached to a carbohydrate moiety; 5'-termini of antisense strand will be labelled with a fluorophore. Impacts of glycosylation on stability, binding affinity, and cellular uptake will be investigated with this luciferase siRNA model (Figure 3.1).

Figure 3.1: Luciferase siRNA sequence

In the future, a tetravalent mannoside **116** will be synthesized in order to increase lectin binding affinity. The bioavailability of tetramannosyl–siRNA conjugate is to be evaluated and compared with dimannosyl- and monomannosyl- conjugates, and nonglycosylated control. Ultimately, this approach may prove to be an effective way to improve the bioavailability of siRNAs as therapeutic agents.

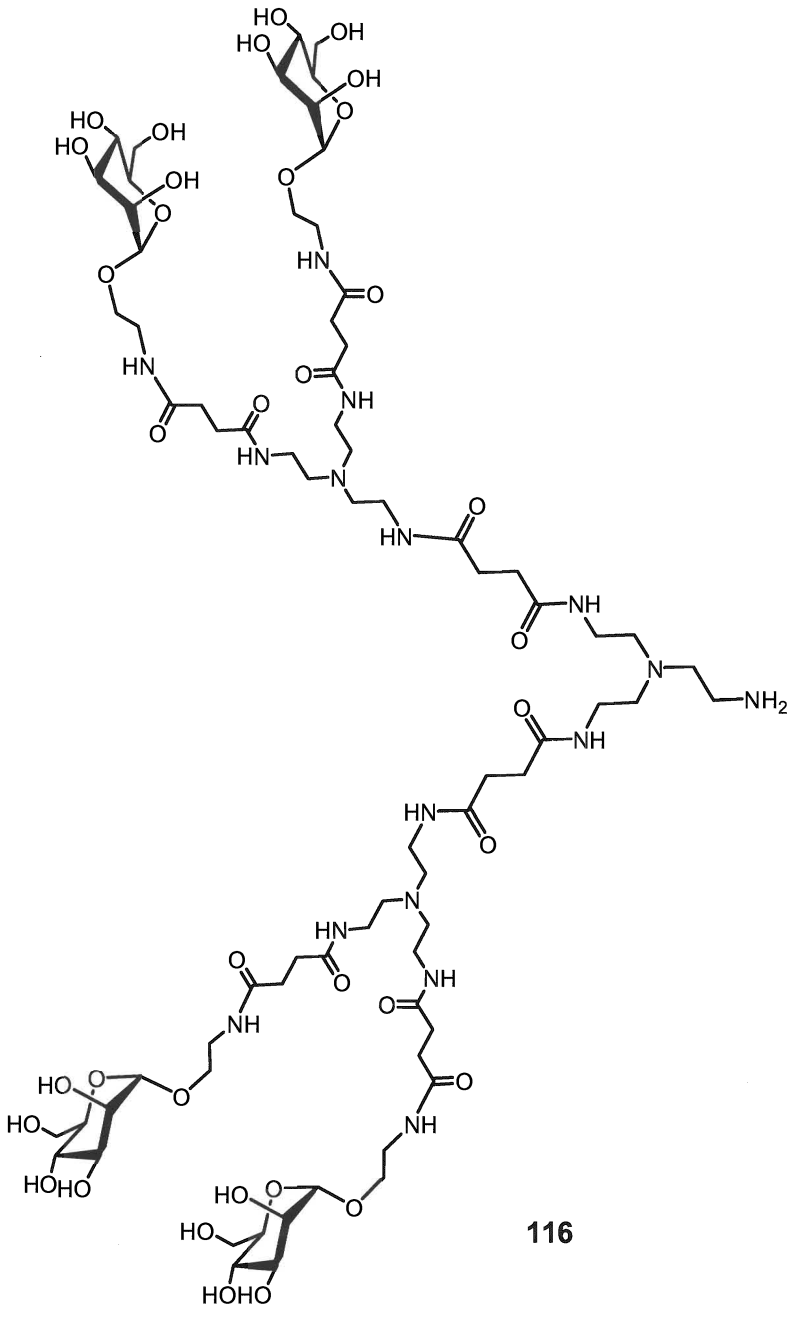

116

In an attempt to prepare aromatic fluorescent ribosides, perbenzylated ribofuranosyl pyrene and phenanthrene were synthesized from perbenzylated ribolactone. However, deprotection of benzyl-protected ribofuranosyl phenanthrene and pyrene by boron tribromide gave ribofuranosyl phenanthrene and ribopyranosyl pyrene, respectively. Mechanism of this unexpected ring expansion in Lewis acid promoted debenzylation of perbenzylated ribofuranosyl pyrene is currently under investigation. Although

phenanthrene and pyrene ribosides derivatives show week fluorescent properties, they may be useful as probes in RNA for examination of base stacking and hydrogen bonding.

4,4-Difluoro-4-bora-3a,4a-diaza-*s*-indacene (BODIPY) **117** is a borondifluoride dipyrrinato complex first reported in 1968.[110] Many BODIPY derivatives display intense fluorescence. Work is currently in progress in our lab to develope BODIPY analogues into fluorophores that could be introduced into oligonucleotides using the phosphoramidite chemistry during solid phase synthesis.[111, 112]

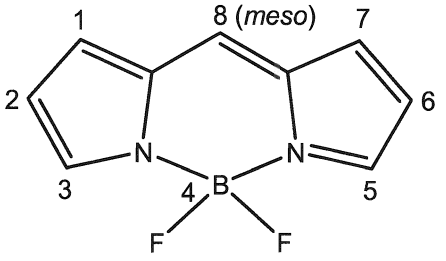

117

BODIPY dyes

Chapter 4 - Experimental

General information

^{1}H NMR spectra were measured at 300 and 600 MHz with a Bruker AV600 spectrometer; tetramethylsilane was used as an internal standard; J values are given in Hz. ^{13}C NMR spectra were measured at 75.5 and 150.9 MHz and ^{31}P NMR spectra were measured at 121.5 MHz with the same spectrometer. Chemical shifts are given in ppm. Mass spectra were recorded on Kratos Concept 1S mass spectrometer (EI, FAB) and Brucker HCT Ultra ESI-MS spectrometer. Desican 60 Å silica gel (230–400 mesh) was used for column chromatography. Thin layer chromatography (TLC) was performed on Silicycle SiliaPlate (60 Å). Reverse phase high-performance liquid chromatography (HPLC) was carried out on a 250×4.6 mm LiChrospher 100® RP-18 5μ column: the column was eluted with water–acetonitrile mixtures [linear gradient of triethylammonium acetate buffer (0.1 *M*, pH 7.0)–acetonitrile (70 : 30 v/v to 20 : 80 v/v) over 15 min and then isocratic elution. Flow rate 1.0 ml/min]. Anion exchange chromatography was carried out on a 250×4 mm DNAPac® PA100 column: the column was eluted with the following program: eluent 1: TrisCl (0.1 *M*, pH 8.0, 10%), eluent 2: water, eluent 3: NaCl (1.0 *M*); flow rate: 1.5 ml/min. Concave gradient of NaCl from 0.1 *M* to 0.55 *M* over 20 min. Melting points were measured with a Kofler hot-stage apparatus and are uncorrected. CHN analysis was performed at Guelph Chemical Laboratories Ltd (Guelph, ON) and Atlantic Microlab, Inc (Norcross, GA). UV absorbance was measured on Unican UV-VIS spectrometer with Vision 32 data system. Quartz cells from Hellma Limited (10 mm and 1 mm path) were used for UV measurement. Fluorescence was measured by QuantaMaster Model QM-2001-4 cuvette based L-format scanning spectrofluorometer. Themal melts was performed by a Varian CARY Model 3E spectrophotometer fitted with a 6-sample thermostatted cell block and a temperature controller.

Dichloromethane was purified by Pure-Solv Solvent Purification Systems (Innovative Technology), and stored over activated 4 Å molecular sieves. Triethylamine, Hünig's base, and pyridine were dried by heating, under reflux, in the presence of calcium

hydride and then distilled under nitrogen. Uridine resin for solid phase synthesis was purchased from Glen Research. 1-(4-Chlorophenyl)-4-ethoxy-1,2,5,6-tetrahydropiperidine and 1,3-dichloro-1,1,3,3-tetraisopropyldisiloxane were purchased from Rasayan Inc. Other chemicals were purchased from Aldrich and VWR and were used without further purification unless stated otherwise.

2,3,4,6-*O*-Tetraacetyl D-(+)-mannose 65

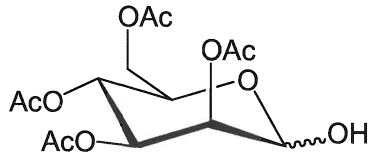

Mannose **63** (1.80 g, 10.0 mmol) was dried under vacuum for 6 h and then dissolved in dry pyridine (30 ml), followed by addition of acetic anhydride (20.0 ml, 0.2 mmol, 20 mol. equiv.). The reaction mixture was stirred overnight under nitrogen, and then quenched by addition of methanol (20 ml). The products were concentrated under reduced pressure. The residue was dissolved in dichloromethane (120 ml) and washed with saturated aqueous sodium hydrogen carbonate (100 ml). The layers were separated and the aqueous layer was back-extracted with dichloromethane (2×20 ml). The combined organic layers were dried ($MgSO_4$) and concentrated under reduce pressure. The residue was redissolved in ethyl acetate (2 ml) and added to hexane (100 ml) under stirring. The precipitate was collected by filtration to give 1,2,3,4,6-*O*-pentaacetyl D-mannose as a white solid. This material was then dissolved in DMF (20 ml), followed by addition of hydrazine acetate (prepared by mixing 720 µl of acetic acid and 600 µl of hydrazine hydrate in 5 ml of dichloromethane, 12 mmol, 1.2 mol equiv.) at room temperature. After 45 min, the products were evaperated under reduced pressure. The residue was redissolved in dichloromethane (120 ml) and extracted with saturated aqueous sodium hydrogen carbonate (100 ml). The layers were separated and the aqueous layer was back-extracted with dichloromethane (2×20 ml). The combined organic layers were dried ($MgSO_4$) and concentrated under reduce pressure. The residue

was purified by column chromatography on silica gel. The approprate fractions, which were eluted with dichloromethane–methanol (97:3 v/v) were combined and evaporated under reduced pressure to give the *title compound* as a white foam (2.23 g, 64.1%).

FAB-MS found M^+ = 349.11642, $C_{14}H_{20}O_{10}$ requires 349.11347.

δ_H[$CDCl_3$, 300 MHz]: 2.01 (3 H, s, CH_3), 2.06 (3 H, s, CH_3), 2.11 (3 H, s, CH_3), 2.17 (3 H, s, CH_3), 3.23 (1 H, br, OH), 4.16 (1 H, m, H-6), 4.25 (1 H, m, H-5), 4.27 (1 H, m, H-6'), 5.25 (1 H, s, H-3), 5.28 (1 H, t, J = 2.5, H-2), 5.33 (1 H, s, H-4), 5.45 (1 H, dd, J = 3.3 and 10.1, H-1)

R_f: 0.41 (dichloromethane–methanol, 95:5 v/v)

2,3,4,6-*O*-Tetraacetyl mannosyl *α*-trichloroacetimidate 66

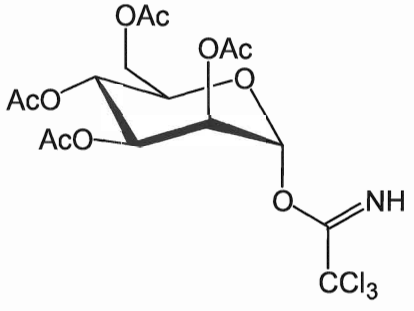

2,3,4,6-*O*-Tetraacetyl D-mannose **65** (4.69 g, 13.5 mmol) was co-evaporated with dry toluene (2×10 ml) and then dissolved in dry dichoromethane (20 ml) and cooled to 0°C (ice-water bath). Trichloroacetonitrile (23.3 ml, 0.232 mol) followed by DBU (820 µl, 5.49 mmol) were added. After 35 min, the reaction mixture was extracted with saturated aqueous sodium hydrogen carbonate (100 ml). The layers were separated and the aqueous layer was back-extracted with dichloromethane (2×20 ml). The combined organic layers were dried ($MgSO_4$) and concentrated under reduce pressure. The residue was purified by column chromatography on silica gel. The approprate fractions, which were eluted with toluene–ethyl acetate (3.5:1 v/v) were combined and evaporated under reduced pressure to give the *title compound* as a white glass (5.31 g, 79.8%).

δ_H[$CDCl_3$, 300 MHz]: 2.02 (3 H, s, CH_3), 2.08 (3 H, s, CH_3), 2.09 (3 H, s, CH_3), 2.21 (3 H, s, CH_3), 4.14 (1 H, m, H-6), 4.22 (1 H, m, H-5), 4.29 (1 H, m, H-6'), 5.41 (1 H, m, H-3), 5.42 (1 H, m, H-2), 5.48 (1 H, m, H-4), 6.29 (1 H, d, J = 1.6, H-1), 8.80 (1 H, s, NH).
δ_C[$CDCl_3$, 75.5MHz]: 20.6 (CH_3), 20.7 (CH_3), 20.8 (CH_3), 60.0 (CH, C-6), 65.4 (CH, C-2), 67.8 (CH, C-4), 68.7 (CH, C-3), 71.2 (CH, C-5), 94.5 (CH, C-1), 159.7 (C, C=NH), 169.6 (C, C=O), 169.7 (C, C=O), 169.8 (C, C=O), 170.6 (C, C=O)
R_f: 0.50 (toluene–ethyl acetate, 3.5:1 v/v)

2,3,4,6-*O*-Tetraacetyl-(2-chloroethyl)-*α*-D-mannoside 67

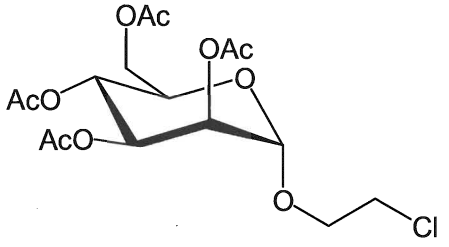

2,3,4,6-*O*-Tetraacetyl D-mannosyl *α*-trichloroacetimidate **66** (5.31 g, 10.8 mmol) was co-evaporated with dry toluene (2×10 ml) and then dissolved in dry dichoromethane (20 ml). Freshly distilled 2-chloroethanol (1.88 ml, 28.0 mmol) and 4 Å activated molecular sieve powder (1.0 g) were added, and the mixture was cooled to -78°C (dry ice-acetone). To this solution was added a pre-cooled solution (-78°C) of boron trifluoride diethyl etherate (2.3 ml, 18.3 mmol) in dry dichloromethane by cannulation. After 1 h, the mixture was warmed up to room temperature, and then extracted with saturated aqueous sodium hydrogen carbonate (100 ml). The layers were separated and the aqueous layer was back-extracted with dichloromethane (2×20 ml). The combined organic layers were dried ($MgSO_4$) and concentrated under reduced pressure. The residue was purified by column chromatography on silica gel. The approprate fractions, which were eluted with hexane–ethyl acetate (3:2 v/v) were combined and evaporated under reduced pressure to give the *title compound* as a white glass (3.17 g, 71.5%).

FAB-MS found $[M+H]^+$ = 411.10556, $C_{16}H_{24}ClO_{10}^+$ requires 411.10580.
δ_H[$CDCl_3$, 300 MHz]: 2.00 (3 H, s, CH_3), 2.06 (3 H, s, CH_3), 2.11 (3 H, s, CH_3), 2.17 (3 H, s, CH_3), 3.67 (2 H, t, J = 5.6, $OCH_2C\underline{H_2}Cl$), 3.83 (1 H, dt, J = 5.3 and 10.6,

$OC\underline{H_2}CH_2Cl$), 3.93 (1 H, dt, J = 5.9 and 11.3, $OC\underline{H_2}CH_2Cl$), 4.12 (1 H, m, H-5), 4.16 (1 H, m, H-6), 4.30 (1 H, m, H-6'), 4.88 (1 H, d, *J* = 1.1, H-1), 5.26–5.38 (3 H, m, H-2, H-3, and H-4)

δ_C[$CDCl_3$, 300 MHz]: 20.6 (CH_3), 20.7 (CH_3), 20.9 (CH_3), 42.4 ($OCH_2\underline{C}H_2Cl$), 62.4 (C-6), 66.0 (CH), 68.6 ($O\underline{C}H_2CH_2Cl$), 68.9 (CH), 69.0 (C-5), 69.4 (CH), 97.8 (C-1), 169.8 (C=O), 169.9 (C=O), 170.0 (C=O), 170.6 (C=O)

R_f: 0.43 (hexane–ethyl acetate, 3:2 v/v)

2,3,4,6-*O*-Tetraacetyl-(2-azidoethyl)-*α*-D-mannoside 68

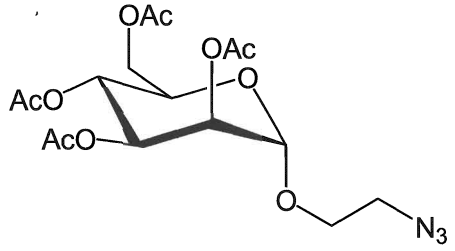

2,3,4,6-*O*-Tetraacetyl-(2-chloroethyl)-*α*-D-mannoside **67** (2.00 g, 4.98 mmol) was dissolved in DMF (30 ml) followed by addition of sodium azide (1.59 g, 24.5 mmol). The mixture was heated at 50°C for 3 d. The mixture was then cooled to room temperature and was filtered. The filtrate was concentrated under reduced pressure and the residue was purified by column chromatography on silica gel. The approprate fractions, which were eluted with hexane–ethyl acetate (3:2 v/v) were combined and evaporated under reduced pressure to give the *title compound* as a white glass (1.94 g, 95.3%).

FAB-MS found $[M+H]^+$ = 418.14481, $C_{16}H_{24}N_3O_{10}^+$ requires 418.14617.

δ_H[$CDCl_3$, 300 MHz]: 2.00 (3 H, s, CH_3), 2.06 (3 H, s, CH_3), 2.11 (3 H, s, CH_3), 2.17 (3 H, s, CH_3), 3.48 (2 H, m, CH_2), 3.68 (1 H, m, $OC\underline{H_2}CH_2N_3$), 3.88 (1 H, m, $OCH_2C\underline{H_2}N_3$), 4.05 (1 H, m, H-5), 4.13 (1 H, dd, *J* = 2.3 and 12.3, H-6), 4.30 (1 H, dd, *J* = 5.3 and 12.3, H-6'), 4.88 (1 H, s, H-1), 5.26–5.39 (3 H, m, H-2, H-3, and H-4)

δ_C[$CDCl_3$, 75.5 MHz]: 20.6 (CH_3), 20.7 (CH_3), 20.8 (CH_3), 20.9 (CH_3), 50.3 ($OCH_2\underline{C}H_2N_3$), 62.4 (CH_2, C-6), 66.0 (CH), 67.0 ($O\underline{C}H_2CH_2N_3$), 68.8 (2×CH), 69.4 (CH), 97.7 (CH, C-1), 169.7 (C=O), 169.8 (C=O), 170.0 (C=O), 170.6 (C=O)

R_f: 0.43 (hexane–ethyl acetate, 4:6 v/v)

α-(2-Aminoethyl)-D-mannoside 69

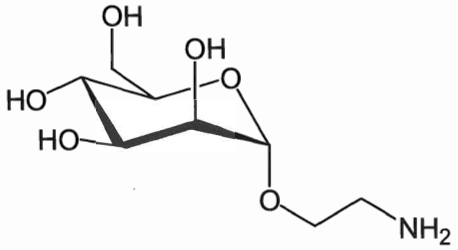

2,3,4,6-*O*-Tetraacetyl-(2-azidoethyl)-α-D-mannoside **68** (0.61 g, 1.46 mmol) was dissolved in methanol (8.0 ml) followed by addition of a solution of sodium methoxide in methanol (25 wt% solution in methanol, 79 µl, 0.36 mmol). After 30 min, pre-washed Amberlite IR 120 (hydrogen form) (1.45 g) was added and stirred for 2 min. The resin was removed by filtration and the filtrate was concentrated under reduced pressure to give α-(2-azidoethyl)-D-mannoside as a colorless gum (0.283 g).

A portion of the above product (0.142 g, 0.57 mmol) was dissolved in water (10 ml) followed by addition of Pd/C (20.0 mg, 5% Pd on charcoal). The mixture was stirred under an atmosphere of hydrogen for 6 h at room temperature. The products were filtered through a bed of celite. The filtrate was concentrated under reduced pressure to give *title compound* as a colorless gum (0.109 g, 66.9% over two steps).

FAB-MS found $[M+H]^+ = 224.11771$, $C_8H_{18}NO_6^+$ requires 224.11341.

δ_H[D_2O, 300 MHz]: 2.74 (2 H, dd, J = 5.5 and 14.4, $OCH_2C\underline{H_2}NH_2$), 3.44 (1 H, m, $OC\underline{H_2}CH_2NH_2$), 3.53–3.81 (6 H, m, H-3, H-4, H-5, H-6, H-6', and $OC\underline{H_2}CH_2NH_2$), 3.87 (1 H, m, H-2), 4.77 (1 H, d, J = 1.6, H-1)

δ_C[D_2O, 75.5 MHz]: 39.8 ($OCH_2\underline{C}H_2NH_2$), 60.9 (C-6), 66.7 (CH), 68.5 ($O\underline{C}H_2CH_2NH_2$), 69.9 (C-2), 70.5 (CH), 72.7 (CH), 99.8 (C-1)

Monovalent mannosyl squarate 73

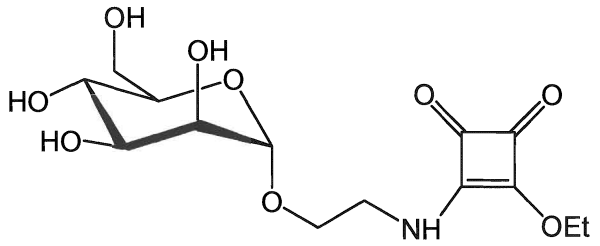

α-(2-Aminoethyl)-D-mannoside (35.5 mg, 0.16 mmol) was dissolved in distilled water (200 µl), followed by addition of methanol (1.8 ml), 3,4-diethoxy-3-cyclobutene-1,2-dione (140 µl, 0.95 mmol), and triethylamine (5 µl). After 5 min, the solvents were quickly removed under reduced pressure. The residue was diluted with distilled water (1.0 ml) and purified by size exclusion column on Bio-Gel P2 gel (fine, 1.6 × 75 cm), eluted with milliQ water. The appropriate fractions were combined and freeze-dried to give the *title compound* as a light yellow amorphous solid (23.0 mg, 41.4%).

FAB-MS found $[M+H]^+ = 348.12946$, $C_{14}H_{22}NO_9^+$ requires 348.12765

δ_H[D_2O, 600 MHz recorded at 10°C]: 1.15 (t, J = 7.0, -$OCH_2C\underline{H}_3$), 1.17 (t, J = 7.0, -$OCH_2C\underline{H}_3$) (these two signals integrate 3 H), 3.26-3.63 (10 H, m, H-2, H-3, H-4, H-5, H-6, H-6', and CH_2), 4.44 (q, J = 7, -$OC\underline{H}_2CH_3$), 4.47 (q, J = 7, -$OC\underline{H}_2CH_3$) (these two signals integrate 2 H), 4.58 (1 H, d, J = 6.0, H-1)

R_f: 0.69 (chloroform–methanol–water, 65:35:5 v/v)

***2*-(Benzyloxycarbonyl)tris(2-aminoethyl)amine 75**

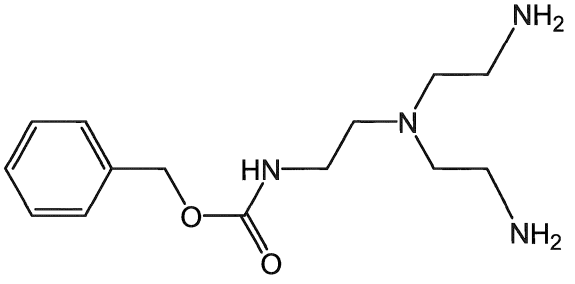

Tris(2-aminoethyl)amine **73** (2.92 g, 20.0 mmol) was dissolved in dry dichloromethane (50 ml) and cooled (ice-water bath). A solution of benzyl chloroformate (1.03 ml, 7.22 mmol) in dry dichloromethane (100 ml) was added over a period of 1 h. The mixture was

allowed to warm up to room temperature slowly. After an additional 1 h, the solvent was removed under reduced pressure. The residue was purified by column chromatography on silica gel. The approprate fractions, which were eluted with chloroform–methanol–amonium hydroxide (10:4:1 v/v) were combined and evaporated under reduced pressure to give the *title compound* as a yellow oil (1.25 g, 61.8% based on benzyl chloroformate).

FAB-MS found $[M+H]^+ = 281.19946$, $C_{14}H_{25}N_4O_2^+$ requires 281.19775.

δ_H[$CDCl_3$, 300 MHz]: 2.51 (4 H, t, J = 6, -$NCH_2C\underline{H_2}NH_2$), 2.56 (2 H, t, J = 5.9, CH_2), 2.72 (4 H, t, $\underline{J}$ = 6, -$NC\underline{H_2}CH_2NH_2$), 3.26 (2 H, br, CH_2), 4.78 (4 H, br, NH_2), 5.10 (2 H, s, -$C\underline{H_2}$Ph), 6.05 (1 H, br, NH), 7.31–7.37 (5 H, m, Ar)

δ_C[$CDCl_3$, 75.5 MHz]: 39.4 (CH_2), 39.6 (CH_2), 53.7 (CH_2), 57.0 (CH_2), 66.5 (CH_2), 128.0 (CH), 128.1 (CH), 128.5 (CH), 136.8 (C), 156.7 (C=O).

R_f: 0.22 (chloroform–methanol–ammonium hydroxide, 10: 4:1 v/v)

2,2'-Bissuccinoyl-2''-(benzyloxycarbonyl)tris(2-aminoethyl)amine 76

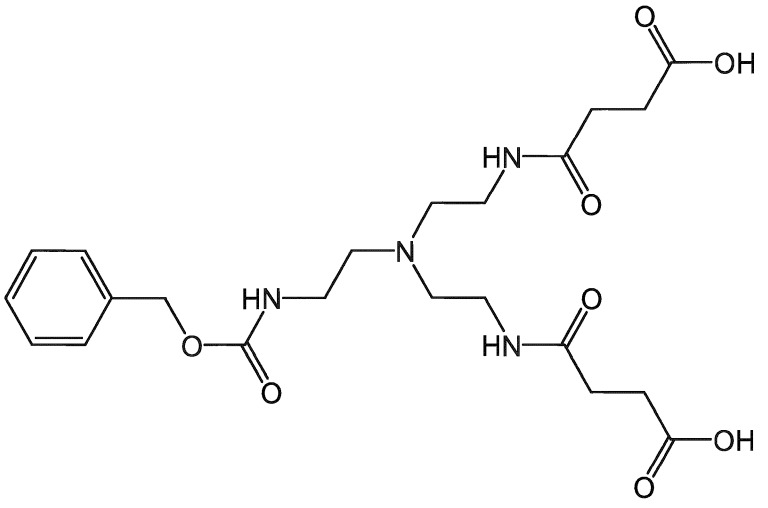

2-(Benzyloxycarbonyl)tris(2-aminoethyl)amine **75** (1.88 g, 6.71 mmol) was co-evaporated with dry toluene (2×10 ml) and then dissolved in dry pyridine (30 ml). Succinic anhydride (1.47 g, 14.7 mmol) was added at room temperature. After 40 min, the products were concentrated under reduced pressure. The residue was dissolved in

methanol (5 ml) and added drop-wise to diethyl ether (300 ml) under stirring. The product was collected by filtration as a white amorphous solid (2.71 g, 84.1%).

ESI-MS found $[M-H]^-$= 479.2, $C_{22}H_{31}N_4O_8^-$ requires 479.2.

δ_H[D_2O, 600 MHz]: 2.37 (4 H, t, J = 6.0, CH_2), 2.41 (4 H, t, J = 6.2, CH_2), 3.26 (6 H, m), 3.39 (5 H, m), 5.01 (2 H, -CH_2Ph), 7.25–7.40 (5 H, Ar)

R_f: 0.12 (chloroform–methanol–ammonium hydroxide, 10: 4:1 v/v)

Trifluoroacetate salt of 2,3,4,6-*O*-tetraacetyl-(2-aminoethyl)-*α*-D-mannoside 70

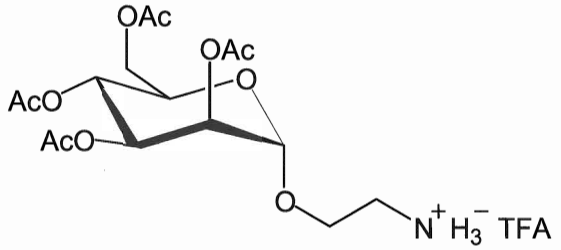

2,3,4,6-*O*-Tetraacetyl-(2-azidoethyl)-*α*-D-mannoside **68** (600.00 mg, 1.44 mmol) was dissolved in methanol (25 ml) followed by addition of Pd/C (42.00 mg, 5% Pd on charcoal) and trifluoroacetic acid (200 µl, 2.65 mmol). The reaction mixture was stirred under an atmosphere of hydrogen for 5 h at room temperature. The products were filtered through a bed of celite. The filtrate was concentrated under reduced pressure and used for the next reaction without further purification.

Fully-protected bivalent mannoside 77

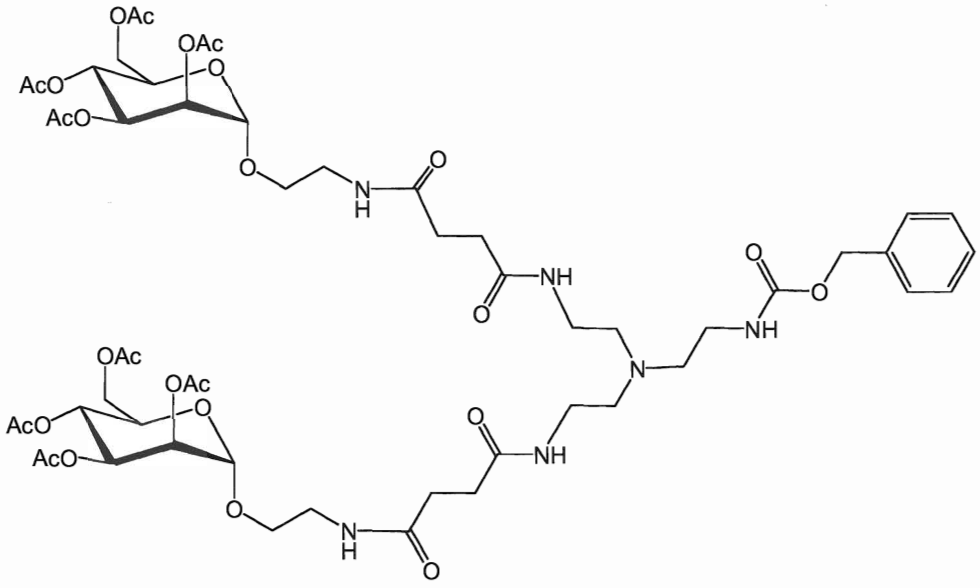

2,2'-Bissuccinoyl-2''-(benzyloxycarbonyl)tris(2-aminoethyl)amine **76** (0.230 g, 0.48 mmol) was dissolved in dry dichloromethane (10 ml). Then (benzotriazol-1-yloxy)tris(dimethylamino)phosphonium hexafluorophosphate (BOP) (0.424 g, 0.96 mmol) followed by Hünig's base (0.75 ml, 4.31 mmol) were added at room temperature. After 20 min, a solution of the trifluoroacetate salt of 2,3,4,6-*O*-tetraacetyl-(2-aminoethyl)-α-D-mannoside **70** (1.44 mmol, prepared as described above) in dry dichloromethane (5 ml) was added. The reaction was allowed to proceed at room temperature for 12 h. The products were then concentrated under reduced pressure. The residue was purified by column chromatography on silica gel. The appropriate fractions, which were eluted with dichloromethane–methanol (95:5 v/v) were combined and evaporated under reduced pressure to give the *title compound* as a white glass (0.309 g, 52.5%).

FAB-MS found $[M+H]^+$ = 1227.60795, $C_{54}H_{79}O_{26}N_6$ requires 1227.50441

δ_H[$CDCl_3$, 300 MHz]: 2.01 (CH_3), 2.07 (CH_3), 2.12 (CH_3), 2.17 (CH_3), 4.00 (2 H, br, H-5man), 4.12 (2 H, dd, J = 2.0 and 12.0, H-6man), 4.29 (2 H, dd, J = 5.0 and 12.0, H-6'man), 4.82 (2 H, s, H-1man), 5.10 (2 H, s, -C$\underline{H_2}$Ph), 5.28–5.31 (6 H, br, m, H-2, H-3, H-4man), 7.36 (5 H, Ar).

R_f: 0.51 (dichloromethane–methanol, 90:10 v/v)

Fully-deprotected bivalent mannoside 78

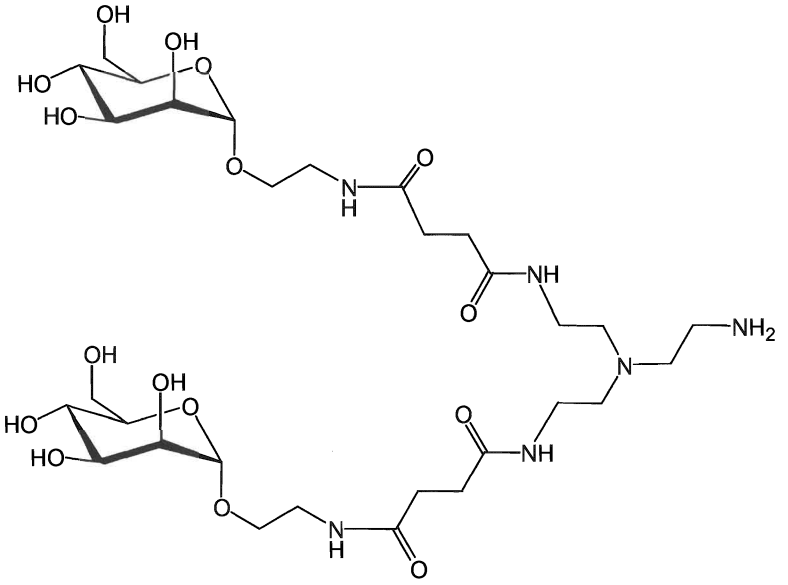

Fully-protected bivalent mannoside **77** (0.194 g, 0.158 mmol) was dissolved in methanol (3 ml) followed by addition of a solution of sodium methoxide in methanol (25 wt%, 9 µl, 0.042 mmol). After 1 h, pre-washed Amberlite IR 120 resin (hydrogen form, 300 mg) was added and stirred for 5 min. The resin was removed by filtration and the filtrate was concentrated under reduced pressure. The residue was redissolved in methanol (15 ml) followed by addition of Pd/C (30.0 mg, 5% Pd on charcoal). The reaction mixture was stirred in an atmosphere of hydrogen at room temperature for 3 h. The products were filtered through a bed of celite. The filtrate was concentrated under reduced pressure and the residue was purified by size exclusion column on Bio-Gel P2 (fine, 1.6 × 75 cm), eluted with aqueous ammonium bicarbonate buffer (30 m*M*). The appropriate fractions were combined and freeze-dried to give the *title compound* as a colorless glass (0.115 g, 96.2%).

FAB-MS found $[M+H]^+$ = 757.40622, $C_{30}H_{58}O_{16}N_6^+$ requires 757.38311

δ_H[D_2O, 600 MHz]: 2.66 (8 H, s, br, CH_2), 2.80 (4 H, s, br, CH_2), 2.85 (2 H, s, br, CH_2), 3.05 (2 H, s, br, CH_2), 3.41 (4 H, s, br, CH_2), 3.50–3.53 (2 H, m, H-6), 3.57–3.60 (2 H, m, H-6'), 3.71–3.75 (4 H, m, CH_2 and H-5), 3.78 (2 H, t, J = 9.6, H-4), 3.86-3.93 (6 H, m, CH_2 and H-3), 4.01 (2 H, d, J = 12, CH_2), 4.07 (2 H, s, H-2), 4.99 (2 H, s, H-1).

δ_C[D_2O, 150.9 MHz]: 31.2 (CH_2), 31.3 (CH_2), 37.2 (CH_2), 39.2 (C-6), 52.62 (CH_2), 61.2 (CH_2), 66.1 (CH_2), 67.0 (C-4), 70.3 (C-2), 70.8 (C-3), 73.1 (C-5), 99.9 (C-1), 175.0 (C=O).

R_f: 0.20 (methanol–ammonium hydroxide, 4:1 v/v)

Squarate-activated bivalent-mannoside 80

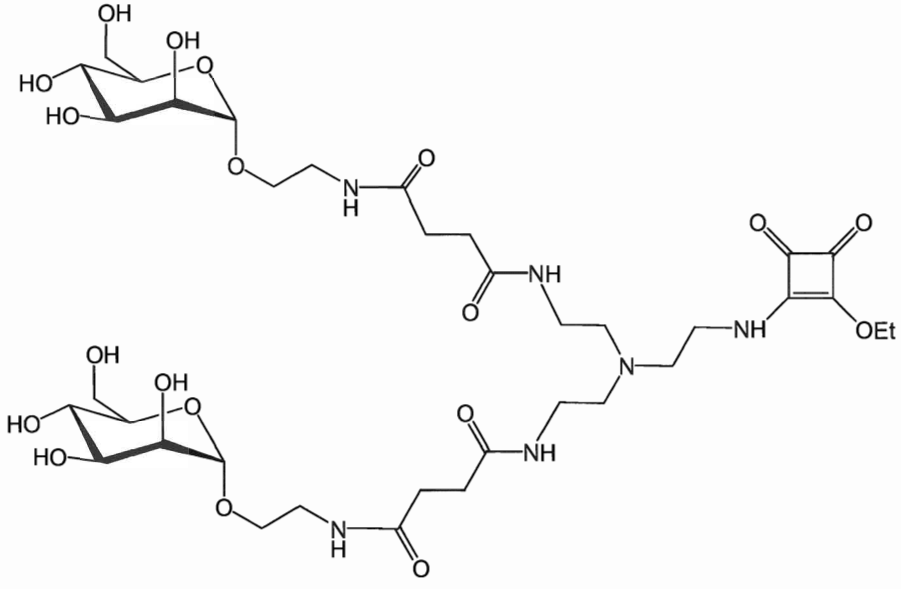

Bivalent mannoside **79** (17.9 mg, 23.7 μmol) was dissolved in distilled water (100 μl), followed by addition of methanol (900 μl), 3,4-diethoxy-3-cyclobutene-1,2-dione (21 μl, 142 μmol), and triethylamine (3 μl). After 7 min, the solvents were quickly removed under reduced pressure. The residue was diluted with distilled water (1.0 ml) and purified by size exclusion column on Bio-Gel P2 resin (fine, 1.6 × 75 cm), eluted with milliQ water. The appropriate fractions were combined and freeze-dried to give the *title compound* as a light yellow amorphous solid (11.6 mg, 55.6%).

FAB-MS found $[M+H]^+$ = 881.38400, $C_{36}H_{61}O_{19}N_6^+$ requires 881.39915

δ_H[D_2O, 600 MHz recorded at 5°C]: 1.07 (t, J = 7.2, -$OCH_2C\underline{H}_3$), 1.08 (7, J = 7.2, -$OCH_2C\underline{H}_3$) (these two signals integrate 3 H), 2.16–2.18 (8 H, m, br, CH_2), 2.36 (4 H, s, br, CH_2), 2.45 (2H, s. br, CH_2), 2.94 (4 H, s, br, CH_2), 2.99–3.02 (2 H, m, H-6), 3.09–3.12 (2 H, m, H-6'), 3.19–3.30 (6 H, m, H-4, H-5, and CH_2), 3.35–3.45 (6 H, m, H-3 and

CH_2), 3.51 (2 H, d, J = 12.0, CH_2), 3.57 (2 H, s, br, H-2), 4.35 (q, J = 7.1, -OC$\underline{H_2}$CH$_3$), 4.39 (q, J = 7.1, -OC$\underline{H_2}$CH$_3$) (these two signals integrate 2 H), 4.49 (2 H, s, H-1).

R_f: 0.45 (methanol–ammonium hydroxide, 4:1 v/v)

3',5'-*O*-(1,1,3,3-Tetraisopropyldisiloxy)-4-*N*-benzoylcytidine 85c

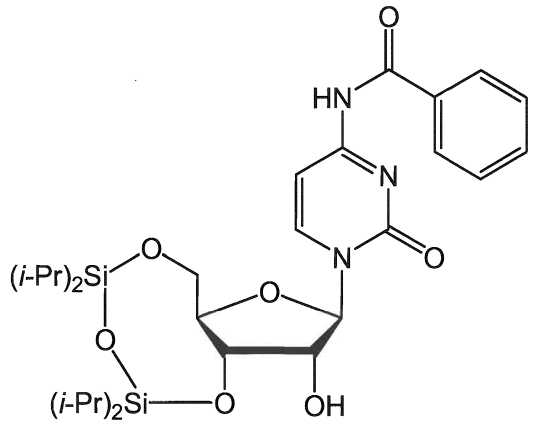

4-*N*-Benzoylcytidine **84c** (5.22 g, 15.0 mmol), which had been dried at 90°C *in vacuo* for 6 h, was co-evaparated with dry pyridine (2×10 ml). The residue was redissolved in dry pyridine (50 ml) and cooled to 0°C followed by addition of 1,3-dichloro-1,1,3,3-tetraisopropyldisiloxane (5.24 g, 16.6 mmol, 1.1 mol equiv.). After stirring at 0°C for 30 min, the mixture was warmed up to room temperature and stirred for another 3.5 h. Then water (5 ml) was added, and after 5 min, the products were concentrated under reduced pressure. The residue was dissolved in dichloromethane (120 ml) and washed with saturated aqueous sodium hydrogen carbonate (100 ml). The layers were separated and the aqueous layer was back-extracted with dichloromethane (2×20 ml). The combined dried ($MgSO_4$) organic layers were concentrated under reduced pressure and the residue was purified by column chromatography on silica gel. The approprate fractions, which were eluted with dichloromethane–methanol (98:2 v/v) were combined and evaporated under reduced pressure to give the *title compound* as a white glass (6.71 g, 75.8%).

FAB-MS found $[M+H]^+$ = 590.27355, $C_{28}H_{43}O_7N_3Si_2^+$ requires 590.27178.

δ_H[$(CD_3)_2SO$, 600 MHz]: 0.97-1.08 (28 H, m, CH_3 and CH), 3.95 (1 H, d, J = 13.1, H-5'), 4.11 (3 H, s, H-2, H-3, and H-4), 4.24 (1 H, d, J = 13.4, H-5''), 5.82 (1 H, d, J = 3.7,

H-1'), 7.37 (1 H, d, J = 7.5, H-5), 7.52 (2 H, t, J = 7.7, CH), 7.63 (1 H, t, J = 7.4, CH), 8.01 (2 H, d, J = 7.7, CH), 8.21 (1 H, d, J = 7.4, H-6), 11.29 (1 H, s, NH).

δ_C[$(CD_3)_2SO$, 150.9 MHz]: 12.3-13.2 (CH_3), 17.2-17.9 (CH), 60.3 (CH_2, C-5'), 68.5 (CH), 74.3 (CH), 81.4 (CH), 91.8 (CH, C-1'), 96.0 (CH, C-5), 128.9 (CH), 133.2 (CH), 144.2 (CH, C-6), 154.6 (C), 163.6 (C), 167.8 (C), 206.9 (C, C=O)

R_f: 0.53 (dichloromethane–methanol, 95:5 v/v)

2'-*O*-[1-(4-Chlorophenyl)-4-ethoxypiperidin-4-yl]-4-*N*-benzoylcytidine 86c

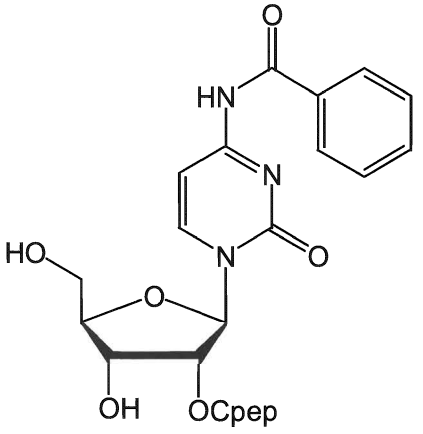

3',5'-*O*-(1,1,3,3-Tetraisopropyldisiloxy)-4-*N*-benzoylcytidine **85c** (6.50 g, 11.0 mmol) and 1-(4-chlorophenyl)-4-ethoxy-1,2,5,6-tetrahydropiperidine (7.87 g, 33.1 mmol, 3 mol equiv.) were co-evaporated with dry toluene (2×10 ml) and then dissolved in dry dichoromethane (40 ml), followed by addition of freshly distilled trifluoroacetic acid (2.1 ml, 20.0 mmol, 2 mol equiv.). After 6 h, triethylamine (3.0 ml, 31.4 mmol, 3 mol equiv.) was added and the products were partitioned between dichloromethane (100 ml) and saturated aqueous sodium hydrogen carbonate (100 ml). The layers were separated and the dried ($MgSO_4$) organic layer was concentrated under reduced presure. The residue was taken up with acetonitrile (30 ml) followed by addition of a solution of tetraethyl ammonium fluoride in acetonitrile (40 ml, 2.2 mol equiv., 1.0 *M*, pH 8.0). After 30 min, the products were concentrated under reduced presure and the residue was purified by column chromatography on silica gel. The appropriate fractions, which were eluted with dichloromethane-methanol (97:3 v/v) were collected and concentrated under reduced pressure to give the *title compound* as a white glass (5.08 g, 79.1%).

FAB-MS found M^+ = 584.20269, $C_{29}H_{33}ClO_7N_4^+$ requires 584.20378.

δ_H[$(CD_3)_2SO$, 600 MHz]: 0.90-0.94 (3 H, m, CH_3), 1.73-1.91 (4 H, m, CH_2), 2.88 (1 H, t, J = 9.5, CH_2), 3.01 (1 H, t, J = 9.5, CH_2), 3.17 (1 H, m, CH_2), 3.26 (1 H, m, CH_2), 3.38 (1 H, m, CH_2), 3.45 (1 H, m, CH_2), 3.63 (1 H, m, H-5'), 3.67 (1 H, m, H-5''), 3.98 (1 H, d, J = 2.2, H-4'), 4.05 (1 H, m, H-3'), 4.44 (1 H, d, J = 5.9, H-2'), 5.18 (1 H, d, J = 5.0, 3'-OH), 5.30 (1 H, t, J = 4.9, 5'-OH), 6.15 (1 H, d, J = 6.7, H-1'), 6.91 (2 H, d, J = 9.0, CH_2), 7.18 (2 H, d, J = 8.9, CH_2), 7.41 (1 H, br, H-5), 7.52 (2 H, t, J = 7.7, CH), 7.63 (1 H, t, J = 7.4, CH), 8.01 (2 H, d, J = 7.7, CH), 8.49 (1 H, br, H-6), 11.31 (1 H, br, NH).

δ_C[$(CD_3)_2SO$, 150.9 MHz]: 13.1 (CH_3), 15.5 (CH), 32.4 (CH_2), 33.7 (CH_2), 45.9 (CH_2), 46.2 (CH_2), 55.4 (CH_2), 56.5 (CH_2), 61.8 (CH, C-5'), 71.2 (CH, C-3'), 74.1 (CH, C-2'), 86.9 (CH, C-4'), 87.8 (CH, C-1'), 98.7 (CH, C-5), 117. 6 (CH), 122.4 (CH), 128.7-129.4 (CH), 146.2 (CH, C-6)

R_f: 0.48 (dichloromethane–methanol, 95:5 v/v)

2'-*O*-[1-(4-Chlorophenyl)-4-ethoxypiperidin-4-yl]-5'-*O*-(4,4'-dimethoxytrityl)-4-*N*-benzoylcytidine 87c

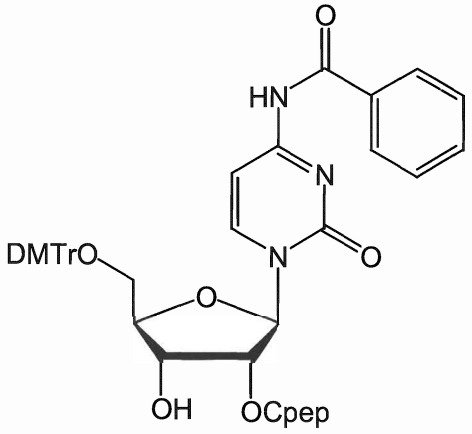

2'-*O*-[1-(4-Chlorophenyl)-4-ethoxypiperidin-4-yl]-4-*N*-benzoylcytidine **86c** (5.32 g, 9.1 mmol) was co-evaporated with dry pyridine (2×5 ml). The residue was redissolved in dry pyridine (45 ml) followed by addition of 4,4'-dimethoxytrityl chloride (3.39 g, 10.0 mmol, 1.1 mol equiv.). After 40 min, triethylamine (5 ml) was added. After another 10 min, the products were partitioned between dichloromethane (100 ml) and saturated aqueous sodium hydrogen carbonate (100 ml). The layers were separated and the dried

($MgSO_4$) organic layer was concentrated under reduced presure. The residue was purified by column chromatography on silica gel. The appropriate fractions, which were eluted with dichloromethane–methanol (98.5:1.5 v/v), were collected and concentrated under reduced pressure to give the *title compound* as a yellow glass (7.71 g, 95.4%).

FAB-MS found M^+ = 886.32870, $C_{50}H_{51}ClO_9N_4^+$ requires 886.33446

δ_H[$(CD_3)_2SO$, 600 MHz]: 0.99 (3 H, t, J = 6.9, CH_3), 1.78-1.94 (4 H, m, CH_2), 2.96 (1 H, t, J = 9.5, CH_2), 3.06 (1 H, t, J = 9.2, CH_2), 3.24-3.31(3 H, m, CH_2), 3.40-3.43 (2 H, m, CH_2), 3.57 (1 H, t, J = 7.7, CH_2), 3.75 (6 H, s, 2×CH_3), 4.11 (1 H, d, J = 2.9, H-4'), 4.22 (1 H, d, J = 4.1, H-3'), 4.59 (1 H, t, J = 5.4, H-2'), 5.31 (1 H, d, J = 5.9, 3'-OH), 6.15 (1 H, d, J = 5.5, H-1'), 6.92-6.95 (6 H, m, Ar), 7.19 (3 H, d, J = 9.0, Ar and H-5), 7.29 (5 H, m, Ar), 7.35 (2 H, t, J = 7.6, Ar), , 7.42 (2 H, d, J = 7.7, Ar), 7.52 (2 H, t, J = 7.7, Ar), 7.63 (1 H, t, J = 7.4, Ar), 8.01 (2 H, d, J = 7.6, Ar), 8.25 (1 H, d, J = 7.3, H-6), 11.34 (1 H, s, NH).

δ_C[$(CD_3)_2SO$, 150.9 MHz]: 15.5 (CH_3), 32.8 (CH_2), 33.5 (CH_2), 46.1 (CH, C-5'), 55.5 (CH_2 and CH_3), 63.8 (CH_2), 70.8 (CH, C-3'), 74.0 (CH, C-2'), 84.5 (CH, C-4'), 86.7 (CH, C-1'), 100.0 (CH, C-5), 113.1-136.5 (CH), 144.9 (CH, C-6)

R_f: 0.54 (dichloromethane–methanol, 95:5 v/v)

2'-*O*-[1-(4-Chlorophenyl)-4-ethoxypiperidin-4-yl]-5'-*O*-(4,4'-dimethoxytrityl)-4-*N*-benzoylcytidine 3'-(2-*O*-cyanoethyl) *N,N*-diethylphosphoramidite 88c

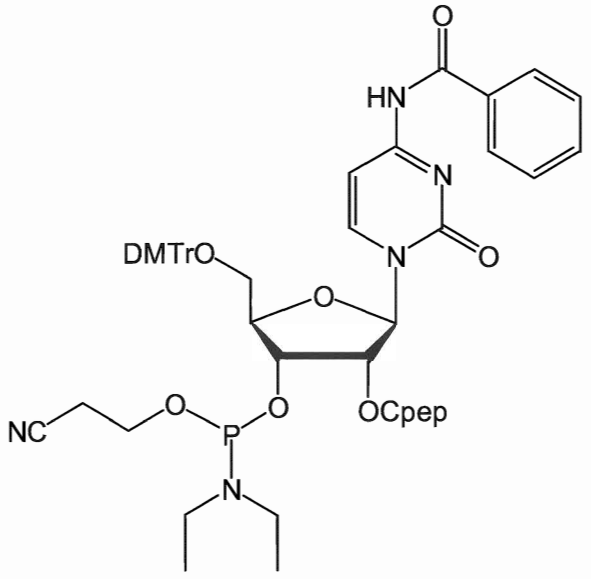

2'-*O*-[1-(4-Chlorophenyl)-4-ethoxypiperidin-4-yl]-5'-*O*-(4,4'-dimethoxytrityl)-4-*N*-benzoylcytidine **87c** (2.00 g, 2.25 mmol) was co-evaporated with dry toluene(2×5 ml). The residue was redissolved in dry THF (30 ml) followed by addition of *N,N*-diisopropylethylamine (978 µl, 5.63 mmol, 2.5 mol equiv.). After 5 min, 2-*O*-cyanoethyl-*N,N*-diethyl phosphorochloridite[113] (0.94 g, 4.51mmol, 2 mol equiv.) was added. After 3 h, the solvent was removed under reduced pressure. The residue was purified by column chromatography on silica gel. The appropriate fractions, which were eluted with hexane–acetone–triethylamine (65:30:2 v/v) were collected and concentrated under reduced pressure to give the *title compound* as a light yellow glass (2.06 g, 85.5%).

δ_H[$CDCl_3$, 300 MHz]: 4.25 (s, H-4'), 4.37 (s, H-4') (these two signals integrate 1 H), 4.51 (1 H, m, H-3'), 4.87 (dd, *J* = 4.6 and 6.5, H-2'), 4.87 (dd, *J* =5.1 and 6.5, H-2') (these two signals integrate 1 H), 6.42 (d, *J* =7.0, H-1'), 6.45 (d, *J* = 6.5, H-1') (these two signals integrate 1 H), 7.02 (d, *J* = 7.5, H-5), 7.03 (d, *J* = 7.5, H-5) (these two signals integrate 1 H), 8.22 (d, *J* = 7.5, H-6), 8.25 (d, *J* = 7.6, H-6) (these two signals integrate 1 H), 6.81-7.93 (22 H, Ar).

δ_P[$CDCl_3$,121.5 MHz]: 149.22 and 150.13

R_f: 0.40 (hexane–acetone–triethylamine, 65:30:2 v/v)

2',3',5'-O-Triacetyl guanosine 82

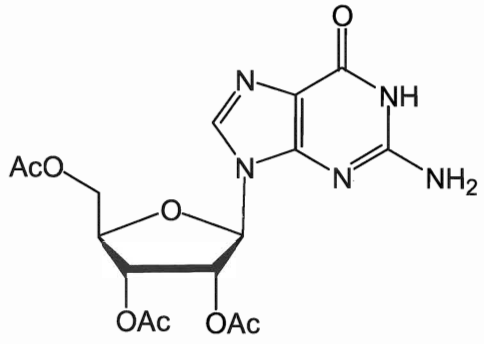

Guanosine **81** (8.50 g, 30.0 mmol) was co-evaporated successively with dry toluene (2×10 ml) and dry pyridine (10 ml). The residue was dissolved in dry DMF (35 ml) and dry pyridine (15 ml), followed by addition of acetic anhydride (18 ml, 0.19 mol, 6 mol. equiv.). The mixture was stirred at room temperature for 1 h, and then heated at 75° C for 2 h. Then the reaction mixture was cooled to room temperature and quenced by addition of methanol (20 ml). The mixture was then concentrated to *ca.* 1/2 of the original volume under reduced pressure to yield a white precipitate. The solid was isolated by filtration. The filtrate was further concentrated under reduced pressure until white solid precipated out of solution. The products from the two crops were combined to yield 2',3',5'-*O*-triacetyl guanosine as a white solid (10.49 g, 85.4%).

δ_H[$(CD_3)_2SO$, 300 MHz]: 2.04-2.11 (9 H, m, CH_3), 4.28-4.35 (3 H, m, H-4', H-5' and H-5''), 5.50 (1 H, m, H-3'), 5.79 (1 H, t, J = 6.0, H-2'), 5.98 (1 H, d, J = 6.2, H-1'), 6.53 (2 H, s, NH_2), 7.93 (1 H, s, H-8), 10.73 (1 H, br, NH).

R_f: 0.64 (dichloromethane–methanol, 90:10 v/v)

2-*N*-Phenylacetylguanosine 83

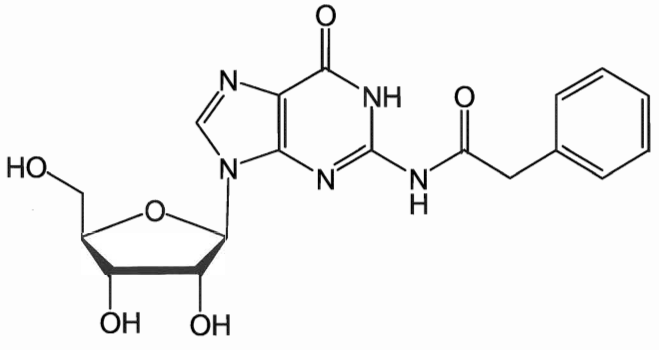

2',3',5'-*O*-Triacetyl guanosine **82** (10.49 g, 25.6 mmol) was co-evaporated with dry toluene (2×10 ml), and then dissolved in acetonitrile (140 ml) and dry pyridine (40 ml). The mixture was stired for 10 min and cooled to 0°C. A solution of phenylacetyl chloride (9.0 ml, 64 mmol, 2.5 mol equiv.) in acetonitrile (30 ml) was added to the above mixture over a period of 30 min at 0°C. This reaction mixture was stirred at room temperature for 1 h and then at 60°C overnight. The reaction was quenched by addition of ice-water (5 ml), followed by addition of toluene (100 ml), and shaked overnight. The organic layer was isolated and concentrated under reduced pressure. The yellow froth residue was dissolved in methanol (140 ml) and cooled to 0°C. Cold NaOH solution (2 *M*, 86 ml) was added over 5 min. The mixture was stirred at 0°C for 10 min, and was then neutralized by addition of hydrochloric acid (2 *M*) to pH 6. After addition of ethyl acetate (100 ml), the percipitate was collected by filtration to give the 2-*N*-phenylacetyl guanosine (2.39 g, 23.3%).

δ_H[$(CD_3)_2SO$, 300 MHz]: 3.81 (2 H, s, CH_2), 3.57 (1 H, m, H-5'), 3.63 (1 H, m, H-5''), 3.91 (1 H, m, H-4'), 4.13 (1 H, t, J = 3.9, H-3'), 4.44(1 H, t, J = 5.1, H-2'), 5.05 (1 H, t, J = 5.1, 5'-OH), 5.18 (1 H, s, 3'-OH), 5.48 (1 H, s, 2'-OH), 5.81 (1 H, d, J = 5.8, H-1'), 7.27-7.35 (5 H, m, CH), 8.26 (1 H, s, H-8), 11.98 (1 H, s, NH).

R_f: 0.32 (dichloromethane–methanol, 95:5 v/v)

2-*N*-Phenylacetyl-3',5'-*O*-(1,1,3,3-tetraisopropyldisiloxy)guanosine 85d

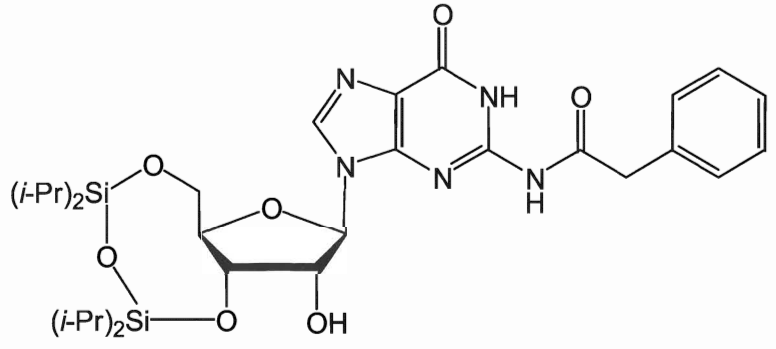

2-*N*-Phenylacetylguanosine **83** (5.59 g, 13.9 mmol), which had been dried at 80°C *in vacuo* for 6 h, was co-evaparated with dry pyridine. The residue was redissolved in dry pyridine (60 ml) and cooled to 0°C followed by addition of 1,3-dichloro-1,1,3,3-

tetraisopropyldisiloxane (4.83 g, 15.3 mmol, 1.1 mol equiv.). After stirring at 0°C for 30 min, the mixture was warmed up to room temperature and stirred for another 3 h. Then water (5 ml) was added, and after 10 min, the products were concentrated under reduced pressure. The residue was dissolved in dichloromethane (120 ml) and washed with saturated aqueous sodium hydrogen carbonate (100 ml). The layers were separated and the aqueous layer was back-extracted with dichloromethane (2×20 ml). The combined dried ($MgSO_4$) organic layers were concentrated under reduced pressure and the residue was purified by column chromatography on silica gel. The approprate fractions, which were eluted with dichloromethane–methanol (97.5:2.5 v/v) were combined and evaporated under reduced pressure to give the *title compound* as a colourless froth (6.73 g, 75.2%).

δ_H[$(CD_3)_2SO$, 300 MHz]: 1.03-1.06 (28 H, m, CH and CH_3, *i*-Pr), 3.82 (2 H, s, CH_2), 3.96 (1 H, dd, *J* = 2.3 and 12.8, H-5'), 4.06 (1 H, m, H – 3'), 4.15 (1 H, dd, *J* = 3.0 and 12.8, H-5''), 4.34 (1 H, m, H-2'), 4.37 (1 H, m, H-4'), 5.71 (1 H, d, *J* = 4.6, H-1'), 5.81 (1 H, s, 2'-OH), 7.27-7.35 (5 H, m, CH), 8.05 (1 H, s, H-8), 11.98 (1 H, s, NH), 12.03 (1 H, s, NH).

R_f: 0.50 (dichloromethane–methanol, 95:5 v/v)

2'-*O*-[1-(4-Chlorophenyl)-4-ethoxypiperidin-4-yl]-2-*N*-phenylacetylguanosine 86d

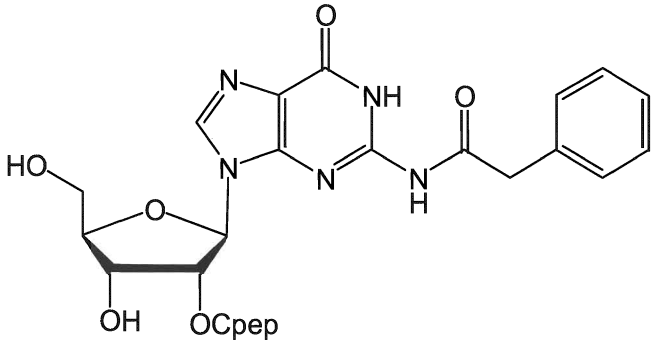

2-*N*-Phenylacetyl-3',5'-*O*-(1,1,3,3-tetraisopropyldisiloxy)guanosine **85d** (6.73 g, 10.4 mmol) and 1-(4-chlorophenyl)-4-ethoxy-1,2,5,6-tetrahydropiperidine (5.69 g, 24 mmol, 2.3 mol equiv.) were co-evaporated with dry toluene (2×10 ml) and then dissolved in dry dichoromethane (60 ml), followed by addition of freshly distilled trifluoroacetic acid

(2.08 ml, 27 mmol, 2.6 mol equiv.). After 6 h, triethylamine (4.4 ml, 31.4 mmol, 3 mol equiv.) was added and the products were partitioned between dichloromethane (100 ml) and saturated aqueous sodium hydrogen carbonate (100 ml). The layers were separated and the dried ($MgSO_4$) organic layer was concentrated under reduced presure. The residue was taken up with acetonitrile (30 ml) followed by addition of a solution of tetraethyl ammonium fluoride in acetonitrile (25 ml, 2.2 mol equiv., 1.0 *M*, pH 8.0). After 1.5 h, the products were concentrated under reduced presure and the residue was purified by column chromatography on silica gel. The appropriate fractions, which were eluted with dichloromethane–methanol (96:4 v/v) were collected and concentrated under reduced pressure to give the *title compound* as a yellow froth (5.97 g, 89.8%).

δ_H[$(CD_3)_2SO$, 300 MHz]: 0.76 (3 H, t, J = 6.9, CH_3), 1.62 (2 H, m, CH_2), 1.82 (2 H, m, CH_2), 2.79 (2 H, m, CH_2), 3.66 (2 H, m, H – 5' and H – 5''), 3.80 (2 H, s, CH_2), 4.01 (1 H, t, J = 3.1, H-4'), 4.13 (1 H, t, J = 4.1, H-3'), 4.73 (1 H, m, H-2'), 5.16 (1 H, d, J = 4.0, 3'-OH), 5.22 (1 H, t, J = 5.1, 5'-OH), 5.98 (1 H, d, J = 7.5, H-1'), 6.82 (2 H, d, J = 9.0, CH), 7.12 (2 H, d, J = 9.0, CH), 7.27-7.35 (5 H, m, CH), 8.35 (1 H, s, H-8), 11.90 (1 H, s, NH), 11.98 (1 H, s, NH).

R_f: 0.51 (dichloromethane–methanol, 90:10 v/v)

2'-*O*-[1-(4-Chlorophenyl)-4-ethoxypiperidin-4-yl]-5'-*O*-(4,4'-dimethoxytrityl)-2-*N*-phenylacetylguanosine 87d

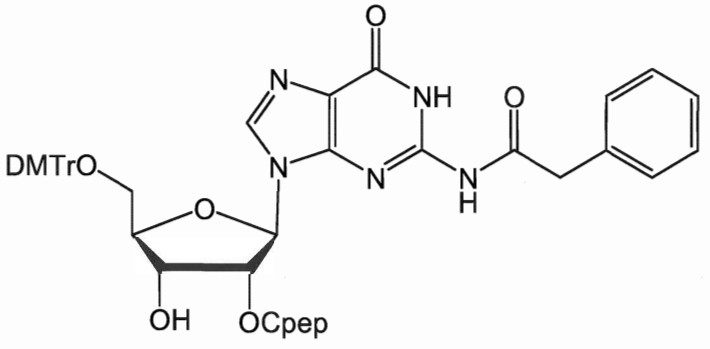

2'-*O*-[1-(4-Chlorophenyl)-4-ethoxypiperidin-4-yl]-2-*N*-phenylacetylguanosine **86d** (5.90 g, 9.23 mmol) was co-evaporated with dry pyridine (2×5 ml). The residue was redissolved in dry pyridine (50 ml) followed by addition of 4,4'-dimethoxytrityl chloride

(3.44 g, 10.15 mmol). After 45 min, triethylamine (5 ml) was added. After another 10 min, the products were partitioned between dichloromethane (100 ml) and saturated aqueous sodium hydrogen carbonate (100 ml). The layers were separated and the dried ($MgSO_4$) organic layer was concentrated under reduced presure. The residue was purified by column chromatography on silica gel. The appropriate fractions, which were eluted with dichloromethane–methanol (96:4 v/v) were collected and concentrated under reduced pressure to give the *title compound* as a yellow froth (8.45 g, 97.4%).

δ_H[$(CD_3)_2SO$, 300 MHz]: 0.76 (3 H, t, J = 6.9, CH_3), 3.73 (6 H, s, CH_3), 4.12 (1 H, s, H-4'), 4.21 (1 H, s, H-3'), 4.92 (1 H, t, J = 6.0, H-2'), 5.28 (1 H, d, J = 4.5, 3'-OH), 6.01 (1 H, d, J = 7.1, H-1'), 8.08 (1 H, s, H-8), 6.83-7.42 (22 H, Ar), 11.8 (1 H, br, NH).
R_f: 0.33 (dichloromethane–methanol, 95:5 v/v)

2'-*O*-[1-(4-Chlorophenyl)-4-ethoxypiperidin-4-yl]-5'-*O*-(4,4'-dimethoxytrityl)-2-*N*-phenylacetyl-guanosine-3'-(2-*O*-cyanoethyl) *N,N*-diethylphosphoramidite 88d

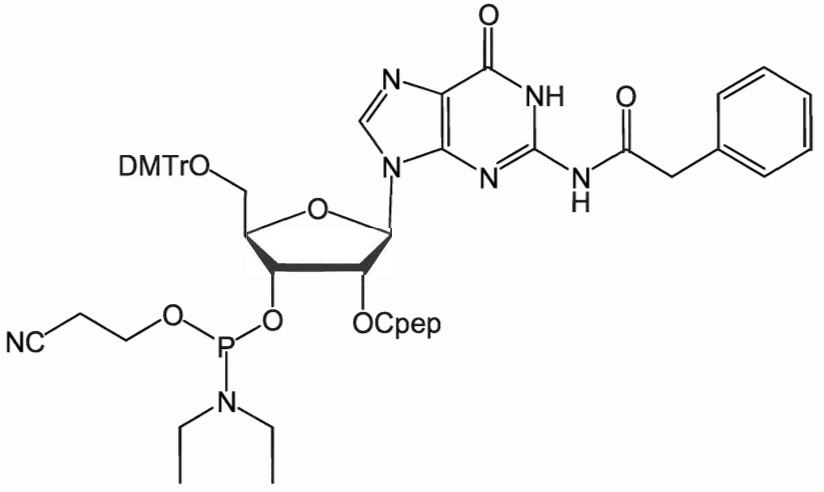

2'-*O*-[1-(4-Chlorophenyl)-4-ethoxypiperidin-4-yl]-5'-*O*-(4,4'-dimethoxytrityl)-2-*N*-phenylacetylguanosine **87d** (1.00 g, 1.06 mmol) was co-evaporated with dry toluene (2×5 ml). The residue was redissolved in dry THF (18 ml) followed by addition of *N,N*-diisopropylethylamine (739 µl, 4.25 mmol, 4 mol equiv.). After 10 min, 2-*O*-cyanoethyl-*N,N*-diethyl phosphorochloridite phosphorochloridite (0.44 g, 2.12 mmol, 2 mol equiv.) was added. After 1 h, the solvent was removed under reduced pressure. The residue was purified by column chromatography on silica gel. The appropriate fractions, which were

eluted with hexane–acetone–triethylamine (50:50:2 v/v) were collected and concentrated under reduced pressure to give the *title compound* as a light yellow glass (0.70 g, 59.4%).

δ_H[$CDCl_3$, 300 MHz]: 4.17 (s, H-4'), 4.34 (s, H-4') (these two signals integrate 1 H), 4.48 (1 H, m, H-3'), 5.33 (dd, J = 4.4 and 7.9, H-2'), 5.34 (H-2') (these two signals integrate 1 H), 6.20 (d, J =7.8, H-1'), 6.21 (d, J = 7.8, H-1') (these two signals integrate 1 H), 8.19 (s, H-2), 8.21 (s, H-2) (these two signals integrate 1 H), 8.49 (1 H, br, NH), 8.61 (s, H-8), 8.64 (s, H-8) (these two signals integrate 1 H), 6.74-7.49 (17 H, Ar).
δ_P[$CDCl_3$, 121.5 MHz]: 148.67 and 150.21
R_f: 0.42 (hexane–acetone–triethylamine, 50:50:2 v/v)

2'-*O*-[1-(4-Chlorophenyl)-4-ethoxypiperidin-4-yl]-5'-*O*-(4,4'-dimethoxytrityl)-6-*N*-pivaloyladenosine-3'-(2-*O*-cyanoethyl) *N*, *N*-diethylphosphoramidite 88b

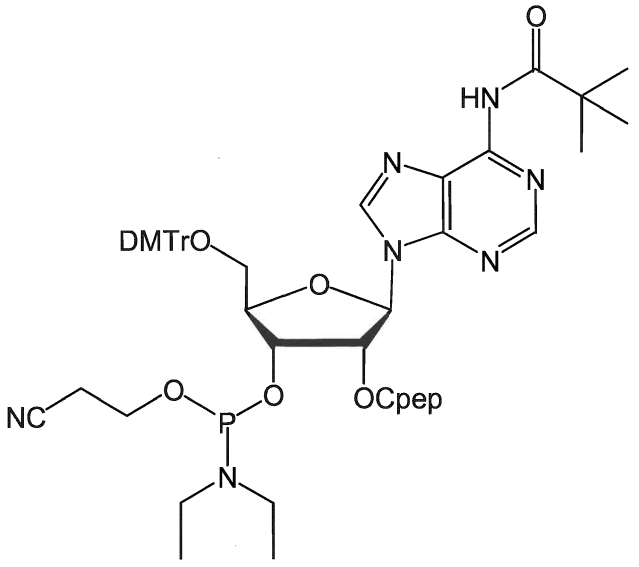

2'-*O*-[1-(4-Chlorophenyl)-4-ethoxypiperidin-4-yl]-5'-*O*-(4,4'-dimethoxytrityl)-6-*N*-pivaloyladenosine **87b** (2.00 g, 2.24 mmol) was co-evaporated with dry toluene (2×5 ml). The residue was redissolved in dry acetonitrile (25 ml) followed by addition of *N,N*-diisopropylethylamine (1.6 ml, 8.96 mmol, 4 mol equiv.). After 5 min, 2-*O*-cyanoethyl-*N,N*-diethyl phosphorochloridite (0.93 g, 4.48 mmol, 2 mol equiv.) was added. After 1.5 h, the solvent was removed under reduced pressure. The residue was purified by column chromatography on silica gel. The appropriate fractions, which were eluted with

hexane–acetone–triethylamine (65:35:2 v/v) were collected and concentrated under reduced pressure to give the *title compound* as a light yellow glass (1.87 g, 77.4%).

δ_H[$CDCl_3$, 300 MHz]: 4.33 (H-4'), 4.43 (H-4') (these two signals integrate 1 H), 4.56 (1 H, m, H-3'), 5.34 (H-2'), 5.42 (dd, J = 5.1 and 7.8, H-2') (these two signals integrate 1 H), 5.86 (d, J = 8.5, H-1'), 6.98 (, J = 8.5, H-1') (these two signals integrate 1 H), 6.74-7.64 (22 H, Ar), 7.83 (s, H-8), 7.86 (s, H-8) (these two signals integrate 1 H).

δ_P[$CDCl_3$, 121.5 MHz]: 149.32 and 150.64

R_f: 0.41 (hexane–acetone–triethylamine, 65:35:2 v/v)

2'-*O*-[1-(4-Chlorophenyl)-4-ethoxypiperidin-4-yl]-5'-*O*-(4,4'-dimethoxytrityl)-uridine-3'-(2-*O*-cyanoethyl) *N*, *N*-diethylphosphoramidite 88a

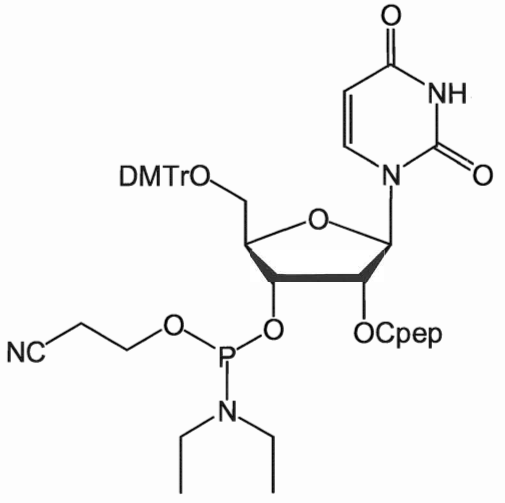

2'-*O*-[1-(4-Chlorophenyl)-4-ethoxypiperidin-4-yl]-5'-*O*-(4,4'-dimethoxytrityl)uridine **88a** (1.00 g, 1.28 mmol) was co-evaporated with dry toluene (2×5 ml). The residue was redissolved in dry acetonitrile (15 ml) followed by addition of *N,N*-diisopropylethylamine (1.1 ml, 6.38 mmol, 5 mol equiv.). After 5 min, 2-*O*-cyanoethyl-*N,N*-diethyl phosphorochloridite (0.53 g, 2.55 mmol, 2 mol equiv.) was added. After 1.5 h, the solvent was removed under reduced pressure. The residue was purified by column chromatography on silica gel. The appropriate fractions, which were eluted with hexane–acetone–triethylamine (65:35:2 v/v) were collected and concentrated under reduced pressure to give the *title compound* as a light yellow glass (0.89 g, 71.8%).

δ_H[$CDCl_3$, 300 MHz]: 4.16 (s, H-4') (these two signals integrate 1 H), 4.29 (s, H-4') (these two signals integrate 1 H), 4.46 (1 H, m, H-3'), 4.67 (dd, *J* = 4.8 and 7.6, H-2'), 4.85 (dd, *J* = 4.8 and 7.9, H-2') (these two signals integrate 1 H), 5.30 (1 H, d, *J* =8.0, H-1'), 6.24 (1 H, t, *J* = 8.0, H-5), 6.80-7.40 (17 H, Ar), 7.77 (d, *J* = 8.1, H-6), 7.80 (d, *J* = 8.1, H-6) (these two signals integrate 1 H).

δ_P[$CDCl_3$, 121.5 MHz]: 149.06 and 150.17

R_f: 0.41 (hexane–acetone–triethylamine, 65:35:2 v/v)

N-(6-Hydroxyhexyl)trifluoroacetamide 91

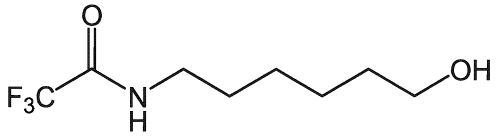

To a solution of 6-hydroxyhexyl-1-amine **90** (1.21 g, 8.53 mmol) in dichloromethane (3 ml) ethyl trifluoroacetate **89** (0.60 g, 4.27 mmol, 0.5 mol equiv.) was added. After 2 h, a second portion of ethyl trifluoroacetate **89** (0.60 g, 4.27 mmol, 0.5 mol equiv.) was added. After another 2 h, the mixture was concentrated under reduced pressure. The residue was purified by column chromatography on silica gel. The appropriate fractions, which were eluted with dichloromethane–methanol (96:4 v/v) were collected and concentrated under reduced pressure to give the *title compound* as a white solid (1.58 g, 86. 9%).

FAB-MS found $[M+H]^+$ = 214.10578, $C_8H_{14}F_3NO_2^+$ requires 214.10549.

δ_H[$(CD_3)_2SO$, 300 MHz]: 1.27-1.31 (4 H, m, CH_2), 1.38-1.43 (2 H, m, CH_2), 1.45-1.50 (2 H, m, CH_2), 3.15-3.18 (2 H, m, CH_2), 3.36-3.39 (2 H, m, CH_2), 4.35 (1 H, s, OH), 9.40 (1 H, s, NH).

δ_C[$(CD_3)_2SO$, 75.5 MHz]: 25.5 (CH_2), 26.5 (CH_2), 26.5 (CH_2), 28.7 (CH_2), 32.9 (CH_2), 39.5 (CH_2), 61.1 (CH_2), 113.6-119.3 (CF_3), 156.2-156.9 (C=O).

R_f: 0.47 (dichloromethane–methanol, 95:5 v/v)

(6-Trifluoroacetamido)hexyl-(2-*O*-cyanoethyl) *N,N*-diisopropylphosphoramidite 92

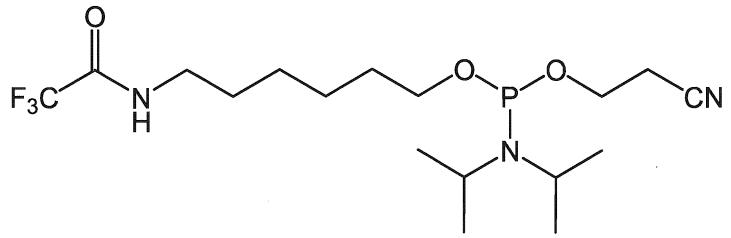

N-(6-Hydroxyhexyl)trifluoroacetamide **91** (0.50 g, 2.35 mmol) was co-evaporated with dry toluene (2×2 ml) and then dissolved in dry dichloromethane (8 ml) followed by addition of *N,N*-diisopropylethylamine (1.6 ml, 9.39 mmol, 4 mol equiv.). After 5 min, 2-*O*-cyanoethyl-*N,N*-diisopropyl phosphorochloridite (1.11 g, 4.69 mmol, 2 mol equiv.) was added. After 15 min, the solvent was removed under reduced pressure and the residue was purified by column chromatography on silica gel. The appropriate fractions, which were eluted with hexane–acetone–triethylamine (80:20:2 v/v) were collected and concentrated under reduced pressure to give the *title compound* as a colorless oil (0.56 g, 57.7%).

δ_P[D_2O, 121.5 MHz]*: 147.28

R_f: 0.68 (hexane–acetone–triethylamine, 80:20:2 v/v)

Solid phase synthesis of oligoribonucleotides

Solid phase synthesis of oligoribonucleotides was performed on an ABI 3400 DNA synthesizer. Standard 1.0 μmol cycle conditions were applied with a coupling time of 2 min. All phosphoramidite solutions (**88a, 88b, 88c, 88d, 92**) are 70 m*M* concentration in dry acetonitrile. A solution of 5-benzylthio-1*H*-tetrazole in dry acetonitrile (0.25 *M*) was used as the activator. Solid phase synthesis of U_9U and A_9A were carried out in "DMTr-off" mode; solid phase synthesis of C_6-amino modifier-U_9U was carried out in "DMTr-on" mode. The average stepwise yield (ASWY), as reported by the synthesizer, was used to evaluate the synthesis efficiency. After synthesis was complete, the resins were incubated in concentrated aqueous ammonia (28%) at 55°C for 12 h. The supernatant

* using D_2O capillary

was subsequently lyophilized to give partially-protected (Cpep protected) oligoribonucleotides.

U_9U 93

ESI-MS found M^- = 5138.5, $C_{207}H_{254}Cl_9N_{29}O_{87}P_9^-$ requires 5138.2.

R_t (C_{18}): 8.53 min.

A_9A 94

ESI-MS found M^- = 5368.7, $C_{217}H_{264}Cl_9N_{59}O_{67}P_9^-$ requires 5168.6.

R_t (C_{18}): 8.90 min.

C_6-amino modifier-U_9U 95

ESI-MS found M^- = 5316.4, $C_{213}H_{268}Cl_9N_{30}O_{90}P_{10}^-$ requires 5317.4.

R_t (C_{18}): 8.52 min.

Man-U_9U 96

Amino-modified U_9U (C_6-amino modifier-U_9U) **95** (0.75 μmol, 1 mol equiv.) was first dissolved in methanol (200 μl), followed by addition of an aqueous solution (70 μl) of squarate-activated monovalent mannoside (3.75 μmol, 5 mol equiv.) and triethylamine (3 μl). The reaction mixture was incubated at 37°C. After 2 h, additional aqueous solution of squarate-activated monovalent mannoside (37 μl, 2 mol equiv.) was added. After an additional period of 3 h, the reaction mixture was lyophilized and was purified by semi-preparative C_{18} RP-HPLC column. The appropriate fractions were collected and lyophilized to give Man-U_9U was obtained as a white solid.

R_t (C_{18}): 7.63 min.

ESI-MS found M^- = 5319.4, $C_{225}H_{283}Cl_9N_{31}O_{98}P_{10}^-$ requires 5618.6.

Bi-Man-U_9U 97

Amino-modified U_9U (0.5 μmol) **95** was dissolved in methanol (300 μl), followed by addition of an aqueous solution (73 μl) of squarate-activated bivalent mannoside (2 μmol) and triethylamine (5 μl). The reaction mixture was incubated at 37°C. Additional

portions of aqueous solution of squarate-activated bivalent mannoside (37 μl, 2 mol equiv.) were added at 3 and 6 h, respectively. After 9 h, the products were lyophilized to give a white solid. The products were purified on a semi-preparative C_{18} RP-HPLC column. The appropriate fractions were collected and lyophilized. The purified Bi-Man-U_9U was characterized by RP-HPLC and ESI-MS.

R_t (C_{18}): 7.34 min.

ESI-MS found M^- = 6152.6, $C_{247}H_{322}Cl_9N_{36}O_{108}P_{10}^-$, requires 6152.2.

General procedures for the removal of Cpep

Substrate (oligoribonucleotides with 2'-Cpep protection, purified previourly by C18 column) was dissolved in DMA (300 μl) followed by addition of triethylammonium formate buffer (TEAF, 200 μl, pH 2.52, 0.5 *M*). The mixture was incubated at 40°C for 6 h. The reaction mixture was then neutralized by addition of triethylammonium acetate buffer (TEAA, pH 10.0). Chloroform (300 μl) was added, followed by vortex and centrifugation. The organic layer was discarded and the aqueous layer was further extracted with chloroform (2×300 μl). The aqueous layer was lyophilized to give a light yellow gel. This material was redissolved in water (30 μl), followed by addition of *n*-butanol (500 μl). After vortexing, the mixture were frozen in liquid nitrogen and centrifuged for 10 min. The butanol layer was discarded. The pellet was dissolved in water (500 μl) and lyophilized to give the fully deprotected-conjugate.

C_6-amino modifier-U_{10} 100

R_t (DNAPac PA100): 3.40 min.

ESI-MS found M^- = 3177.7, $C_{96}H_{124}N_{21}O_{81}P_{10}^-$, requires 3177.8.

Man-U_{10} 101

R_t (DNAPac PA100): 3.66 min.

ESI-MS found M^- = 3479.1, $C_{108}H_{139}N_{22}O_{89}P_{10}^-$, requires 3479.1.

Bi-Man-U_{10} 102

R_t (DNAPac PA100): 2.70 min.

ESI-MS found M^- = 4012.6, $C_{130}H_{178}N_{27}O_{99}P_{10}^-$ requires 4012.7.

U_{10} 98

ESI-MS found M^- = 2998.4, $C_{90}H_{110}N_{20}O_{78}P_9^-$ requires 2998.7.

R_t (DNAPac PA100): 2.79 min.

A_{10} 99

ESI-MS found M^- = 3229.2, $C_{100}H_{120}N_{50}O_{58}P_9^-$ requires 3229.1.

R_t (DNAPac PA100): 2.95 min

Enzymatic stability of U_{10}, Man-U_{10}, and Bi-Man-U_{10}

0.183 ODU of substrate (U_{10} **98**, Man-U_{10} **101**, and Bi-Man-U_{10} **102**) was dissolved in 200 µl of Tris-Cl buffer (pH 8.0). Rnase A (100× dilute of stock solution, 5 µl) and alkaline phosphatase (100× dilute of stock solution, 5 µl) were added. The stock solutions of Rnase A were obtained by dissolving Rnase A (0.001 g) in 0.1 *M* Tris-Cl buffer (pH 8.0, 1.0 ml) and bacterial alkaline phosphatase was obtained by dissolving *ca.* 2 units of enzyme in 1.0 ml of the same buffer. The mixture was incubated at 37°C. Aliquots (20 µl) were withdrawn at the following time, 0, 2, 5, 10, 15, 20, 40, and 60 min. To the aliquots were added an aqueous solution of aluminon (5 µ*M*, 20 µl) and the mixtures were frozen in liquid nitrogen immediatedly. All aliquots were analyzed with anion exchange HPLC (DNAPac PA100).

UV Thermal denaturation studies

0.15 A_{260} units of the A_{10} **99** was mixed with 12 A_{260} units of each of the oligoribonucleotides (U_{10} **98**, Man-U_{10} **101**, and Bi-Man-U_{10} **102**) and the oligomers were dried using a speed-vacuum. The pellet was resuspended in a 90 m*M* sodium chloride, 10 m*M* sodium phosphate, and 1 m*M* EDTA buffer (pH 7.0) solution. The mixtures were heated to 90°C for 10 minutes then allowed to cool to room temperature for 30 minutes and finally stored at 4 °C overnight. Denaturation curves were obtained by monitoring the OD at 260 nm while the cells were being heated from 10°C to 90°C at a rate of

0.5°C/minute using a Varian CARY Model 3E spectrophotometer fitted with a 6-sample thermostatted cell block and a temperature controller.

Methyl 2, 3, 5-tri-*O*-benzyl-D-(-)-riboside 108

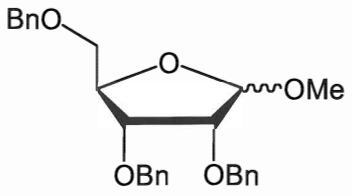

D-(-)-Ribose **106** (3.00 g, 19.98 mmol) was dissolved in a solution of HCl-methanol (1:99 v/v, 50 ml). After the reaction mixture was stirred at room temperature for 24 h, solid sodium bicarbonate (1.0 g) was added. The procucts were evaporated under reduced pressure to *ca.* 1/3 of the original volume, and then filtered. The filtrate was concentrated under reduced pressure to give methyl riboside as a yellow oil. This material was azeotroped with dry toluene (2×10 ml). The residue was dissolved in dry DMF (60 ml) and cooled (ice-water bath), followed by addition of sodium hydride (4.00 g, 100 mmol, 5 mol equiv.). After 20 min, benzyl bromide (17.10 g, 100 mmol, 5 mol equiv.) was added dropwise at 0°C. The reaction mixture was allowed to warm up to room temperature and stirred overnight. After the reaction was quenched by addition of methanol (10 ml), the solvents were removed under reduced pressure. The residue was redissolved in dichloromethane (120 ml) and extracted with saturated sodium hydrogen carbonate (100 ml). The aqueous layer was back extracted with dichloromethane (20×2 ml) and the combined organic layers were dried ($MgSO_4$) and evaporated under reduced pressure. The residue was purified by column chromatography on silica gel (dichloromethane–methanol 99.5:0.5 v/v). Methyl 2,3,5-tri-*O*-benzyl-D-riboside **108** (5.32 g, 61.4% over two steps) was obtained as a light yellow oil.

δ_H[$CDCl_3$, 600 MHz]: 3.56 (1 H, dd, J = 5.82 and 10.68, H-5'), 3.67 (1 H, dd, J = 3.54 and 10.50, H-5''), 3.89 (1 H, d, J = 4.56, H-2'), 4.07 (1 H, t, J = 5.52, H-3'), 4.40 (1 H, m, H-4'), 4.50 (1 H, d, J = 11.82, CH), 4.59 (1 H, d, J = 11.22, CH), 4.60 (1 H, d, J = 11.52, CH), 4.63 (1 H, d, J = 12.24, CH), 4.66 (1 H, d, J = 12.18, CH), 4.72 (1 H, d, J = 12.00, CH), 4.97 (1 H, s, H-1').

δ_C[$CDCl_3$, 600 MHz]: 71.4 (CH, C-5'), 72.3 (CH_2), 72.5 (CH_2), 73.2 (CH_2), 78.4 (CH, C-3'), 79.7 (CH, C-2'), 80.5 (CH, C-4'), 106.4 (CH, C-1'), 127.6-138.4 (CH and C).

R_f: 0.58 (dichloromethane–methanol, 98:2 v/v)

2, 3, 5-Tri-*O*-benzyl lactone 110

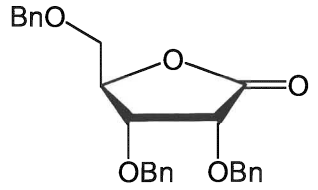

Methyl 2,3,5-tri-*O*-benzyl-D-riboside **108** (2.00 g) was dissolved in a mixture of dioxane and 0.12 *M* hydrochlorid acid (4:1 v/v, 75 ml). The solution was heated, under reflux, overnight. The products were concentrated and purified by column chromatography on silica gel (dichloromethane–methanol 98:2 v/v). 2,3,5-Tri-*O*-benzyl-D-ribose **109** (1.62 g, 83.5%) was obtained as a light yellow oil.

2,3,5-Tri-*O*-benzyl-D-ribose **109** (4.87 g, 11.6 mmol) was co-evaporated with dry toluene (2×10 ml) and then dissolved in dry DMSO (15.8 ml, 232 mmol, 20 mol equiv.), followed by addition of acetic anhydride (10.9 ml, 116 mmol, 10 mol equiv.) at room temperature. After 20 h, methanol (15 ml) was added, and the products were concentrated under reduced pressure. Upon addition of ice water (100 ml) to the residue, a yellow syrup was formed around the flask. The syrus was dissolved in dichloromethane (120 ml), and the aqueous layer was back-extracted with dichloromethane (100 ml). The combined organic layers were dried ($MgSO_4$) and concentrated under reduced pressure. The residue was purified by column chromatography on silica gel (hexane–ethyl acetate 80:20 v/v). The 2,3,5-tri-*O*-benzyl lactone **110** was obtained as a white solid (3.85 g, 79.4%).

FAB-MS found $[M+H]^+$ = 419.16902, $C_{26}H_{27}O_5^+$ requires 419.18585.

δ_H[$CDCl_3$, 600 MHz]: 3.58 (1 H, dd, J = 2.64 and 11.04, H-5'), 3.69 (1 H, dd, J = 2.82 and 11.04, H-5''), 4.13 (1 H, dd, J = 1.89 and 5.67, H-2'), 4.43 (1 H, t, J = 5.88, H-3'), 4.44 (1 H, d, J = 11.76, CH), 4.52 (1 H, d, J = 11.88, CH), 4.58 (1 H, m, H-4'), 4.57 (1 H,

d, J = 11.94, CH), 4.73 (1 H, d, J =11.82, CH), 4.77 (1 H, d, J =11.94, CH), 4.97 (1 H, d, J =11.94, CH), 7.19-7.41 (15 H, m).

δ_C[$CDCl_3$, 150.9 MHz]: 68.8 (CH, C-5'), 72.4 (CH, C-4'), 72.8 (CH_2), 73.7 (CH_2), 73.8 (CH, C-3'), 75.4 (CH, C-2'), 81.8 (CH_2), 127.5-138.6 (CH and C), 173.8 (C=O).

R_f: 0.54 (hexane–ethyl acetate, 70:30 v/v)

1-(2,3,5-Tri-*O*-benzyl-*β*-D-ribofuranosyl)phenanthrene 112a

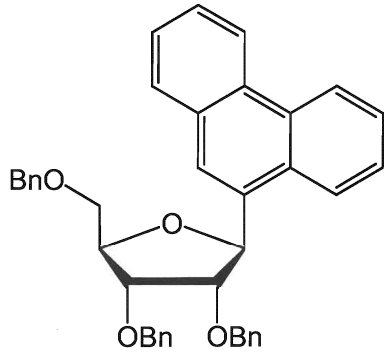

9-Bromophenanthrene **113a** (0.922 g, 3.59 mmol) was co-evaporated with dry toluene (2×5 ml) and dissolved in dry THF (20 ml). The solution was then cooled to -78°C (acetone-dry ice bath) followed by addition of *n*-butyllithium (2.24 ml, 1.6 *M* solution in hexane, 3.58 mmol) over 2 min. After 40 min, a pre-cooled (-78°C) solution of 2,3,5-tri-*O*-benzyl lactone **110** (1.00 g, 2.39 mmol) in dry THF (5 ml), which was prepared by first co-evaporating 2,3,5-tri-*O*-benzyl lactone **110** with dry toluene (2×5 ml) followed by dissolving in dry THF, was added over 2 min. Stirring was continued for 3 h at the same temperature. The reaction mixture was then allowed to warm up to room temperature over a period of 2 h. Solid carbon dioxide (1.0 g) followed by saturated aqueous sodium hydrogen carbonate (10 ml) were added. The products were concentrated under reduced pressure and the residue was taken up in dichloromethane (40 ml) and extracted with saturated aqueous sodium hydrogen carbonate (2×20 ml). The aqueous layer was back extracted with dichloromethane (10 ml) and the combined organic layers were dried ($MgSO_4$) and evaporated under reduced pressure. The residue was further co-evaporated with dry toluene (2×5 ml), and then dissolved in dry dichloromethane (40 ml). After the solution was cooled to -78°C (acetone-dry ice bath), triethylsilane (2.3 ml, 14.4 mmol) followed by boron trifluoride diethyl etherate (1.7 ml,

13.7 mmol) were added over a period of 5 min. The reaction mixture was stirred at the same temperature for 30 min, and was then allowed to warm up to room temperature over a period of 3 h. The products were partitioned between dichloromethane (100 ml) and saturated aqueous sodium hydrogen carbonate (100 ml). The aqueous layer was back extracted with dichloromethane (2×10 ml) and the combined organic layers were dried ($MgSO_4$) and evaporated under reduced pressure. The residue was purified by column chromatography on silica gel. The appropriate fractions, which were eluted by hexane–ethyl acetate (90:10 v/v) were combined and evaporated under reduced pressure to give the *title compound* as a pale yellow solid (0.72 g, 51.9%). Colourless needles were obtained after re-crystallization from methanol. M.p. 79–80°C. Found, in material recrystallized from methanol: C, 82.60; H, 6.26. Calc. for $C_{40}H_{36}O_4$: C, 82.76; H, 6.25.

EI-MS found M^+ = 580.26233, $C_{40}H_{36}O_4$ requires 580.26136.

δ_H[$CDCl_3$, 600 MHz]: 3.84 (1 H, dd, *J* = 3.3 and 10.6, H-5'), 4.01 (1 H, dd, *J* = 2.7 and 10.6, H-5''), 4.19 (1 H, t, *J* = 4.2, H-2'), 4.24 (1 H, dd, *J* = 4.5 and 6.5, H-3'), 4.53 (1 H, ddd, *J* = 2.7, 6.2 and 6.2, H-4'), 4.57 (1 H, d, *J* = 11.6, C$\underline{H_2}$), 4.58 (1 H, d, *J* = 11.8, C$\underline{H_2}$), 4.65 (1 H, d, *J* = 11.8, C$\underline{H_2}$), 4.69 (1 H, d, *J* = 11.8, C$\underline{H_2}$), 4.74 (1 H, d, *J* = 11.8, C$\underline{H_2}$), 4.81 (1 H, d, *J* = 11.6, C$\underline{H_2}$), 5.83 (1 H, d, *J* = 4.2, H-1'), 7.28-7.67 (20 H, m), 8.10-8.14 (2 H, m), 8.66 (1 H, d, *J* = 8.3), 8.75 (1 H, d, *J* = 8.3).

δ_C[$CDCl_3$, 150.9 MHz]: 69.6 (CH, C5'), 72.7 (CH_2), 73.2 (CH_2), 73.5 (CH_2), 78.2 (CH, C3'), 80.3 (CH, C4'), 81.7 (CH, C1'), 82.3 (CH, C2'), 122.3 (CH, Ar), 123.2 (CH, Ar), 124.2 (CH, Ar), 124.5 (CH, Ar), 126.2 (CH, Ar), 126.5 (CH, Ar), 126.6 (CH, Ar), 126.7 (CH, Ar), 127.6, 127.7, 127.8, 128.4, 128.5, 129.1 (CH, Ar), 130.1, 130.6, 131.5, 134.2, 138.0, 138.2, 138.2, 138.4.

R_f: 0.40 (hexane–acetone, 80:20 v/v)

9-(2,3,5-Tri-*O*-benzyl-*β*-D-ribofuranosyl)pyrene 112b

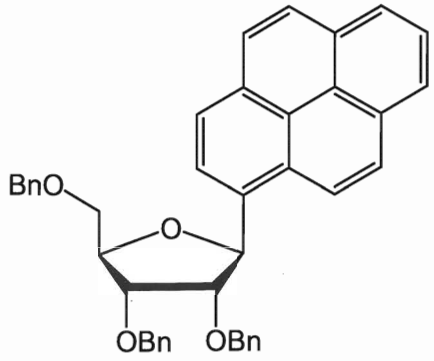

The *title compound* was synthesized following the procedure described above for the synthesis of 2,3,5-tri-*O*-benzyl-*β*-D-ribofuranosyl phenanthrene **112a**. After column chromatography on silica gel (hexane–ethyl acetate 93:7 v/v), the *title compound* was obtained as a pale yellow solid (34.3%). M.p. 104–105°C (material re-crystallized from methanol). Found, in material recrystallized from methanol: C, 83.40; H, 6.03. Calc. for $C_{42}H_{36}O_4$: C, 83.42; H, 6.00.

EI-MS found M^+ = 604.26000, $C_{42}H_{36}O_4$ requires 604.26136.

δ_H[$CDCl_3$, 600 MHz]: 3.82 (1 H, dd, *J* = 3.6 and 10.4, H-5'), 3.93 (1 H, dd, *J* = 3.6 and 10.4, H-5''), 4.18 (1 H, dd, *J* = 5.2 and 6.2, H-2'), 4.24 (1 H, dd, *J* = 4.8 and 5.0, H-3'), 4.45 (1 H, d, *J* = 11.9, C$\underline{H_2}$), 4.56 (1 H, m, H-4'), 4.56 (1 H, d, *J* = 11.8, C$\underline{H_2}$), 4.66 (1 H, d, *J* = 11.9, C$\underline{H_2}$), 4.67 (1 H, d, *J* = 12.1, C$\underline{H_2}$), 4.74 (1 H, d, *J* = 11.9, C$\underline{H_2}$), 4.75 (1 H, d, *J* = 12.1, C$\underline{H_2}$), 6.14 (1H, d, *J* = 6.2, H-1'), 7.13-7.43 (15 H, m), 8.04-8.14 (5 H, m), 8.22 (2 H, m), 8.33 (1 H, d, *J* = 8.0), 8.49 (1 H, d, *J* = 9.2).

δ_C[$CDCl_3$, 150.9 MHz]: 69.6 (CH, C5'), 72.7 (CH_2), 73.2 (CH_2), 73.5 (CH_2), 78.2 (CH, C3'), 80.3 (CH, C4'), 81.7 (CH, C1'), 82.3 (CH, C2'), 122.3 (CH, Ar), 123.8 (CH, Ar), 124.7, 124.8, 125.0, 125.1, 125.9, 127.2, 127.5, 127.6, 127.7, 127.8,127.9, 128.1, 128.2, 128.3, 128.4, 128.5, 130.7, 131.4, 133.9, 137.8, 138.0, 138.3.

R_f: 0.35 (hexane–acetone, 80:20 v/v)

1-D-Ribofuranosyl phenanthrene

1-(2,3,5-Tri-*O*-benzyl-*β*-D-ribofuranosyl)phenanthrene **112a** (0.550 g, 0.95 mmol) was co-evaporated with dry toluene (2×5 ml), and then dissolved in dry dichloromethane (60

ml). The solution was cooled to -78°C (acetone-dry ice bath), followed by addition of boron tribromide (0.1 *M* in a mixture of hexane and dichloromethane 1:9 v/v, 33.2 ml, 3.32 mmol) over a period of 30 min. The reaction was allowed to proceed for 2 h at the same temperature and was then quenched by addition of aqueous methanol (20 ml, methanol–water 4:1, v/v). The mixture was then allowed to warm up to room temperature. After 2 h, the products were concentrated under reduced pressure and then further co-evaporated with methanol (3×10 ml) under reduced pressure. The residue was purified by column chromatography on silica gel. The appropriate fractions, which were eluted with dichloromethane–methanol (98:2 to 95:5 v/v) were combined and evaporated under reduced pressure. The α- and β-anomers were obtained as light yellow glasses in 39.0% (0.114 g) and 24.3% (0.071 g) yields, respectively.

1-*α-D-Ribofuranosyl phenanthrene* **114b**

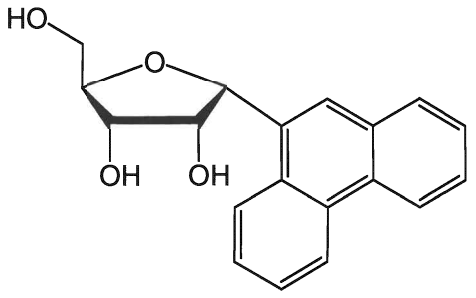

EI-MS found M^+ = 310.12077, $C_{19}H_{18}O_4$ requires 310.12051.

δ_H[$(CD_3)_2SO$, 600 MHz]: 3.58 (1 H, ddd, *J* = 4.7, 4.9 and 11.8, H-5'), 3.79 (1 H, ddd, *J* = 2.5, 4.9, and 11.8, H-5''), 4.02 (1 H, ddd, *J* = 2.3, 4.7 and 8.6, H-4'), 4.32 (1 H, ddd, *J* = 4.3, 7.9 and 8.7, H-3'), 4.43 (1 H, dd, *J* = 4.4 and 7.9, H-2'), 4.47 (1 H, d, *J* = 4.5, 2'-OH), 4.82 (1 H, t, *J* = 5.7, 5'-OH), 4.89 (1 H, d, *J* = 7.5, 3'-OH), 5.75 (1 H, d, *J* = 2.7, H-1'), 7.61–7.71 (4 H, m), 7.96 and 7.98 (2 H), 8.11 (1 H, d, *J* = 8.1), 8.81 (1 H, d, *J* = 7.9), 8.88 (1 H, d, *J* = 8.1).

δ_C[$(CD_3)_2SO$, 150.9 MHz]: 62.2 (CH, C5'), 73.0 (CH, C2'), 73.2 (CH, C3'), 79.8 (CH, C1'), 82.3 (CH, C4'), 123.1 (CH, Ar), 123.8 (CH, Ar), 124.1 (CH, Ar), 125.3 (CH, Ar), 126.6 (CH, Ar), 126.8 (CH, Ar), 127.2 (CH, Ar), 127.3 (CH, Ar), 128.9 (CH, Ar), 129.8, 130.1, 130.2, 131.6, 133.6.

R_f: 0.57 (dichloromethane–methanol, 90:10 v/v)

1-*β-D-Ribofuranosyl phenanthrene* **114a**

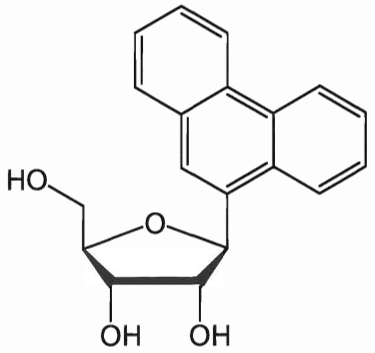

EI-MS found M^+ = 310.12031, $C_{19}H_{18}O_4$ requires 310.12051.

δ_H[$(CD_3)_2SO$, 600 MHz]: 3.69 (1 H, ddd, *J* = 5.2, 5.5 and 11.8, H-5'), 3.83 (1 H, ddd, *J* = 2.8, 5.6, and 11.9, H-5''), 3.90 – 3.99 (3 H, m, H-3', H-4' and H-2'), 4.96 (1 H, t, *J* = 5.7, 5'-OH), 4.97 (1 H, d, *J* = 6.1, 3'-OH), 5.31 (1 H, d, *J* = 5.2, 2'-OH), 5.41 (1 H, d, *J* = 3.7, H-1'), 7.63-7.74 (4 H, m), 7.96 (1 H, dd, *J* = 1.2 and 8.1), 8.13 (1 H, s), 8.25 (1 H, dd, *J* = 1.2 and 8.1), 8.81 (1 H, d, *J* = 8.1), 8.89 (1 H, dd, *J* = 1.2 and 8.1).

δ_C[$(CD_3)_2SO$, 150.9 MHz]: 61,7 (CH, C5'), 70.8 (CH, C3'), 76.5 (CH, C2'), 82.7 (CH, C1'), 83.5 (CH, C4'), 123.2 (CH, Ar), 123.8 (CH, Ar), 124.0 (CH, Ar), 125.0 (CH, Ar), 127.0 (CH, Ar), 127.2 (CH, Ar), 127.3 (CH, Ar), 127.4 (CH, Ar), 129.1 (CH, Ar), 129.9, 130.1, 130.4, 131.5, 135.6.

R_f: 0.54 (dichloromethane–methanol, 90:10 v/v)

9-D- ribopyranosyl pyrene 115

9-(2,3,5-Tri-*O*-benzyl-*β*-D-ribofuranosyl) pyrene **112b** (0.570 g, 0.94 mmol) was deprotected following the same procedure as described above for the debenzylation of 1-(2,3,5-tri-*O*-benzyl-*β*-D-ribofuranosyl) phenanthrene **112a**. After column chromatography on silica gel (dichloromethane–methanol 98:2 to 97:3, v/v), the *β* and *α*-anomers (**115a** and **115b**) were obtained as a light brown solid (0.041 g, 13.2%) and a light yellow glass (0.039 g, 12.3%), respectively.

9-α-D- ribopyranosyl pyrene **115b**

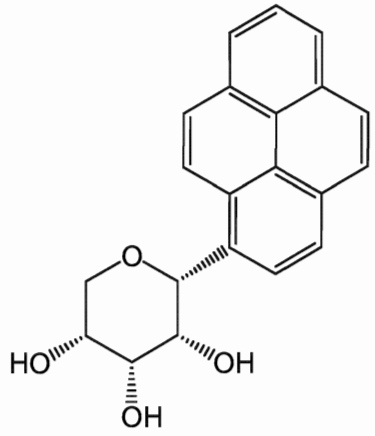

EI-MS found M^+ = 334.12096, $C_{21}H_{18}O_4$ requires 334.12051.

δ_H[$(CD_3)_2SO$, 600 MHz]: 3.87-3.89 (1 H, br, m, H-5' and H-4'), 3.96 (1 H, br, m, H-2'), 4.04 (1 H, ddd, *J* = 3.0, 3.3 and 6.2, H-3'), 4.15 (1 H, dd, *J* = 1.7 and 12.2, H-5''), 4.65 (1 H, d, *J* = 8.0, 2'-OH), 4.91 (1 H, d, *J* = 6.7, 3'-OH), 5.23 (1 H, d, *J* = 6.1, 4'-OH), 5.54 (1 H, s, H-1'), 8.07 (1 H, t, *J* = 7.6), 8.17 (2 H, s), 8.22 (1 H, d, *J* = 9.3), 8.28-8.31 (4 H, m), 8.37 (1 H, d, *J* = 9.3).

δ_C[$(CD_3)_2SO$, 150.9 MHz]: 69.2 (CH, C3'), 70.0 (CH, C4'), 72.0 (CH, C5'), 73.6 (CH, C2'), 77.9 (CH, C1'), 123.3 (CH, Ar), 124.2, 124.6, 124.8 (CH, Ar), 125.4 (CH, Ar), 125.6 (CH, Ar), 126.3 (CH, Ar), 126.5 (CH, Ar), 126.7, 127.3 (CH, Ar), 127.7 (CH, Ar), 127.9 (CH, Ar), 130.2, 130.6, 131.3, 134.5.

R_f: 0.64 (dichloromethane–methanol, 90:10 v/v)

9-β-D- ribopyranosyl pyrene **115a**

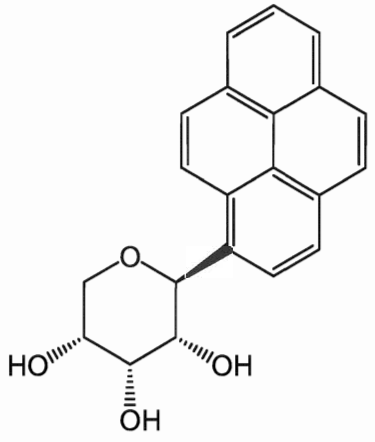

EI-MS found M^+ = 334.12007, $C_{21}H_{18}O_4$ requires 334.12051.

δ_H[$(CD_3)_2SO$, 600 MHz]: 3.68-3.71 (1 H, dd, *J* = 5.4 and 10.2, H-5'), 3.76 (1 H, t, *J* = 10.4, H-5''), 3.82–3.86 (2 H, m, H-2' and H-4'), 4.08 (1 H, br, m, H-3'), 4.63 (1 H, d, *J* = 7.3, 2'-OH), 4.81 (1 H, d, *J* = 6.6, 4'-OH), 4.98 (1 H, d, *J* = 3.4, 3'-OH), 5.39 (1 H, d, *J* = 9.6, H-1'), 8.07 (1 H, t, *J* = 7.6), 8.15-8.20 (4 H, m), 8.28 – 8.30 (3 H, m), 8.47 (1 H, d, *J* = 9.4).

δ_C[$(CD_3)_2SO$, 150.9 MHz]: 66.4 (CH, C5'), 67.9 (CH, C2' or C4'), 72.0 (CH, C3'), 72.8 (CH, C2' or C4'), 73.7 (CH, C1'), 124.3, 124.2, 124.7 (CH, Ar), 125.1 (CH, Ar), 125.3 (CH, Ar), 125.5 (CH, Ar), 125.8 (CH, Ar), 126.6 (CH, Ar), 127.2 (CH, Ar), 127.6 (CH, Ar), 127.9 (CH, Ar), 129.7, 130.5, 130.7, 131.3, 135.2.

R_f: 0.57 (dichloromethane–methanol, 90:10 v/v)

Chapter 5 - References

(1) Franklin, R. E.; Gosling, R. G. *Nature* **1953**, *171*, 740-741.
(2) Watson, J. D.; Crick, F. H. C. *Nature* **1953**, *171*, 737-738.
(3) Wilkins, M. H. F.; Stokes, A. R.; Wilson, H. R. *Nature* **1953**, *171*, 738-740.
(4) Patil, S. D.; Rhodes, D. G.; and Burgess, D. J. *AAPS J.* **2005**, *7*, E61-77.
(5) Kurreck, J. In *Therapeutic Oligonucleotides;* RSC Publishing: Cambridge, US, 2008.
(6) Fire, A.; Xu, S.; Montgomery, M. K.; Kostas, S. A.; Driver, S. E.; Mello, C. C. *Nature* **1998**, *391*, 806-811.
(7) Novina, C. D.; Sharp, P. A. *Nature* **2004**, *430*, 161-164.
(8) Kim, D. H.; Rossi, J. J. *Nat. Rev. Genet.* **2007**, *8*, 173-184.
(9) Elbashir, S. M.; Lendeckel, W.; Tuschl, T. *Genes Dev.* **2001**, *15*, 188-200.
(10) Elbashir, S. M.; Harborth, J.; Lendeckel, W.; Yalcin, A.; Weber, K.; Tuschl, T. *Nature* **2001**, *411*, 494-498.
(11) Elbashir, S. M.; Martinez, J.; Patkaniowska, A.; Lendeckel, W.; Tuschl, T. *EMBO J.* **2001**, *20*, 6877-6888.
(12) Beal, J. *Drug Discovery Today* **2005**, *10*, 169-172.
(13) Paroo, Z.; Corey, D. R. *Trends Biotechnol.* **2004**, *22*, 390-394.
(14) Braasch, D. A.; Jensen, S.; Liu, Y.; Kaur, K.; Arar, K.; White, M. A.; Corey, D. R. *Biochemistry* **2003**, *42*, 7967-7975.
(15) Braasch, A.; Paroo, Z.; Constantinescu, A.; Ren, G.; Öz, O. K.; Mason, R. P.; Corey, D. R. *Bioorg. Med. Chem. Lett.* **2004**, *14*, 1139-1143.
(16) Amarzguioui, M.; Holen, T.; Babaie, E.; Prydz, H. *Nucleic Acids Res.* **2003**, *31*, 589-595.
(17) Czauderna, F.; Fechtner, M.; Dames, S.; Aygün, H.; Klippel, A.; Pronk, G. J.; Giese, K.; Kaufmann, J. *Nucleic Acids Res.* **2003**, *31*, 2705-2716.
(18) Kawasaki, A. M.; Casper, M. D.; Freier, S. M.; Lesnik, E. A.; Zounes, M. C.; Cummins, L. L.; Gonzalez, C.; Cook, P. D. *J. Med. Chem.* **1993**, *36*, 831-841.
(19) Chiu, Y. L.; Rana, T. M. *RNA* **2003**, *9*, 1034-1048.
(20) Soutschek, J., et al *Nature* **2004**, *432*, 173-178.
(21) Allerson, C. R.; Sioufi, N.; Jarres, R.; Prakash, T. P.; Naik, N.; Berdeja, A.; Wanders, L.; Griffey, R. H.; Swayze, E. E.; Bhat, B. *J. Med. Chem.* **2005**, *48*, 901-904.
(22) Schwarz, D. S.; Hutvágner, G.; Haley, B.; Zamore, P. D. *Mol. Cell.* **2002**, *10*, 537-548.
(23) Lorenz, C.; Hadwiger, P.; John, M.; Vornlocher, H. P.; Unverzagt, C. *Bioorg. Med. Chem. Lett.* **2004**, *14*, 4975-4977.
(24) Lichtenstein, J.; Cohen, S. S. *J. Biol. Chem.* **1960**, *235*, 1134-1141.
(25) Halder, J.; Kamat, A. A.; Landen, C. N.; Han, L. Y.; Lutgendorf, S. K.; Lin, Y. G.; Merritt, W. M.; Jennings, N. B.; Chavez-Reyes, A.; Coleman, R. L.; Gershenson, D. M.; Schmandt, R.; Cole, S. W.; Lopez-Berestein, G.; Sood, A. K. *Clin. Cancer Res.* **2006**, *12*, 4916-4924.
(26) Akhtar, S.; Benter, I. F. *J. Clin. Invest.* **2007**, *117*, 3623-3632.
(27) Zhang, C.; Tang, N.; Liu, X.; Liang, W.; Xu, W.; Torchilin, V. P. *J. Control. Release* **2006**, *112*, 229-239.
(28) Zimmermann, T. S., et al *Nature* **2006**, *441*, 111-114.

(29) Gariepy, J.; and Kawamura, K. *Trends Biotechnol.* **2001**, *19*, 21-28.
(30) Morris, M. C.; Chaloin, L.; Heitz, F.; Divita, G. *Curr. Opin. Biotechnol.* **2000**, *11*, 461-466.
(31) Mahato, R. I. *J. Drug Targeting* **1997**, *7*, 249-268.
(32) Morris, M. C.; Vidal, P.; Chaloin, L.; Heitz, F.; Divita, G. *Nucleic Acids Res.* **1997**, *25*, 2730-2736.
(33) Simeoni, F.; Morris, M. C.; Heitz, F.; Divita, G. *Nucleic Acids Res.* **2003**, *31*, 2717-2724.
(34) Song, E.; Zhu, P.; Lee, S. K.; Chowdhury, D.; Kussman, S.; Dykxhoorn, D. M.; Feng, Y.; Palliser, D.; Weiner, D. B.; Shankar, P.; Marasco, W. A.; Lieberman, J. *Nat. Biotechnol.* **2005**, *23*, 709-717.
(35) Matta, H.; Hozayev, B.; Tomar, R.; Chugh, P.; Chaudhary, P. M. *Cancer. Biol. Ther.* **2003**, *2*, 206-210.
(36) Wu, X.; Li, Y.; Crise, B.; Burgess, S. M. *Science* **2003**, *300*, 1749-1751.
(37) Tomar, R. S.; Matta, H.; Chaudhary, P. M. *Oncogene* **2003**, *22*, 5712-5715.
(38) Monsigny, M.; Midoux, P.; Mayer, R.; Roche, A. *Biosci. Rep.* **1999**, *19*, 125-132.
(39) Rogers, J. C.; Kornfeld, S. *Biochem. Biophys. Res. Commun.* **1971**, *45*, 622-629.
(40) Davis, B. G.; Robinson, M. A. *Curr. Opin. Drug Discov. Devel.* **2002**, *5*, 279-288.
(41) Wu, G. Y.; Wu, C. H. *J. Biol. Chem.* **1987**, *262*, 4429-4432.
(42) Yan, H.; Tram, K. *Glycoconj. J.* **2007**, *24*, 107-123.
(43) Zatsepin, T. S.; Oretskaya, T. S. *Chem & Biodiversity* **2004**, *1*, 1401-1417.
(44) Bonfils, E.; Mendes, C.; Roche, A. C.; Monsigny, M.; Midoux, P. *Bioconjug. Chem.* **1992**, *3*, 277-284.
(45) Haensler, J.; Szoka, F. C. *Bioconjug. Chem.* **1993**, *4*, 85-93.
(46) Hasegawa, T.; Fujisawa, T.; Numata, M.; Matsumoto, T.; Umeda, M.; Karinaga, R.; Mizu, M.; Koumoto, K.; Kimura, T.; Okumura, S.; Sakurai, K.; Shinkai, S. *Org. Biomol. Chem.* **2004**, *2*, 3091-3098.
(47) Akhtar, S.; Routledge, A.; Patel, R.; Gardiner, J. M. *Tetrahedron Lett.* **1995**, *36*, 7333-7336.
(48) Wang, Y.; Sheppard, T. L. *Bioconjug. Chem.* **2003**, *14*, 1314-1322.
(49) Yamada, Y.; Matsuura, K.; Kobayashi, K. *Bioorg. Med. Chem.* **2005**, *13*, 1913-1922.
(50) Akasaka, T.; Matsuura, K.; Emi, N.; Kobayashi, K. *Biochem. Biophys. Res. Commun.* **1999**, *260*, 323-328.
(51) Forget, D.; Boturyn, D.; Renaudet, O.; Defrancq, E.; Dumy, P. *Nucleosides Nucleotides Nucleic Acids* **2003**, *22*, 1427-1429.
(52) Sando, S.; Matsui, K.; Niinomi, Y.; Sato, N.; Aoyama, Y. *Bioorg. Med. Chem. Lett.* **2003**, *13*, 2633-2636.
(53) Michelson, A. M.; Todd, A. R. *J. Chem. Soc.* **1955**, 2632-2638.
(54) Khorana, H. G.; Razzell, W. E.; Gilham, P. T.; Tener, G. M.; Pol, E. H. *J. Am. Chem. Soc.* **1957**, *79*, 1002-1003.
(55) Letsinger, R. L.; Lunsford, W. B. *J. Am. Chem. Soc.* **1976**, *98*, 3655-3661.
(56) Beaucage, S. L.; Caruthers, M. H. *Tetrahedron Lett.* **1981**, *22*, 1859-1862.
(57) Hall, R. H.; Todd, A.; Webb, R. F. *J. Chem. Soc.* **1957**, 3291-3296.
(58) Sinha, N. D.; Biernat, J.; McManus, J.; Koster, H. *Nucleic Acids Res.* **1984**, *12*, 4539-4557.

(59) Alvarado-Urbina, G.; Sathe, G. M.; Liu, W. C.; Gillen, M. F.; Duck, P. D.; Bender, R.; Ogilvie, K. K. *Science* **1981**, *214*, 270-274.
(60) McCollum, C.; Andrus, A. *Tetrahedron Lett.* **1991**, *32*, 4069-4072.
(61) Reese, C. B. *Org. Biomol. Chem.* **2005**, *3*, 3851-3868.
(62) Kuusela, S.; Lönnberg, H. *J. Chem. Soc. Perkin Trans. 2* **1994**, *1994*, 2109-2113.
(63) Griffin, B. E.; Reese, C. B.; Stephenson, G. F.; Trentham, D. R. *Tetrahedron Lett.* **1966**, *7*, 4349-4354.
(64) Hayes, J. A.; Brunden, M. J.; Gilham, P. T.; Gough, G. R. *Tetrahedron Lett.* **1985**, *26*, 2407-2410.
(65) Ogilvie, K. K.; Sadana, K. L.; Thompson, E. A.; Quilliam, M. A. *Tetrahedron Lett.* **1974**, *33*, 2861-2863.
(66) Westman, E.; Stromberg, R. *Nucleic Acids Res.* **1994**, *22*, 2430-2431.
(67) Jones, S. S.; Reese, C. B. *J. Chem. Soc. Perkin Trans. 1* **1979**, 2762-2764.
(68) Reese, C. B.; Trentham, D. R. *Tetrahedron Lett.* **1965**, *29*, 2467-2472.
(69) Griffin, B. E.; Reese, C. B. *Tetrahedron Lett.* **1964**, 2925-2931.
(70) Reese, C. B.; Saffhill, R.; Sulston, J. E. *Tetrahedron* **1970**, *26*, 1023-1030.
(71) van Boom, J. H.; van Deursen, P.; Meeuwse, J.; Reese, C. B. *J. Chem. Soc. , Chem. Commun.* **1972**, 766-767.
(72) Reese, C. B.; Serafinowska, H. T.; Zappia, G. *Tetrahedron Lett.* **1986**, *27*, 2291-2294.
(73) Reese, C. B.; Thompson, E. A. *J. Chem. Soc. Perkin Trans. 1* **1988**, 2881-2885.
(74) Faja, M.; Reese, C. B.; Song, Q.; Zhang, P. *J. Chem. Soc. Perkin Trans. 1* **1997**, 191-194.
(75) Lloyd, W.; Reese, C. B.; Song, Q.; Vandersteen, A. M.; Visintin, C.; Zhang, P. *J. Chem. Soc. Perkin Trans. 1* **2000**, 165-176.
(76) Schwartz, M. E.; Breaker, R. R.; Asteriadis, G. T.; deBear, J. S.; Gough, G. R. *Bioorg. Med. Chem. Lett.* **1992**, *2*, 1019-1024.
(77) Gough, G. R.; Miller, T. J.; Mantick, N. A. *Tetrahedron Lett.* **1996**, *37*, 981-982.
(78) Cieslak, J.; Kauffman, J. S.; Kolodziejski, M. J.; Lloyd, J. R.; Beaucage, S. L. *Org. Lett.* **2007**, *9*, 671-674.
(79) Scaringe, S. A.; Wincott, F. E.; Caruthers, M. H. *J. Am. Chem. Soc.* **1998**, *120*, 11820-11822.
(80) Pitsch, S.; Weiss, P. A.; Jenny, L.; Stutz, A.; Wu, X. *Helv. Chim. Acta.* **2001**, *84*, 3773-3795.
(81) Wada, T.; Tobe, M.; Nagayama, T.; Sekine, M.; Furusawa, K. *Tetrahedron Lett.* **1995**, *36*, 1683-1684.
(82) Ohgi, T.; Masutomi, Y.; Ishiyama, K.; Kitagawa, H.; Shiba, Y.; Yano, J. *Org. Lett.* **2005**, *7*, 3477-3480.
(83) Zhou, C.; Honcharenko, D.; Chattopadhyaya, J. *Org. Biomol. Chem.* **2007**, *5*, 333-343.
(84) Cieslak, J.; Grajkowski, A.; Kauffman, J. S.; Duff, R. J.; Beaucage, S. L. *J. Org. Chem.* **2008**, *73*, 2774-2783.
(85) Kamath, V. P.; Diedrich, P.; and Hindsgaul, O. *Glycoconj. J.* **1996**, *13*, 315-319.
(86) Yan, H.; Aguilar, A. L.; Zhao, Y. *Bioorg. Med. Chem. Lett.* **2007**, *17*, 6535-6538.
(87) Figdor, C. G.; van Kooyk, Y.; Adema, G. J. *Nat. Rev. Immunol.* **2002**, *2*, 77-84.
(88) Drickamer, K.; Taylor, M. E. *Annu. Rev. Cell Biol.* **1993**, *9*, 237-264.

(89) Hanessian, S. In *Preparative carbohydrate chemistry;* Marcel Dekker: New York, 1997; pp 648.
(90) Lundquist, J. J.; Toone, E. J. *Chem. Rev.* **2002**, *102*, 555-578.
(91) Brunel, J. M.; Salmi, C.; Letourneux, Y. *Tetrahedron Lett.* **2005**, *46*, 217-220.
(92) Le-Nguyen, D.; Heitz, A.; Castro, B. *J. Chem. Soc. Perkin Trans. 1* **1987**, *1987*, 1915-1919.
(93) Piton, N.; Mu, Y.; Stock, G.; Prisner, T. F.; Schiemann, O.; Engels, J. W. *Nucleic Acids Res.* **2007**, *35*, 3128-3143.
(94) Noe, C. R.; Winkler, J.; Urban, E.; Gilbert, M.; Haberhauer, G.; Brunar, H. *Nucleosides Nucleotides Nucleic Acids* **2005**, *24*, 1167-1185.
(95) Beaucage, S. L.; Iyer, R. P. *Tetrahedron* **1993**, *49*, 1925-1963.
(96) Bloom, L. B.; Otto, M. R.; Beechem, J. M.; Goodman, M. F. *Biochemistry* **1993**, *32*, 11247-11258.
(97) Ren, R. X.; Chaudhuri, N. C.; Paris, P. L.; Rumney, S.; Kool, E. T. *J. Am. Chem. Soc.* **1996**, *118*, 7671-7678.
(98) Schweitzer, B. A.; Kool, E. T. *J. Am. Chem. Soc.* **1995**, *117*, 1863-1872.
(99) Chaudhuri, N. C.; Kool, E. T. *Tetrahedron Lett.* **1995**, *36*, 1795-1798.
(100) Postema, M. H. D. *Tetrahedron* **1992**, *48*, 8545-8599.
(101) Kraus, G. A.; Molina, M. T. *J. Org. Chem.* **1988**, *53*, 752-753.
(102) Krohn, K.; Heins, H.; Wielckens, K. *J. Med. Chem.* **1992**, *35*, 511-517.
(103) Hildbrand, S.; Leumann, C. *Angew. Chem. Int. Ed. Engl.* **1996**, *35*, 1968-1970.
(104) Sollogoub, M.; Fox, K. R.; Powers, V. E. C.; Brown, T. *Tetrahedron Lett.* **2002**, *43*, 3121-3123.
(105) Reese, C. B.; Wu, Q. P. *Org. Biomol. Chem.* **2003**, *1*, 3160-3172.
(106) Liu, L.; Li, C. P.; Cochran, S.; Ferro, V. *Bioorg. Med. Chem.* **2004**, *14*, 2221-2226.
(107) Austin, P. W.; Hardy, F. E.; Buchanan, J. G.; Baddiley, J. *J. Chem. Soc.* **1964**, *1964*, 2128-2137.
(108) Timpe, W.; Dax, K.; Wolf, N.; Weidmann, H. *Carbohydrate Research* **1975**, *39*, 53-60.
(109) Lacowicz, J. R. In *Principles of Fluorescence Spectroscopy;* Springer: US, 2006; pp 54-55.
(110) Treibs, A.; Kreuzer, F. *J ust. Lieb. Ann. Chem.* **1968**, *718*, 208-223.
(111) Tram, K.; McIntosh, W.; Yan, H. *Tetrahedron Lett.* **2009**, *50*, 2278-2280.
(112) Tram, K.; Yan, H.; Jenkins, H. A.; Vassiliev, S.; Bruce, D. *Dyes Pigms.* **2009**, *82*, 392-395.
(113) Rao, M. V.; Reese, C. B.; Schehimann, V.; Yu, P. S. *J. Chem. Soc. Perkin Trans. 1* **1993**, *1993*, 43-55.